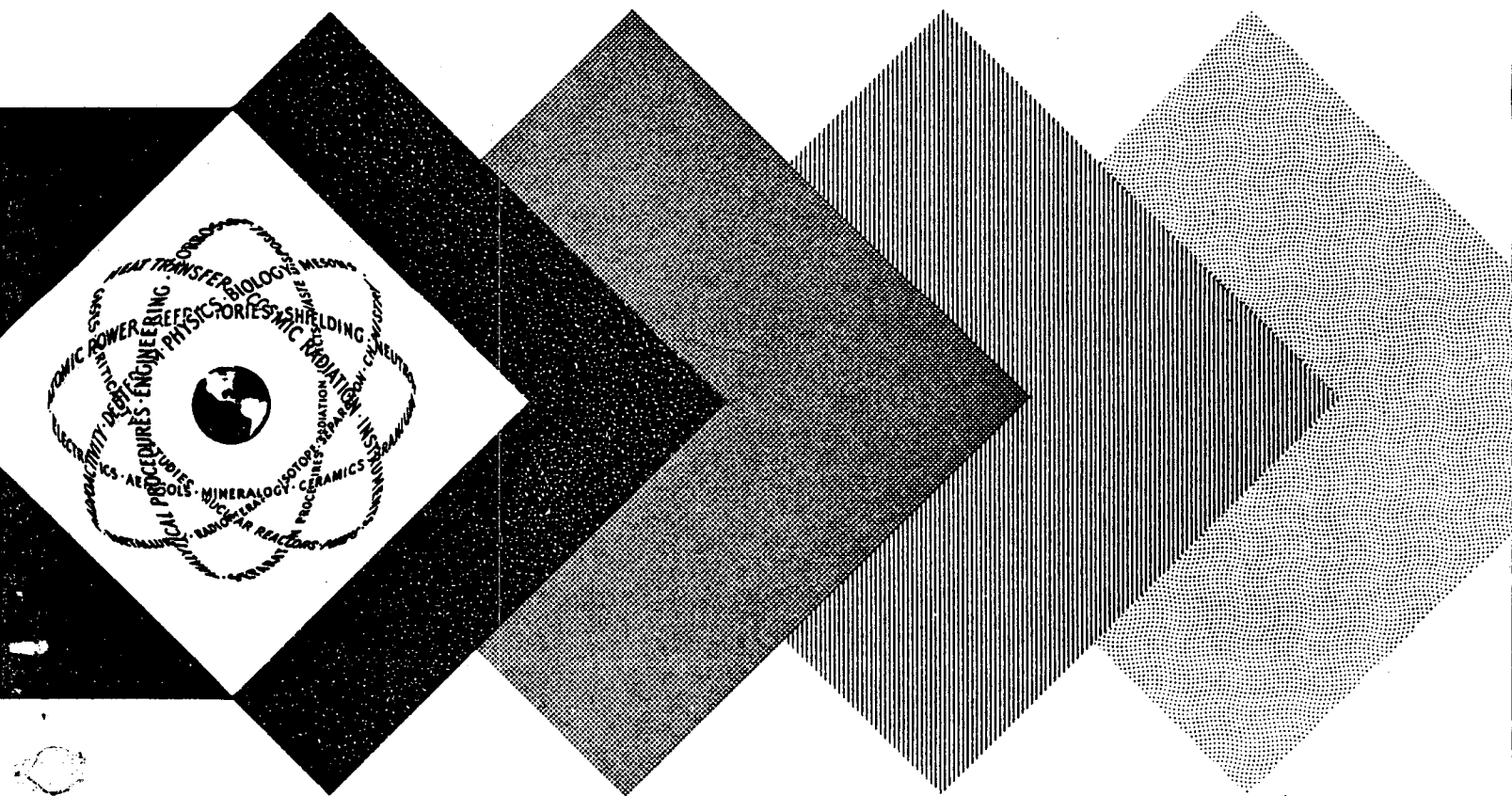# HYDRODYNAMIC ASPECTS OF BOILING HEAT TRANSFER (thesis)

By
Novak Zuber

June 1959

Research Laboratory
Los Angeles and Ramo-Wooldridge Corporation
University of California
Los Angeles, California

LEGAL NOTICE

This report has been reproduced directly from the best available copy.

Printed in USA. Price $2.00. Available from the Office of Technical Services, Department of Commerce, Washington 25, D. C.

DISCLAIMER

DISCLAIMER

Portions of this document may be illegible in electronic image products. Images are produced from the best available original document.

UNIVERSITY OF CALIFORNIA, LOS ANGELES

Hydrodynamic Aspects

of Boiling Heat Transfer

A dissertation submitted in partial satisfaction of the

requirements for the degree Doctor of Philosophy

in Engineering

by

Novak Zuber

June, 1959

TABLE OF CONTENTS

TABLE OF FIGURES

vii

NOMENCLATURE

a	=	thermal diffusivity
A	=	area
b	=	a numerical constant equal to 1 or $\pi/2$
c	=	specific heat at constant pressure
C	=	propagation velocity of a disturbance
D_c	=	diameter of a nucleating cavity
D_d	=	diameter of a bubble departing from a horizontal surface
D_m	=	maximum bubble diameter
f	=	frequency
g	=	acceleration due to gravity
h	=	heat transfer coefficient
H_o	=	amplitude of a disturbance

$$Ja = \frac{(T_w - T_s)c\rho_L}{L\rho_v} = \text{Jakob Modulus}$$

I_o	=	modified Bessel function of the first kind
K_o	=	modified Bessel function of the second kind
k	=	thermal conductivity
L	=	latent heat of vaporization
m	=	wave number
M	=	vapor mass flow rate per unit area
n	=	number of bubbles

P = pressure

q = heat flux density from solid to liquid

q_b = heat flux density from bubble interface to bulk liquid

q_c = critical heat flux

q_m = minimum heat flux in transitional boiling

r_o = radius of a surface cavity

R = bubble radius

R_m = maximum bubble radius in subcooled boiling

t_c = contact time, i.e., the time needed to superheat the liquid

t_d = the time needed for a bubble to reach the diameter D_d

t_m = the time needed for a bubble to reach the radius R_m

T_L = temperature of the bulk liquid

T_o = temperature of the superheated liquid

T_s = saturation temperature

T_w = temperature of the solid, i.e., of the wall and therefore of the liquid in contact with it

$T = T_o - T_s = T_w - T_s$ = liquid superheat temperature difference

U_v = velocity of the vapor

U_L = velocity of the liquid

U = velocity of rise of deformed bubbles

X_s = thickness of the superheated liquid film adjacent to the heating surface

α = conical angle of a nucleating cavity

δ = thickness of the thermal boundary layer

λ = wave length

η = disturbance of a plane interface

ζ = disturbance of a cylindrical interface

ω = angular frequency

ρ = density

σ = surface tension

Θ = contact angle

Subscripts

v = vapor

L = liquid

ACKNOWLEDGEMENTS

Mojim dobrim roditeljima - tamo daleko,

and to Corinne close by.

Na Vidovdan 1959

ABSTRACT

An analytical expression is presented which permits
the prediction of the critical heat flux density in pool
boiling of saturated or subcooled liquids. The theore-
tical results are in good agreement with experimental
data.

The hydrodynamic characteristics of transitional
boiling from a horizontal surface are analyzed; the
phenomenon is interpreted in terms of Taylor instability.
It is shown that the minimum heat flux is limited by the
effect of Taylor instability only; an equation is derived
which permits the prediction of this heat flux density.

The hydrodynamic characteristics of nucleate boiling
from a horizontal surface are analyzed. The similarity
between bubble formation at an orifice and bubble
formation in nucleate boiling is investigated. This
similarity indicates a relation between the diameter of
a quasi-static bubble departing from the surface and the
radius of the nucleating cavity. An equation is derived
also for the product bubble diameter times frequency of
bubble emission; the predicted values are in good
agreement with experimental data of Jakob. It is
possible thus to estimate the maximum frequency of the

release of single bubbles in nucleate boiling. The similarity between nucleate boiling and the process of gas bubbling from a porous surface is discussed. The similarity indicates that the critical heat flux is a hydrodynamic phenomenon known as "flooding".

The nucleation from a solid surface is reviewed. The analysis of available experimental data indicates that the diameter of a nucleating cavity can be related to the heat flux density and to the superheat temperature difference. Further experimental investigations are needed.

The problem of bubble growth is discussed. It is pointed out that the original formulation of the problem as given by Bosnjakovic and Jakob contains the essential features of the problem. The theory of Bosnjakovic and Jakob is extended to include the effects of a non-uniform temperature field.

INTRODUCTION

Developments in nuclear reactors and rocket engines where exceedingly high heat transfer rates occur in comparatively small areas, have focused attention on boiling as a mode of transferring heat at high flux densities. To attain these high heat transfer rates by forced convection would require excessively high velocities with resulting high pressure drops. With nucleate boiling, however, they can be reached at much lower bulk velocities. For this reason extensive experimental and theoretical studies of this phenomenon are conducted in this country and abroad.

The phenomenon is complex because three different regimes exist: nucleate, transition and film boiling. The change from one regime to another is accompanied by marked changes in the hydrodynamic and thermal state of the system. These regimes are illustrated in Figure I. When the temperature of the heating surface is below the fluid saturation temperature heat is transferred by convection, forced or natural, depending on the system. This non-boiling region (AB) has been extensively investigated and equations have been derived which permit the prediction of heat transfer rates.

Y-axis: HEAT FLUX, q, $(BTU/HR\ FT^2)$

10^6

10^5

10^4

X-axis: 10^1 10^2 10^3 10^4

Labels on curve: A, B, C, D, E

TEMPERATURE DIFFERENCE BETWEEN WALL AND LIQUID $(T_W-T_L)(^\circ F)$
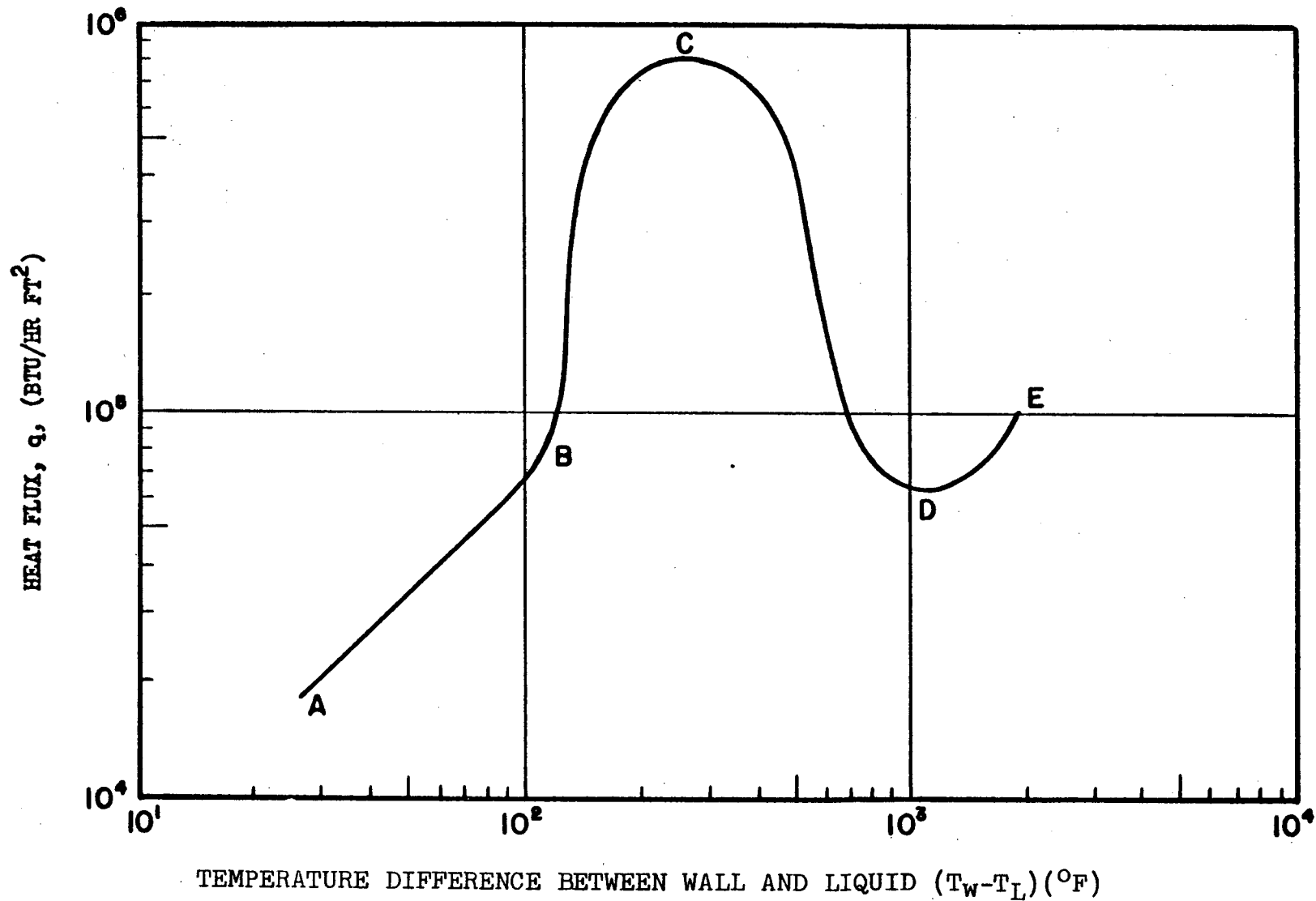
FIGURE I.   A TYPICAL CURVE OF HEAT FLUX DENSITY VERSUS SURFACE TEMPERATURE IN BOILING

Nucleate boiling (BC) starts when the temperature of the surface exceeds the saturation by a few degrees. Adjacent to the surface a thin layer of superheated liquid is formed in which bubbles nucleate and grow from some preferred spots on the surface. The thermal resistance of this superheated liquid film is greatly reduced by the agitation produced by the bubbles. An increase of the wall temperature is accompanied by a large increase of the bubble population causing in turn a sharp increase of the heat flux. However, as the temperature increases, bubbles become so numerous that their motions intereact. Under these conditions the nucleate heat flux reaches its peak. If the temperature is further increased transition boiling begins. Westwater and Santangello (1) have found that in this region (CD) no liquid-solid contact exists. The surface is blanketed by an unstable, irregular film of vapor which is in violent motion. In transition boiling an increase of temperature is followed by a decrease of heat flux until a minimum value is reached at which point film boiling starts. This new regime is characterized by an orderly discharge of large bubbles with a regular frequency and at regular intervals. In the film boiling region the heat flux increases with an increase of temperature but at a much slower rate than in nucleate

boiling. Consequently, at high heat transfer rates the
temperature of the heating surface can exceed the melting
temperature and "burnout" occurs. It is of great
practical interest to operate in the nucleate region
because of the favorable heat transfer. The problem is
to avoid the "burnout" phenomenon.

The temperatures of the wall in nucleate boiling
are quite low, for example, with boiling water the tem-
perature of the surface at the point C exceeds the fluid
saturation temperature by about $50^{\circ}F$ at 14.6 psia and
by only $10^{\circ}F$ at 2000 psia. Therefore, in many designs
the exact surface temperatures are of secondary
importance. This is especially true for constant heat-
input systems such as a nuclear reactor. The essential
information needed by a designer is the limit to the
heat transfer rates given by the critical heat flux,
i.e., by the flux corresponding to point C. The tem-
perature at point C is relatively unimportant. An
investigation of the conditions leading to this maximum
heat flux is therefore of practical and theoretical
interest. Such a study, as applied to a horizontal
plate, is reported in this dissertation. The study is
concerned with determining the limiting hydrodynamic
conditions which characterize nucleate and transitional

boiling. The critical heat flux (point C) and the minimum heat flux (point D) are derived from these hydrodynamic limits.

An understanding of the conditions leading to the changes in the regimes of boiling requires an understanding of the processes which characterize each regime separately. Because of this, both nucleate and transitional boiling are investigated and discussed. The dissertation is divided into six chapters according to the problem under consideration. Results of experimental investigation of nucleate boiling are discussed in Chapter I, which is, therefore, a review section. The problem of bubble growth is discussed in this dissertation because nucleate boiling is characterized by the action of vapor bubbles. In Chapter II, the bubble growth theory of Bosnjakovic and Jakob is extended to include the effect of a non-uniform temperature field. In Chapter III, the hydrodynamic aspect of nucleate boiling is analyzed, whereas the hydrodynamic aspect of transitional boiling is investigated in Chapter IV. The minimum and the critical heat flux are analyzed in Chapters V and VI respectively.

CHAPTER I

A REVIEW OF NUCLEATE BOILING

The first systematic investigation of nucleate boiling was undertaken by Jakob, Fritz and Linke, the results of which were reported in a series of outstanding papers (2, 3, 4, 5, 6). The high heat transfer rates in nucleate boiling were attributed to bubbles which induce locally a strong agitation of the liquid near the heating surface. The effect of bubble agitation on the heat flux was further investigated and confirmed by Gunther and Kreith (7) and by Rohsenow and Clark (8).

Jakob and Fritz (2) noted that the high heat transfer rates, which are caused by local flow oscillations that exist in the vicinity of growing and rising bubbles, can be induced also by liquid jets flowing in between rising bubble columns and impinging on the heating surface. The total heat flux from the heating surface to the liquid is the sum of such local heat transfer rates. Consequently, in order to gain an understanding of nucleate boiling it is necessary to understand the local processes which are associated with single bubbles. It is necessary thus to investigate

three aspects of the problem: the nucleation of a bubble, the growth of a bubble, and finally, the hydrodynamics of a bubble departing from the heating surface. These three aspects of the problem, which were investigated by Jakob and co-workers as well as by other investigators, will be discussed in the sections which follow.

I-1. Nucleation from a Solid Surface

The effect of a surface on the process of nucleation will be discussed in some detail because, as it will be seen in the sections which follow, the conditions of the surface determine the temperature at which the bubble will generate and, thus, determine the subsequent history of a growing bubble.

It is experimentally observed that in boiling liquids bubbles nucleate at liquid superheat temperatures which are considerably less than those which would be predicted by classical nucleation theories. It is known, also, that bubbles originate from specific nucleating centers located on the heated surface. The question of whether these nucleating centers are roughness projections or cavities in the surface was examined in detail by Bankoff (9). By comparing the theoretical superheat temperatures which would be required to generate a bubble from a flat or projecting surface, with the superheats which are observed in experiments, Bankoff concluded

that only pits or scratches which contain gas or vapor are possible sites for nucleation. These deductions were conclusively verified by the experimental results of Clark, Strenge and Westwater (10).

The nucleation process from a cavity was investigated by Jakob and co-workers (2, 3, 4, 5); by Dzhandzhgava (11); Nesis (12); Courty and Foust (13, 14); Ellion (15); Bankoff (9); Clark, Strenge and Westwater (10); and by Griffith and Wallis (16). The problem can be resolved into two parts: one, an investigation of the conditions necessary to entrap gas and/or vapor into surface capillaries (pits or scratches) and, two, an investigation of conditions which would permit the release of this vapor in the form of a bubble.

The process of entrapment of a gas and/or vapor into a cavity and the related problem of investigating whether this cavity will remain stable in time, i.e., whether or not the entrapped gas will diffuse and whether the entrapped vapor can condense, are of importance in an analysis of transient boiling and of boiling hysteresis. Since these latter two processes are not the topic of the present investigation, the entrapment and the stability of a cavity will not be discussed here. The reader is referred to the papers by Courty (13), Bankoff (17, 18) and by Sabersky and

Gates (19) for a discussion and investigation of this problem. An analysis of transient boiling will be presented in a future report where the entrapment process will be taken up also.

We shall proceed with the discussion of the conditions which permit the release of a gas or vapor from a cavity, a problem which was first analyzed by Courty and Foust (13, 14) in this country and by Nesis (12) in Russia.

I-2. Bubble Generation from a Cavity

Consider an amount of gas or vapor which is entrapped in a cylindrical capillary with vertical walls shown in Figures I-1 and I-2, which are reproduced from Nesis' paper (12). When the liquid wets the solid, i.e., when the contact angle Θ , is less than 90° (Figure I-1), the pressure in the cavity is given by:

$$P = P_L + \frac{2\sigma}{r} \qquad \text{I-1}$$

where r is the radius of the curvature of the interface and P_L is the pressure in the liquid. The maximum pressure in the cavity occurs when the radius, r , is minimum. In expanding from stage I to stage VI, the minimum curvature occurs when the interface turns around the corner. The minimum value of r , ($r_{min} = r^*$) is
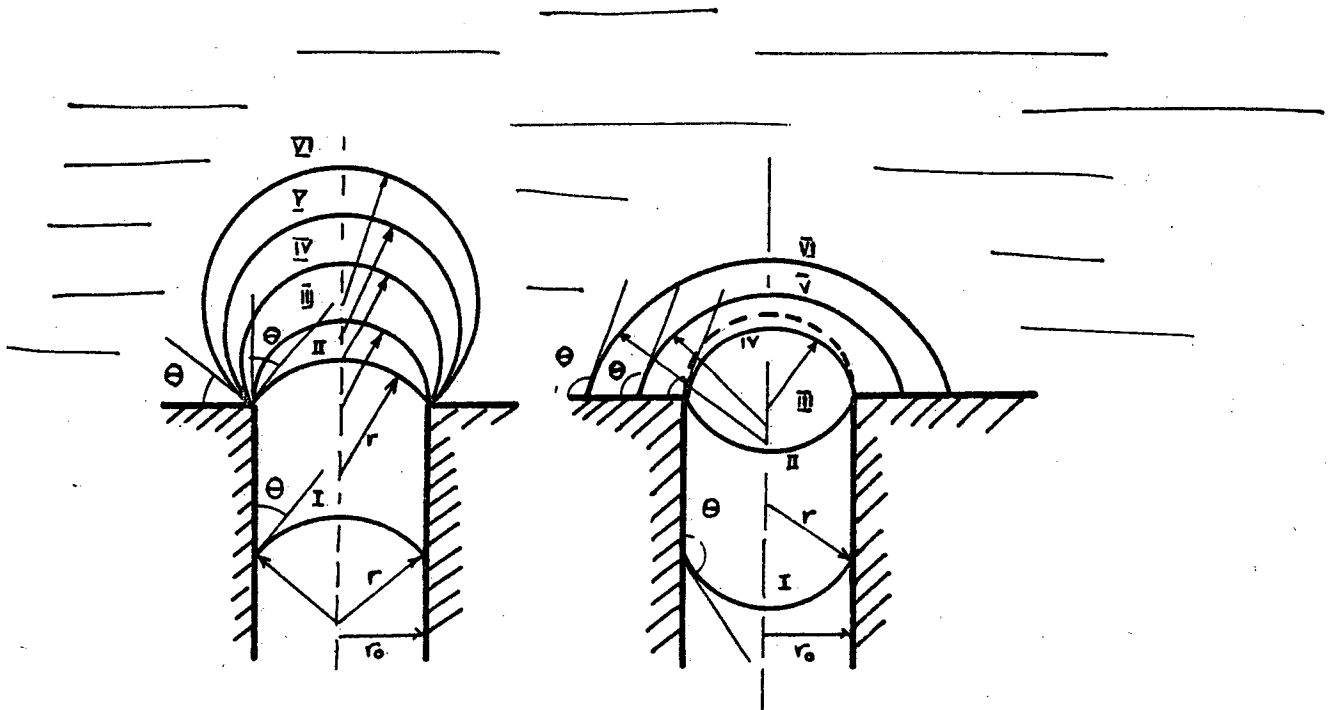
Figure I-1.

Liquid Wets
the Solid

Figure I-2.

Liquid Does
Not Wet
the Solid

Nucleation from a Cavity

(These figures are reproduced from
the paper by Nesis (12).)

equal then to the radius r_o, of the cylindrical capillary, thus $r^* = r_o$. Consequently, if the cavity is to be active, i.e., if it is to be a nucleating center, the pressure within it must reach the maximum value, corresponding to $r = r^*$. Using Clausius-Clapeyron's equation:

$$\frac{P_v(r_o) - P_s}{T_w(r_o) - T_s} = \frac{L}{T(v_v - v_L)} \qquad \text{I-2}$$

This maximum pressure difference can be related to a temperature difference. For a cavity which contains only vapor, and for a uniformly superheated liquid, the superheat temperature which will activate a cavity of radius r_o, is given by Equations I-1 and I-2, thus

$$T_w(r_o) - T_s = \frac{2\sigma}{r_o} \frac{T(v_v - v_L)}{L} \qquad \text{I-3}$$

It should be noted here that r_o is a characteristic of the surface. Consequently, for a given cavity at a given pressure different starting superheat temperatures can be obtained by varying the value of the surface tension.

If the cavity contains both, vapor and gas, the temperature of the superheated liquid, $T_w(r_o)$, will be reduced by an amount corresponding to the partial

pressure of the gas.

When the cavity does not wet the solid ($\theta > 90°$),
the interface is concave (see Figure I-2), and the
pressure within the cavity is given by

$$P = P_L - \frac{2\sigma}{r}$$

In expanding, the interface changes from concave to
convex; the maximum pressure occurs when the radius of
the convex interface establishes the contact angle θ ,
at the entrance of the cavity. Since the radius of
curvature, r , and the radius of the cavity, r_0 ,
are related by

$$r^* = \frac{r_0}{\sin \theta}$$

it follows from Equations I-1, I-2 and I-5 that with a
non-wetting liquid the cavity will be activated at a
lower superheat temperature difference $T_w - T_s$.

Similar deductions can be derived for conical
cavities, which were investigated by Courty (13),
Bankoff (17), and Wallis (16). Since the radius of
curvature of the interface in a conical cavity (see
Figure I-3) is given by
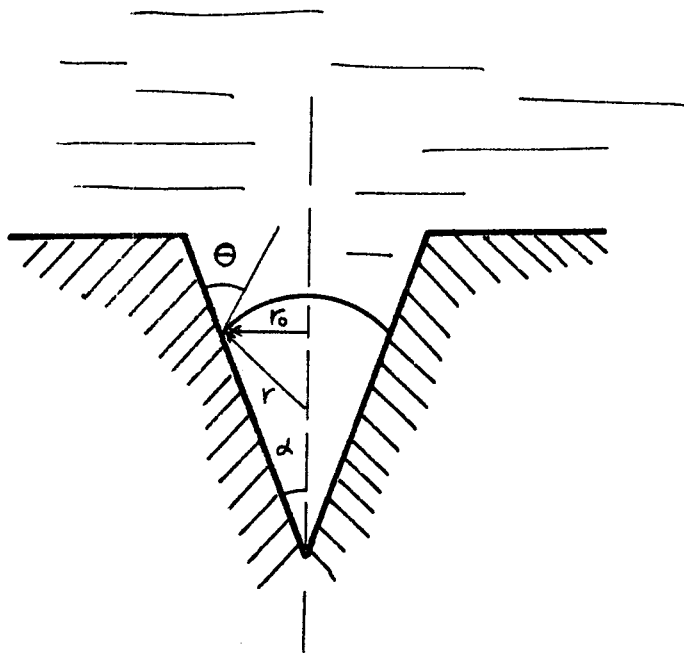
Figure I-3.

Nucleation from a Conical Cavity

$$r = \frac{r_0}{\cos(\theta - \alpha)} \qquad \text{I-6}$$

the maximum superheat temperature will depend on the contact angle θ , as well as on the relative magnitude of α and θ .

The above considerations were verified recently by Griffith and Wallis (16) in experiments which were conducted by reducing the pressure on the system (note that this has the same effect as of uniformly super-heating the liquid). The results of these careful and important experiments showed that when $\alpha < \theta < 90^\circ$ the temperature which activated a cavity of given radius r_0 , was given indeed by Equation I-3. However, when the same experiments were performed by heating the surface it was found that the wall superheat temperature, $T_w - T_s$, required to nucleate a bubble from the same cavity was $20^\circ F$ instead of $3^\circ F$ as predicted by Equation I-3. Similar results were reported by Clark, Strenge and Westwater (10).

Four conclusions can be drawn from these experiments and from the analysis discussed in this section.

1) Pits and cavities which contain entrapped gas
     or vapor are nucleating centers in boiling

from a solid surface.

2) The dimensions of the cavity are important in the nucleating process from a heated surface.

3) For a <u>given</u> cavity size a larger superheat is required to nucleate a bubble in a non-uniform than in a uniform temperature field.

4) The nucleating propensity of a surface will depend upon the size distribution of cavities. For a given surface this cavity distribution will remain an invariant for variations of pressure or of liquid properties. This important fact was shown also by Griffith and Wallis.

In the next section we shall discuss experimental results which pertain to bubbles growing and rising from a horizontal heated surface in nucleate, pool boiling, i.e., in absence of forced convection.

I-3. <u>The Dynamics of a Bubble Departing from a Horizontal, Heated Surface</u>

Following the nucleation from a cavity the bubble grows in a superheated liquid film which exists adjacent to the solid wall. The thickness of this superheated liquid film is of the order of 10^{-1} to 10^{-2} cm. (2, 3, 4, 5, 7, 20). The bubble remains attached to the surface until, at time t_d, it reaches a characteristic

diameter D_d , and departs from the heating surface.
The departure is governed by the dynamics of the sur-
rounding liquid as well as by the buoyant and adhesion
forces. The dynamic effect of the surrounding liquid
upon a bubble departing from the surface has not been
evaluated quantitatively yet. The problem was analyzed
by Wark (21), Fritz (22) and by Nesis (12), who con-
sidered a static equilibrium between the buoyant and
adhesive forces. For such a static condition the
problem becomes an analogue to the problem of determining
the maximum volume of a sessile drop hanging from a
horizontal surface, a problem which was analyzed by
Bashfort and Adams (23). Using their numerical results,
Fritz (22) derived the following expression for the
diameter D_d , of a bubble departing from a horizontal
surface, thus

$$D_d = 0.0208\,\theta \left[\frac{\sigma}{g(\rho_L - \rho_v)} \right]^{1/2} \qquad \text{I-7}$$

where the contact angle θ , is measured in degrees.

The problem of bubble detachment was investigated
experimentally by Jakob and Linke (5) and by Fritz and
Ende (24). From a detailed study of motion pictures of
steady boiling at low heat flux densities (of the order
of 20,000 kcal/m^2hr), Jakob and Linke (5) found that

diameters of departing bubbles D_d , are given by a statistical distribution about a mean value. The values of D_d varied from 1.5 mm to 4.5 mm with a maximum at about $D_d = 2.8 \times 10^{-1}$ cm. This maximum value was in agreement with the value predicted by Equation I-7 for a contact angle of $\theta = 50^{\circ}$. It was observed also that preceding the detachment, bubbles become elongated (see Figure 1-4). Immediately after the detachment, i.e., after the elongated connection snaps, the lower surface of the bubble reenters causing a deformation. Thus, immediately after departure, the bubble takes first a mushroom-like form and later a lenticular shape.

It was observed in these experiments that the nucleation and bubble growth from a given nucleating center is a periodic process. Following the departure of a bubble the colder liquid comes in contact with the solid and gets heated during a "contact time", t_c , at the end of which time another bubble is nucleated from the same center. This new bubble grows until, at time t_d , it in turn departs from the surface, and the process is repeated. The contact time, t_c , during which the liquid in the vicinity of the nucleating cavity becomes superheated was found to be approximately equal to the growth time t_d . Thus, the total frequency of bubble emission
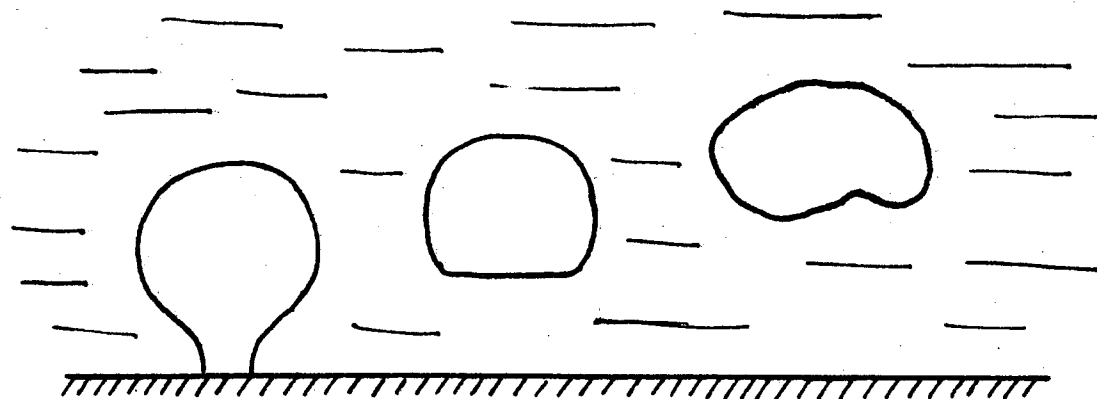
Figure I-4.

Deformation of a Bubble Departing from

a Heated Horizontal Surface According to Jakob (3).

$$f = \frac{1}{t_c + t_d} \qquad \text{I-8}$$

was found to be a constant for a given nucleating center, although for different cavities a statistical distribution was observed. In the range of low heat flux densities, i.e., in the range which was investigated by Jakob and Linke and Fritz and Ende it was found that both the diameter D_d , and the frequency f , were independent of the heat flux. The effect of increasing the heat flux was to increase only the number of active nucleating centers. Consequently the product of the diameter D_d , and the frequency f , is a constant,

$$D_d \cdot f = const. \qquad \text{I-9}$$

Recently a study of bubble dynamics in the entire range of nucleate boiling with methanol was reported by Perkins and Westwater (25). It was observed that the average bubble diameter as well as the average frequency remained constant for heat fluxes up to 80% of the critical heat flux. At higher flux densities both the diameter as well as the frequency increased. In these

experiments at high heat transfer rates the contact time, t_c , was found to be approximately zero, i.e., the bubbles form immediately after each other. A similar observation was reported by Donald and Haslam (26).

This change of bubble generation from intermittent to continuous was investigated by Yamagata and Nishikawa (27). These experiments were carried out with water at atmospheric pressure with heat flux densities ranging from 6,000 to 18,000 $kcal/m^2hr$. It should be noted here that for water at atmospheric pressure the critical heat flux is approximately 10^6 $kcal/m^2hr$. From a study of their experimental data, Yamagata and Nishikawa classified bubbles into four groups, i.e., sphere type, bell type, precession type and tandem type. Figure I-5, which is reproduced from their report, shows the different bubble forms.

The formation of sphere and bell type bubbles was essentially identical, consequently they were classified as "simple bubbles"; whereas the precession and the tandem bubbles were called "multiple bubbles" because they were formed by bubble coalescence. All four bubble types were generated intermittently. A contact time, t_c , and a growth time, t_d , were observed for simple bubbles. The product of $D_d \cdot f$ was constant for simple bubbles, whereas the data for multiple bubbles showed a

a) Sphere Type

b) Bell Type
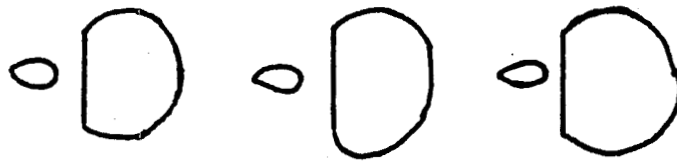
c) Precession Type

d) Tandem Type

e) Continuous Vapor Column

Figure I-5. Types of Vapor Bubbles Departing from
a Horizontal Heated Surface as Reported by
Yamagata and Nishikawa (Reference 27).

larger scatter. Simple bubbles were generated at lower
heat flux densities when a smaller number of nucleating
centers were active. Multiple bubbles were formed at
higher heat flux density when the bubble columns were
more numerous. Yamagata and Nishikawa noted that when
the heat flux is increased beyond a certain limit "the
bubbles were not generated intermittently, but formed
a continuous vapor column. These whirls were often
generated at two or more spots interferring with each
other." Such an observed continuous vapor column is
shown in Figure I-5. It is important to note that
continuous vapor columns can be seen also in the high
speed movies taken by Perkins and Westwater.

We shall now summarize the experimental evidence
concerning the dynamics of bubbles departing from a
horizontal surface in nucleate, pool boiling.

1) At low heat flux densities the mechanism
governing the departure can be approximated
by a quasi-static equilibrium between the
buoyant and adhesive forces. Consequently,
the statistical mean value of the diameters
can be approximated by Equation I-7.

2) Immediately after the departure a bubble
undergoes a deformation.

3) At low heat transfer rates bubbles are generated intermittently with a characteristic constant frequency.

4) As the heat flux is increase the contact time, t_c , decreases. Bubbles change from simple to multiple type which are formed by a coalescence of several bubbles.

5) At high heat transfer rates the contact time decreases until bubbles form immediately after each other.

6) At still higher heat transfer rates the diameters and the frequency of bubble formation increase until a continuous vapor column is formed.

7) It appears that at low heat transfer rates the effect of increasing the heat flux is to increase the number of active nucleating centers, ie., of bubble columns. Whereas at higher heat flux density this effect appears to change the bubble generation from an intermittent to a continuous process. The characteristic of the phenomenon thus appears to be a change from a column consisting of single, rising bubbles to a continuous vapor column, i.e., a vapor jet.

I-4. The Relation Between Heat Flux Density, Surface
Roughness and Temperature in Nucleate Boiling

In the two previous sections we have reviewed the
nucleation of a single bubble from a cavity and the
departure of a bubble from a heated surface. In this
section we shall discuss the interdependence of the heat
flux density, surface roughness, superheat temperature
difference and bubble dynamics in nucleate boiling. The
phenomenon will be described in more detail in order
that, in Chapter III, it may be more easily compared to
the process of a gas bubbling through a porous plate.
The discussion in this section is based to a large extent
upon a penetrating study of nucleate boiling which was
reported by Courty (13) and Courty and Foust (14).

Consider a surface with cavities which contain
some entrapped gas or vapor and let the heat flux
density increase so that the temperature of the solid
surface exceeds the saturation temperature, i.e., the
liquid adjacent to the wall becomes superheated. At
some superheat temperature difference, $T_w - T_s$, a
few bubbles will start growing from some nucleating
centers located at random. At what particular superheat
temperature this nucleation can start will depend, as
discussed in Section I-2, upon the dimensions of the
cavities, contact angle and the amount of entrapped

gas or vapor. Consequently, surfaces with different
surface characteristics will have different "starting"
superheat temperatures. The heat flux starts deviating
from the values corresponding to natural convection when
few of these active bubble centers appear. If the heat
flux density is increased again, the superheat temper-
ature increases (though at a lower rate than in natural
convection), and the active bubbling sites become centers
of patches of more violent boiling. Courty and Foust
observed that, in nucleate, patchwise boiling, wide
variations occur in the temperature of the surface. The
areas covered with bubbles are considerably cooler than
the bubble-free areas. Also, widely varying temperature
readings were recorded by thermocouples located in the
surface. The magnitude of these fluctuations were,
however, not reported. Since the original bubbling
centers are located at random, the patches of active
boiling are also randomly distributed.

Courty and Foust discussed two processes by which
patchwise boiling can be established around an active
nucleating center. The first is a pressure fluctuation
mechanism, and the second is a vapor trapping process.
The pressure fluctuation mechanism bears similarity to
cavitation. During the bubble growth the liquid is
pushed away from the nucleating center; after the

departure of the bubble, the liquid rushes back. These oscillations of the fluid and the possible vortex formation with attendant pressure variations can induce nucleation.

The second mechanism is a vapor-trapping process. Suppose that in the vicinity of the active center are cavities which are, originally, filled with liquid. The bubble growing from the active nucleus may blanket some of these neighboring cavities. After the bubble breaks off, the liquid advances over the area which was covered by vapor and may trap some vapor in the neighboring capillaries. If the heating rate is sufficiently high and the rate of penetration of the advancing liquid comparatively slow, the liquid may become superheated before it refills the capillary. Under these conditions the neighboring capillaries may in turn become active nucleating centers. It is seen that this process depends upon the dimensions of the capillaries as well as upon two rates, the rate of heating the liquid and the rate of penetration of the liquid into cavities. This problem was analyzed recently by Bankoff (18).

The process of seeding, i.e., of activating cavities around the original active nucleating center, will continue until, depending upon the heating rate, the original nucleus can co-exist independently with

another nucleus. The intermediately located nucleating centers will be starved out. Such starving of a nucleus by a new active cavity was described recently by Clark, Strenge and Westwater (10). At a given heat flux density the spreading of boiling patches will cease when there are no cavities, within the range of activation, that can support a new bubble column at the prevailing heating rate and superheat temperature, $T_w - T_s$.

If the heat flux density is increased again, the temperature of the non-bubbling, ie., the bare area which surrounds the boiling patch, increases. Consequently, within the range of activation new, smaller cavities (which require higher superheats) can be activated and at the higher heating rates additional bubble columns can be maintained. This spreading mechanism continues with increasing heat flux densities until the whole area is populated with nucleating centers, i.e., with bubble columns.

Two important facts should be stressed now. It was observed already that the superheat temperature difference, $T_w - T_s$, at which bubbling starts depends upon the conditions of the surface. Different "starting" superheats are needed for different cavities. It was noted also that when boiling occurs in patches, the increase of superheat temperature which follows an

increase of the heat flux density depends on the size

distribution of cavities. Different superheat temper-

atures are needed to activate new nucleating centers.

Thus in nucleate boiling, at moderate heating rates at

least, the rate of increase of the superheat temperature

$T_w - T_s$, with an increase of the heat flux density

depends upon the characteristics of the surface. This

is shown on Figure I-6 which is reproduced from the

paper by Courty and Foust. It is seen that different

"starting" superheat temperatures, different nucleate

boiling curves with different slopes can be obtained

with the same metal surface having different roughness

characteristics. Thus, the heat flux density is not a

single valued function of the temperature. In order to

determine the relation between the heat flux and the

temperature, the characteristics of the surface must be

specified.

The question which arises - whether this dependence

upon the surface roughness is a characteristic of the

entire nucleate boiling curve - is not resolved yet.

Experimental results of Jakob (3) and of Averin (28)

indicate that, for water at atmospheric pressure,

nucleate boiling curves for surfaces of different

roughness merge when the heat flux density reaches a

value of 150,000 to 200,000 kcal/m^2hr. Note that the
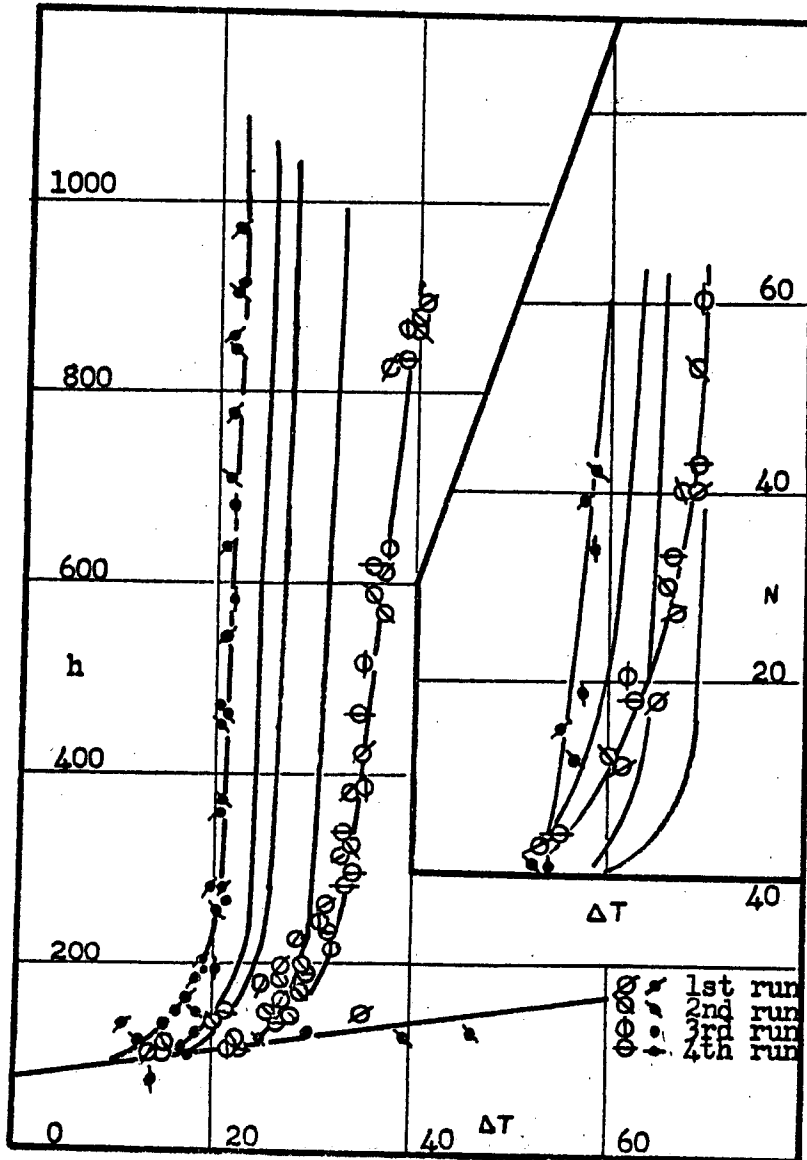
FIGURE I-6. THE EFFECT OF DIFFERENT AMOUNTS OF
ROUGHNESS ON THE HEAT TRANSFER IN NUCLEATE BOILING
($h = q/\Delta T$, BTU/HR FT^2°F; N = BUBBLES/IN^2).
THIS FIGURE IS REPRODUCED FROM THE PAPER BY CLAUDE
CORTY AND ALLAN S. FOUST (13, 14).

critical heat flux is 10^6 kcal/m^{2}hr. The dependence of the nucleate boiling curve upon the surface roughness can be expected to manifest itself in the low flux region because boiling in patches occurs at lower heat flux densities. The merging of the nucleate boiling curves could be interpreted then as a change in the boiling process, i.e., the termination of boiling in patches. A large number of active nucleating centers would tend to decrease the effects of different surface roughness. It was discussed in the preceding section that with increasing heat transfer rates bubbles change from simple to multiple, and the bubble generation changes from an intermittent to a continuous process. It is possible that with the spreading and the subsequent disappearance of boiling patches a gradual change in the bubble types and in the bubble generation mechanism takes place over most of the surface area. Such a change, together with the termination of boiling in patches, could account for the change in the boiling process.

It appears also that the effect of the surface roughness disappears for surfaces which have "aged", i.e., from which boiling was maintained over a period of a week or so. The experiments of Jakob and Linke (4) and of Zysina-Molozhen (29) indicated that both the superheat temperature difference, $T_w - T_s$, and the

number of nucleating centers, n , approach a limit value
with prolonged boiling. These limiting values were
independent of the original roughness, but dependent
upon the metal of the heating surface. Zysina-Molozhen
noted that the number of nucleating centers and,
therefore, the superheat temperature, become constant
(for a given surface) once a stable oxide film has
formed. She made the following observation: "Evidently
the factor controlling the numerical value of the heat
transfer coefficient in ordinary heating surfaces is
the thermal conductivity of the oxide film, which makes
it impossible to determine the true value of the heat
transfer coefficient." Note that her statement implies
the uncertainty of determining the superheat temperature
$T_W - T_s$, for a given heat flux density. We shall return,
in Chapter III, to discuss this effect in connection
with the coupling of the thermal properties of the solid
and liquid during the transient temperature oscillations
which occur in boiling. In the following we shall sum-
marize the discussion of this section.

1) The superheat temperature difference, $T_W - T_s$,
at which nucleate boiling sets in depends upon
the characteristics of the surface and upon
the amount of gas and vapor which is entrapped
in cavities. The first nucleating centers are

located at random.

2) At low heat transfer rates boiling takes place in patches which are located around the first nucleating centers.

3) During this non-uniform, patchwise boiling spatial and time variations occur in the temperature of the surface.

4) In the boiling patches, growing and departing bubbles strongly agitate the superheated film; colder fluid is brought in contact with the heating surface resulting in high heat transfer rates.

5) With an increase of the heat flux density, the superheat temperature, $T_w - T_s$, increases so as to alter the number of nucleating sites. The increase of active cavities and, therefore, of the superheat, is such that the agitation of the superheated film due to all bubble columns can accommodate the new heat flux.

6) In nucleate boiling, at moderate heat transfer rates at least, the heat flux is not a single-valued function of the temperature. In order to determine the relation between the heat transfer rate and the temperature of the surface, the characteristics of the surface

must be specified.

7) It appears that, at higher heat flux densities,
    the effect of the surface roughness upon the
    $q - \Delta T$ relation vanishes, indicating a more
    uniform boiling (disappearance of patches)
    with a possible change in the types of bubbles
    and in the bubble generation process (from
    intermittent to continuous).

8) It appears also that the effect of the surface
    roughness on nucleate boiling disappears once
    a stable oxide film coats the surface. Under
    these circumstances it appears that the
    thermal conductivity of the oxide film becomes
    the controlling factor.

In this part of the dissertation we have discussed
the results of analytical and experimental investigations
which pertain to the nucleation process, to the hydro-
dynamics of bubbles departing from surface and to the
effects of surface roughness. We shall proceed, in
Chapter II, with the problem of bubble growth.

CHAPTER II

THE PROBLEM OF BUBBLE GROWTH

II-1. The Dynamics of Vapor Bubbles in a Uniform

Temperature Field - Historical Background

The growth of a bubble in a superheated liquid
was first analyzed by Bosnjakovic (30). According to
his theory the vaporization process is maintained by an
energy transfer from the superheated liquid to the
bubble interface. The temperature drop which maintains
this process is localized in a thin boundary layer which
surrounds the bubble. This model is shown on Figure II-1.
A relation between the bubble growth rate, the temperature
drop and the heat transfer coefficients is obtained from
an energy balance, thus

$$h \, (T_o - T_s) \; = \; L \, \rho_v \, \frac{dR}{dt} \qquad\qquad \text{II-1}$$

The theory of Bosnjakovic was tested experimentally
by Jakob and co-workers (2, 3, 4, 5), Prüger (31) and
Fritz and Ende (24); good agreement was reported. In
the discussion of their experimental results Fritz and
Ende noted that, for a liquid which is initially uniformly

34

$$\frac{dR}{dt}$$

$$\frac{dR}{dt}$$

Vapor

R

T_s

δ = thickness of the thin boundary layer

$T_o - T_s$ = temperature drop across δ

$$q = h(T_o - T_s) =$$
$$= L \rho_v \frac{dR}{dt}$$

$$\frac{dR}{dt}$$

Liquid at temperature: T_o
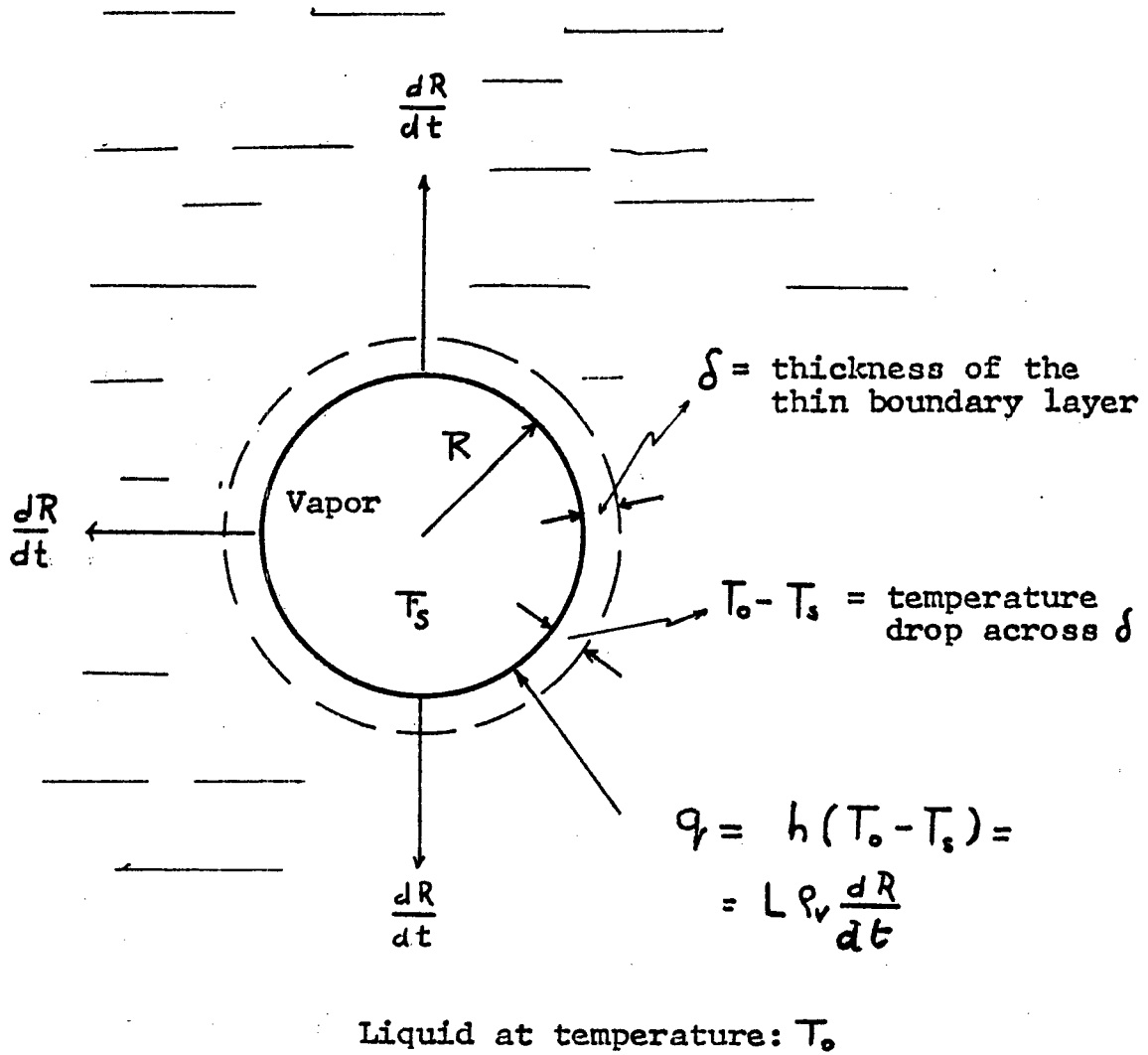
Figure II-1. Bosnajakovic's Analytical Model of
a Bubble Growing in a Uniformly
Superheated Liquid

superheated, the bubble growth problem was similar to the one dimensional, transient heat conduction problem, i.e., to

$$a \frac{\partial^2 T}{\partial x^2} = \frac{\partial T}{\partial t}$$

$$t = 0 \; : \; T(x, 0) = T_o - T_s$$

$$t > 0 \; : \; T(0, t) = 0 \qquad\qquad \text{II-2}$$

The heat transfer coefficient for a growing bubble can be obtained from the gradient at the bubble wall (x = 0), thus

$$h (T_o - T_s) = \kappa \left(\frac{\partial T}{\partial x} \right)_{x=0} \qquad \text{II-3}$$

The temperature gradient is obtained by solving Equation II-2, thus

$$\left(\frac{\partial T}{\partial x} \right)_{x=0} = \frac{T_o - T_s}{\sqrt{\pi a t}} \qquad \text{II-4}$$

Substituting Equation II-3 and II-4 into Equation II-1, the bubble growth rate is given by

$$L \rho_v \frac{dR}{dt} = \kappa \frac{T_o - T_s}{\sqrt{\pi a t}} \qquad \text{II-5}$$

Using high speed movies Fritz and Ende determined the bubble growth velocity, and from Equation II-1 computed the heat transfer coefficient. This value was then

compared to the value computed from Equations II-1 and II-4; the two values of h, thus determined, were found to be in good agreement with each other.

At first this agreement could appear as fortuitous. The real bubble is spherical; its interface represents a moving boundary whereas the system described by Equation II-2 represents a semi-infinite slab with stationary boundary. Also, the effects of liquid inertia and of surface tension were neglected in the analysis. Nevertheless, subsequent more detailed studies of the bubble growth problem only corroborated the theory of Bosnjakovic and the analysis of Jakob, Fritz and Ende which contains the essential feature of the phenomenon.

The first mathematical formulation which took into account the effects of liquid inertia, surface tension, sphericity and of the moving boundary is due to Plesset and Zwick (32, 33) and to Romie (34). The problem is formulated by considering Rayleigh's equation of motion:

$$ R \ddot{R} + \frac{3}{2} \dot{R}^2 + \frac{2\sigma}{\rho_L R} = \frac{P_v(t) - P_s}{\rho_L} \qquad \text{II-6} $$

Clausius-Clapeyron's equation:

$$\frac{P_v(t) - P_s}{T_v(t) - T_s} = \frac{L \rho_v \rho_L}{T(\rho_L - \rho_v)} \qquad \text{II-7}$$

and the energy equation:

$$a\left[\frac{\partial^2 T}{\partial r^2} + \frac{2}{r}\frac{\partial T}{\partial r}\right] = \frac{\partial T}{\partial t} + \frac{\partial T}{\partial r}\dot{r}$$

$$t = 0 : \quad T(r,0) = T_0 - T_s \qquad \text{II-8}$$

$$t > 0 : \quad \kappa\left(\frac{\partial T}{\partial r}\right)_{r = R(t)} = L\rho_v \dot{R}$$

$$T(\infty, t) = T_0 - T_s$$

The problem was analyzed in References 32, 33 and in 34, 35. The results of these studies were in agreement with each other and with experimental data reported by Dergarabedian (36). It was found that during the growth of a bubble the effect of liquid inertia and of surface tension are not important. Consequently, the growth of a vapor bubble is governed by the heat transfer process. Plesset and Zwick derived the following expression for the bubble growth rate

$$L\rho_v \dot{R} = \sqrt{3}\ \kappa \frac{T_0 - T_s}{\sqrt{\pi a t}} \qquad \text{II-9}$$

Whereas Forster and Zuber obtained

$$L \rho_v \overset{\bullet}{R} = \frac{\pi}{2} \kappa \frac{T_o - T_s}{\sqrt{\pi a t}} \qquad \text{II-10}$$

It should be noted that, in both of these studies, the assumption was made that the temperature drop is localized in a "thin boundary layer" near the bubble wall. Thus, the "thermal boundary layer" assumption of Bosnjakovic was reintroduced in the problem.

Recently, Birkhoff, Margulies and Horning (37) and Scriven (38) solved the energy problem (Equation II-8) without making recourse to the "thin boundary layer" approximation. It was shown that this assumption is valid when the Jakob number* is large, that is when:

$$J_a \overset{\triangle}{=} \frac{(T_o - T_s) c \rho_L}{L \rho_v} \gg 1 \qquad \text{II-11}$$

It was found also, that for large Jakob numbers the bubble growth rate is given by Equation II-9.

---

* This dimensionless group was recently proposed by Savic (39) to be referred to as the "Jakob Number" in honor of the late Professor Max Jakob.

Comparing Equation II-9 and II-10 with Equation II-5 it is seen that, apart from a numerical constant, these equations are identical. A larger growth rate could have been expected for spherical bubbles than for a plane interface because the temperature gradient at a spherical surface is given by (40)

$$\left(\frac{\partial T}{\partial r}\right)_{r=R} = (T_o - T_s)\left[\frac{1}{\sqrt{\pi a t}} + \frac{1}{R}\right] \qquad \text{II-12}$$

It follows for Equation II-4 and II-12 that the plane approximation is valid when

$$\frac{\sqrt{\pi a t}}{R} \ll 1 \qquad \text{II-13}$$

It is important to note that, for growing vapor bubbles, Equation II-9 and Equation II-10 indicate that the effect of sphericity is only to increase the gradient by a constant factor whose value lies between 1 and $\sqrt{3}$, with $\pi/2$ an intermediate value.

We can conclude this section by noting that for a growing vapor bubble the effects of liquid inertia and surface tension are not important. The growth rate, i.e., the rate of evaporation is given by an equation of the form:

$$L \rho_v \dot{R} = b \kappa \frac{T_0 - \bar{T_s}}{\sqrt{\pi a t}} \qquad \text{II-14}$$

Where the value of the constant is $b = 1$ for "plane" bubbles, or $b = \pi/2$ or $\sqrt{3}$ when correcting for the curvature. The mathematical formulation originally given by Fritz and Ende, and the theory of Bosnjakovic and Jakob contain, therefore, the essential feature of the phenomenon. In the next section we shall extend the theory of Bosnjakovic and Jakob to include the effect of a non-uniform temperature field.

II-2. The Growth of a Vapor Bubble in a Non-Uniform Temperature Field

In 1932 Jakob (3) described the heat transfer process which occurs at the interface of a bubble growing on a heated surface as follows: "It can be imagined that during the small explosion which starts the growth of a bubble, the interface temperature, because of the heat of vaporization, drops immediately from the superheat temperature to the saturation temperature, for example from 110°C to 100°C . . . As a consequence of the heat transfer from the liquid to the vapor bubble the liquid envelope is being cooled progressively from the inside toward the outer boundary; a temperature

boundary layer is created with a constantly decreasing temperature drop. This thermal boundary increases in thickness until the thermal wave, which advances from the vapor bubble interface into the liquid, has reached the outer limit of the hydrodynamic boundary layer. The decrease in thickness of the hydrodynamic boundary layer because of the evaporation at the interface is, initially, a small fraction of the total thickness." This model is shown on Figure II-2.

It is important to point out now the difference between the growth of a bubble in a uniformly superheated liquid and the growth in a non-uniform temperature field. In a uniformly superheated liquid (see Figure II-1) the thickness of the thermal boundary layer δ, constantly increases; however, since the liquid was initially at a uniform temperature T_o, the total temperature difference $T_o - T_s$, across the thermal boundary remains constant. In a non-uniform temperature field (see Figure II-2) the thickness of the thermal boundary layer δ, also increases as the thermal waves advance into the liquid. However, in this case, since the initial temperature in the liquid was not uniform, the temperature drop across the thermal boundary layer δ, constantly decreases as δ increases. In other words, whereas in a uniform thermal field only one heat transfer process occurs,

Initial temperature distribution in the hydrodynamic boundary layer.
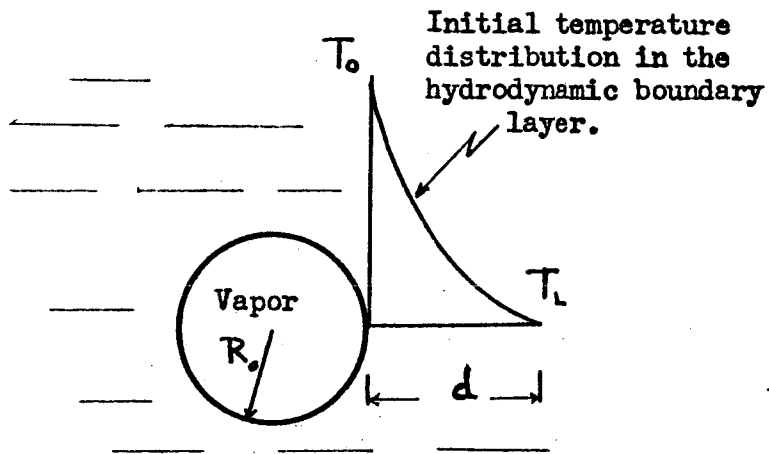
d = thickness of the hydrodynamic boundary layer

R_o = initial radius

δ = Thickness of the thermal boundary layer, i.e., of the distance travelled by the heat wave.

FIGURE II-2.a.   INITIAL TEMPERATURE
              DISTRIBUTION

FIGURE II-2.b.   TEMPERATURE DISTRIBUTION FOR
              A GROWING BUBBLE

FIGURE II-2.   JAKOB'S ANALYTICAL MODEL OF A BUBBLE GROWING
              IN A NON-UNIFORM TEMPERATURE FIELD

43

in a non-uniform temperature field two transfers of energy take place. One is the heat transfer across the film δ ; this process maintains the evaporation at the bubble interface. The second is the heat transfer to the bulk liquid.

The theory of Bosnjakovic and Jakob can be extended to include the effect of the non-uniform temperature by making an energy balance per unit transfer area. For a plane bubble the rate of evaporation is then given by:

$$L \rho_v \mathring{R} = K \frac{T_0 - T_s}{\sqrt{\pi a t}} - q_b \qquad \text{II-15}$$

where the second term on the right hand side is the heat transfer rate to the bulk liquid. For a uniformly superheated liquid $q_b = 0$ and Equation II-15 becomes Equation II-5. In view of the results which were discussed in the previous section it can be expected that a correction for the curvature can be made by multiplying the right hand side of Equation II-15 by b= $\pi/2$, thus

$$L \rho_v \mathring{R} = b \left[K \frac{T_0 - T_s}{\sqrt{\pi a t}} - q_b \right] \qquad \text{II-16}$$

with b=1 or b = $\pi/2$. The bubble radius is then given
by

$$R = b \frac{2}{\pi} \frac{\Delta T c \rho_L}{L \rho_v}\left[1 - \frac{q_b}{\kappa \Delta T} \frac{\sqrt{\pi a t}}{2}\right] \sqrt{\pi a t} \quad \text{II-17}$$

In order to make use of Equation II-17 we must
determine the heat flux q_b , to the bulk liquid.
Consider an instant just prior to the nucleation of a
bubble. A temperature gradient exists in the liquid
adjacent to the heating surface. It is this gradient
which transfers the energy from the solid wall to the
liquid. Consider now the instant just after the nucle-
ation of a plane bubble. The effect of introducing,
locally, the vapor phase between the solid and the liquid
is to insulate, locally, the liquid from the heating
solid. Assuming that no great distortions and dis-
turbances occur in the liquid during this transition
instant, the temperature gradient between the vapor
interface and the liquid is approximately equal to the
gradient which existed between the solid wall and the
liquid before the bubble was nucleated. In the sections
which follow we shall identify therefore, q_b with the
heat transfer rate from the heating surface, q . This
appears a rather drastic assumption; we shall justify

it a posteriori in the sections which follow after we examine the physical process in greater detail.

It is seen that Equation II-17 relates the bubble radius to the superheat temperature ($\Delta T = T_w - T_s$) and the heat flux which exist <u>locally</u> around a nucleating center. It was discussed in Chapter I that, in nucleate boiling at low heat flux density, both the temperature of the surface and the heat transfer rate vary over the heated area. The values which are usually reported are average values. It is known also from the experiments of Jakob and Linke (5), of Ellion (15) and of Treschov (41) that the diameters of bubbles departing from or collapsing on a heated surface follow a distribution curve. Therefore, if we introduce into Equation II-17 the average heat flux and superheat we can expect to predict only the growth of an average bubble and not of a specific bubble (unless it coincides with the average one) whose growth was recorded on a motion picture. Keeping this fact in mind we shall examine first the growth of a bubble in a liquid whose bulk is at saturation temperature.

II-3. The Bubble Growth in Liquids at Saturation
Temperature

In this section the bubble growth rate predicted
by Equation II-17 will be compared to experimental
results reported by Fritz and Ende (24) and by Zmola
(42). In Section I-3 the experiments of Jakob and
Linke (5) were discussed; in these experiments the
diameters of bubbles departing from a heated surface
varied between 1.5 mm and 4.5 mm with a maximum at
about D_d = 2.81 x 10^{-1} cm. Because Jakob and Linke
did not report the values of the superheat temperature
$T_w - T_s$, and the heat flux density q , Equation II-17
cannot be used for comparison with their results. This
can be done, however, with the data for water reported
by Fritz and Ende which is tabulated below.

TABLE II-1

Experimental Data of Fritz and Ende

Bubble Number	$\frac{q}{\frac{Kcal}{hrm^2}}$	$T_w - T_s$ °C	t_c sec	t_d sec	D_d cm
BM1	19000	.9	0.0225	0.023	5.42 x 10^{-1}
BM3	19000	9	0.0025	0.018	4.04 x 10^{-1}
BR8	19000	9	0.01675	0.020	4.64 x 10^{-1}

Inserting the above values of superheat temperature $T_w - T_s$, heat flux q, and time at departure t_d, into Equation II-17 the corresponding diameters at departure for two values of the constant b are given below.

TABLE II-2

Diameters at Departure Predicted

by Equation II-17

Bubble Number	D_d (cm) $b = 1$	D_d (cm) $b = \frac{\pi}{2}$
BM1	2.91×10^{-1}	4.58×10^{-1}
BM3	2.68×10^{-1}	4.18×10^{-1}
BR8	2.76×10^{-1}	4.33×10^{-1}

It is seen that the predicted values are in better agreement with experiments when the correction for the sphericity is taken into account. This could have been expected because for large bubbles the liquid laminae over the bubble are stretched thus increasing the temperature gradients. We note, however, that even if this correction was not included, the predicted values for the "plane" bubble, i.e., $b = 1$, are in agreement with the average value observed by Jakob and Linke, i.e., $D_d = 2.81 \times 10^{1}$ cm.

In order to investigate whether Equation II-17
is in agreement with experimental data over a longer
time interval we can compare it to the experimental
data reported by Zmola (42) and shown on Figure II-3.
For these experiments the heat flux was $q = 9.6 \times 10^3$
Btu/hr ft^2, and the superheat temperature $T_w - T_s = 9.4^{\circ}F$.
Inserting these values into Equation II-17, the pre-
dicted growth rate for $b = \pi/2$ is shown on Figure II-3
also.

To the writer's knowledge no other experimental
data for liquids at saturation are available in the
literature for further comparison. On the basis of
present results it appears that at atmospheric pressure,
at low heat flux densities, and for liquids at saturation
temperature, Equation II-17 with $b = \pi/2$ approximates
experimental data adequately.

The agreement of Equation II-17 with experimental
data indicates some areas for further investigation and
offers interesting possibilities. We shall discuss
some of them before proceeding with the analysis of
the growth and collapse of bubbles in subcooled liquids.
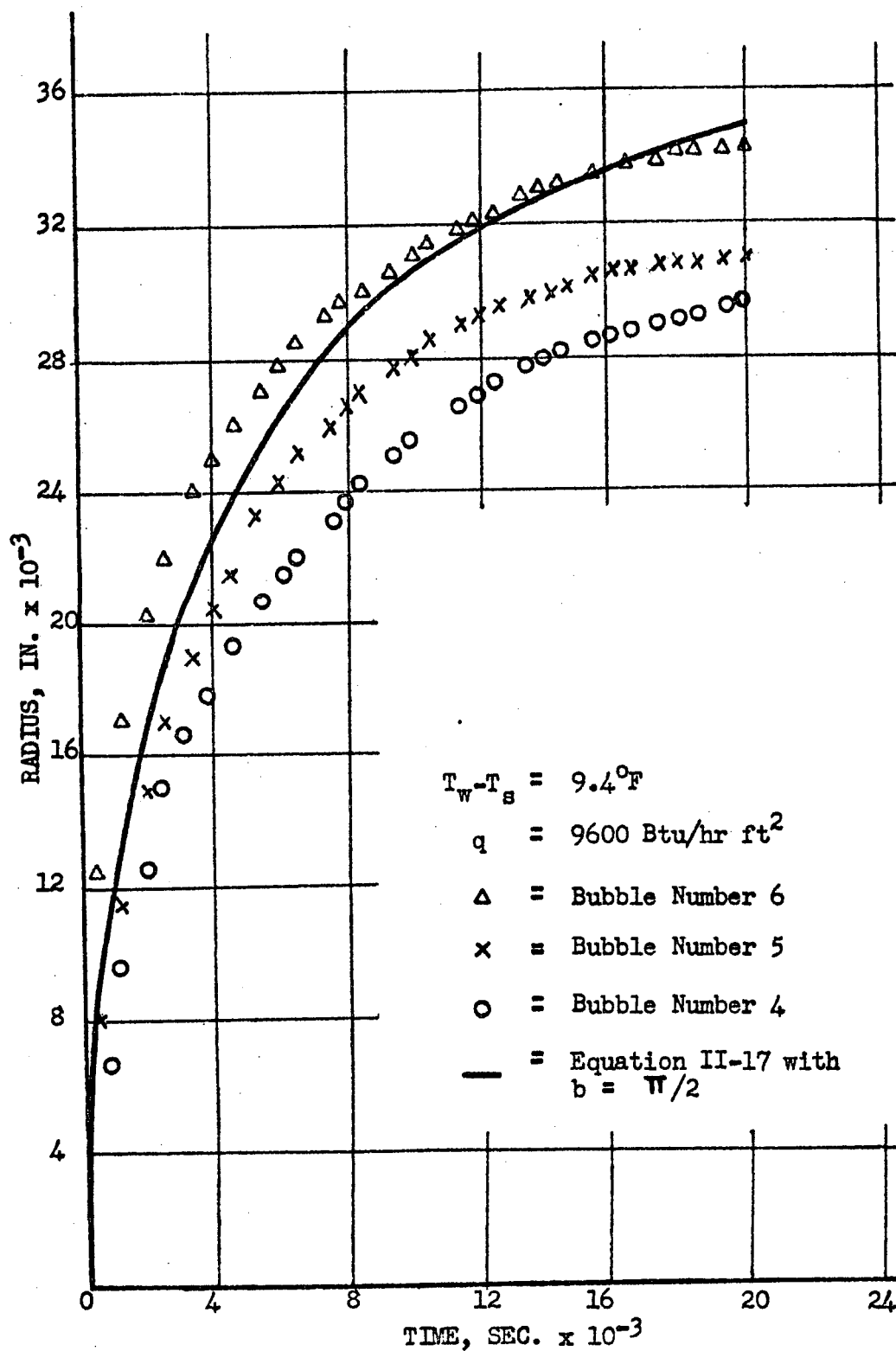
FIGURE II-3. COMPARISON OF EQUATION II-17 WITH ZMOLA'S (42) EXPERIMENTAL DATA FOR BUBBLES IN POOL BOILING OF WATER AT SATURATION TEMPERATURE

II-4. Maximum Bubble Diameter and the Thickness of the Superheated Liquid Film

It is seen from Equation II-16 that the bubble will stop growing when

$$\sqrt{\pi a t} = \frac{\kappa \Delta T}{q} \qquad \text{II-21}$$

That is, when the diffusion length becomes equal to the thickness X_s , of the superheated liquid film adjacent to the heating surface. The maximum bubble diameter is given then by

$$D_m = \frac{\Delta T c \rho_L}{L \rho_v} \frac{\kappa \Delta T}{q} \qquad \text{II-22}$$

which is equivalent to:

$$\frac{D_m}{X_s} = \frac{\Delta T c \rho_L}{L \rho_v} \qquad \text{II-23}$$

This is not surprising since it is in energy balance - nil novi sub sole. Consider a surface area A, and a liquid film of thickness X_s , adjacent to it. If this liquid film is superheated by ΔT degrees the internal energy of the liquid is given by: $A X_s \Delta T c \rho_L$. If all this stored energy is used for vaporization, the maximum distance the vapor front can advance is given by:

$$A \, D_m \, L \, \rho_v = A \, X_s \, \Delta T \, c \, \rho_L \qquad\qquad \text{II-24}$$

It follows from Equation II-23 that, in boiling, the significance of Jakob's number is that it represents the ratio of the maximum bubble radius to the thickness of the superheated liquid film.

For the experiments of Zmola, Equation II-23 predicts a maximum radius $R_m = 36.6 \times 10^{-3}$ in., which would be reached when $\overset{o}{R} = 0$. It is interesting to note that the growth curves on Figure II-3 show almost zero velocity at $t = 20 \times 10^{-3}$ sec.; indicating a deficiency of energy available to maintain the vaporization process.

II-5. The Thickness of the Superheated Liquid Film

The nucleation from a cavity was discussed in Section I-2; it was noted that the dimensions of a cavity is important in the nucleation process from a heated surface. The results of the previous section indicated the importance of the thickness of the superheated liquid film. Both the nucleation and the thickness of the superheated film affect the dynamics of a bubble. One is lead therefore to investigate whether or not a relation exists between the diameter $D_c = 2r_o$, of the

cavity and the thickness of the superheated film given
by

$$X_s = K \frac{T_w - T_s}{q} \qquad \text{II-26}$$

For the experiments of Griffith and Wallis (16) the
superheat which initiated boiling was: $T_w - T_s = 20°F$,
and the heat flux was q = 40,000 Btu/hr ft^2. Substi-
tuting these values into Equation II-26 the film
thickness becomes X_s = 2.39 x 10^{-3} in. The diameter of
the cavity in the experiments of Griffith and Wallis
was D_c = 2.7 x 10^{-3} in. Such a close agreement is rather
surprising. To explore further this relation the experi-
mental data for pentane and ether reported by Clark,
Strenge and Westwater (10) are reproduced on the fol-
lowing table together with the corresponding values of
X_s computed from Equation II-26. For some pits two
values of the superheat temperature were reported; the
second was the observed value whereas the first one was
corrected to smooth the data. The accuracy of the heat
flux density q, and of the superheat temperature $T_w - T_s$,
were not evaluated for these experiments.

TABLE II-3

Comparison of Computed Film Thickness with the Diameters

of Active Cavities in Westwater-Strenge's Experiments

Site	Diam or Width in.	ΔT °F	q Btu / hr ft^2	X_s in.
Pit				
1	0.0003	14	13400	0.0010
2	0.0003	50	8100	0.0057
3	0.00088	23-35	12300	0.0019-0.0029
4	0.0082	12	5400	0.0021
5	0.0018	11-19	2600	0.0040-0.0068
6	0.0018	23-35	12300	0.0017-0.0024
7	0.0020	22-30	13000	0.0017-0.0023
8	0.0022	23-35	12300	0.0018-0.0029
9	0.0022	27-42	15600	0.0017-0.0026
10	0.0023	14	4900	0.0026
11	0.0025	21-31	13200	0.0015-0.0022
12	0.0026	27-41	15600	0.0017-0.0025
13	0.0033	10	3400	0.0028
Scratch				
1	0.00008	50	8100	0.00058
2	0.00018	14	8900	0.0015
3	0.00044	23-35	12300	0.0017-0.0027
4	0.00075	13	17600	0.00069

It is seen from the above table that, with exception of Pits No. 1 and No. 2, the computed thickness X_s, appears to be of the same order as the diameters of active cavities D_c. For scratches such an agreement is not indicated.

A relation between D_c and X_s such as that indicated by these experiments offers interesting possibilities in an analysis of boiling heat transfer and initial

boiling transients. We shall note only one here.

Since the diameter of a cavity is a characteristic of the surface, a relation between D_c and X_s implies that for a given heat flux the local superheat temperature $T_w - T_s$, is determined by the diameter of the active cavity. In steady boiling at low heat transfer rates, a known distribution of cavities would permit then a derivation of an equation relating the average superheat temperature to the average heat flux.

In view of the indicated relation between the cavity diameter and the thickness of the superheated liquid film, and in view of the possibilities that this relation offers, it appears that further experimental and theoretical investigations are warranted.

II-6. Implications and Limitations of the Model

In this section will be discussed some implications and limitations of the extended Bosnjakovic-Jakob model. In order to bring these implications and limitations into focus we shall describe first the actual physical process. This brief description is based on an excellent discussion of the bubble growth problem given by Ellion (15).

A thin superheated liquid film with a steep temperature profile exists adjacent to the heating surface. Following the nucleation, the bubble starts

growing in this superheated liquid film. The bubble is, initially, hemispherical; it is probable that the bottom of the bubble is separated from the wall by a thin layer of liquid since the viscous and adhesion forces in the liquid prevent the bubble from wiping the wall clear of water and the evaporation rate may not be sufficiently large to evaporate any appreciable thickness of liquid at the bubble base. Ellion was not able to verify the existence of this thin film because of the limited resolution of the camera lens. In view of the presence of the nucleating cavity, the existence of a "dry" point appears probable also.

The superheated liquid film that was initially above the nucleating cavity is pushed away from the wall by the bubble, see Figure II-4. As the bubble grows, the film becomes stretched and this results in higher temperature gradients. Heat is removed from the displaced superheated film by conduction and convection to the bulk liquid and by evaporation at the bubble interface. Evaporation occurs also at the base of the bubble. The rate of evaporation and, consequently, the rate of growth decreases as the superheated film becomes cooler. As the bubble decelerates the momentum that was stored in the liquid and the buoyant force tend to pull the bubble away from the surface. Because
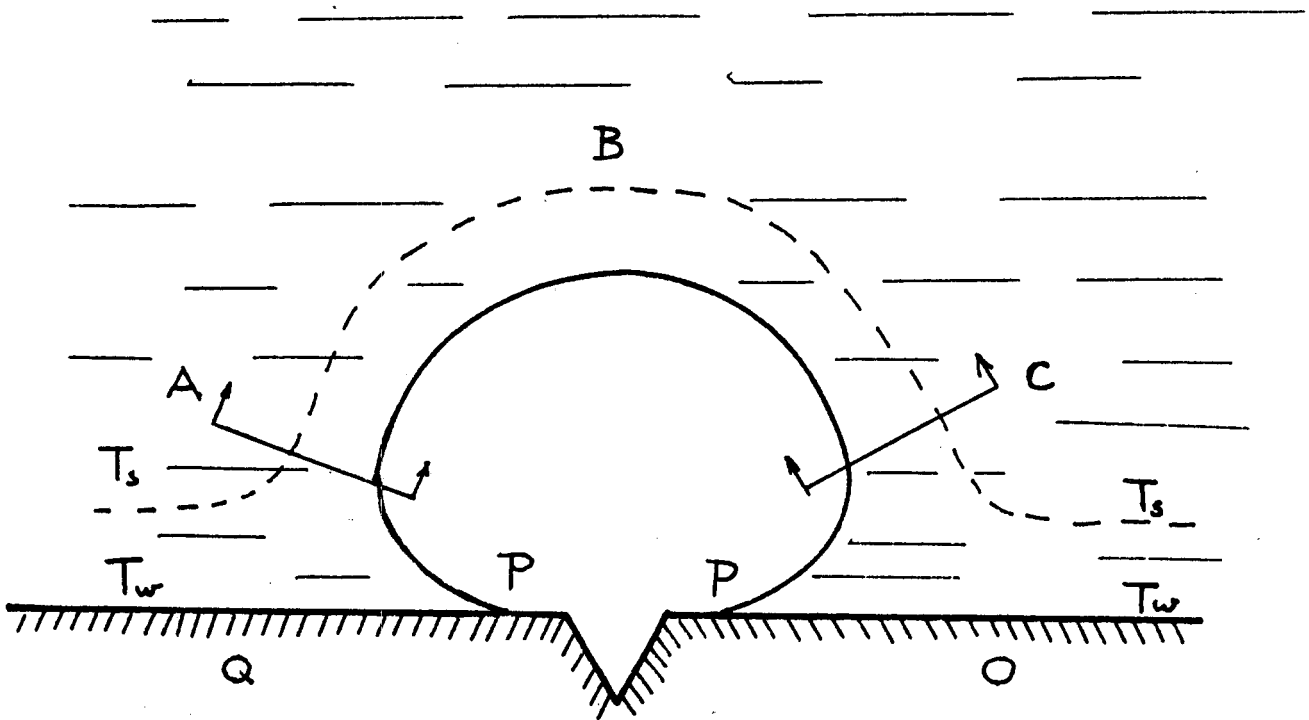
Figure II-4.   The Probable Bubble Form and
the Approximation of the Model

of the adhesion forces and the resistance to motion the
bubble becomes deformed. If the bulk liquid is at
saturation temperature the bubble will depart from the
surface; if it is subcooled the bubble will collapse.

It is seen from this brief description that a
complete analysis of the bubble growth problem on a
heated surface should take into account the hydrodynamic
aspect as well as the energy aspect of the problem.
Since the process takes place in such a vicinity of
the solid surface it is apparent that the viscous
effects of the liquid as well as the inertial should be
retained in the analysis. In addition, because of the
liquid-vapor interface and of the solid-liquid-vapor
interface, both the surface tension and the contact
angle become important. Because evaporation takes
place over the entire interface the energy equation
should take into account the transfer of energy from
the wall to the liquid and the interface in the regions
QAP and OCP, during the entire bubble lifetime. As a
consequence of this energy transfer the temperature
distribution in the solid in the region OPQ will not
be uniform. Thus, the problem involves two energy
equations, one for the solid and the second for the
liquid with a matching problem along an unknown moving
boundary.

In view of the complexity of the problem any agreement of predicted growth rates by the simple model with experimental data is rather surprising. It can be seen from Figure II-4 that the model considers only the energy transfer in the region ABC. The motion of the interface depends only on the amount of stored energy which existed originally in the superheated film.

The limitations of the model now become apparent. The model cannot take into account any temperature change due to heating after the growth has started, i.e., after the vapor has insulated locally the liquid from the solid. Since the regions QAP and OCP are not considered, the effect of additional heating during the growth process is not accounted for. We note, however, that it appears that this restriction could be removed; it will be discussed in a future report. Because the hydrodynamic effects were not considered, the effect of the distortion of the bubble on the temperature field is neglected.

It is seen from these limitations that if any agreement is to be expected the effect of evaporation in the regions QAP and OCP should be small when compared to the evaporation in the region ABC. To achieve this, two conditions must be satisfied. First, the transfer area in the regions QPA and OPC should be

small in comparison with the transfer area ABC. Second, the rate of vaporization in the region ABC should be fast so that any change of the temperature field in the regions QPA and OPC, caused by heating during the growth process is small. The effect of the bubble distortion on the process of vaporization in the region ABC will be small if the distortion occurs at the end of the growth process. In view of the agreement of predicted growth rates with experimental data it appears that either these conditions were satisfied, or that the effects of various assumptions tend to compensate each other.

Another important limitation should be noted before closing this section; it is concerned with the "thin thermal boundary layer" assumption. It was noted in Section II-1 that for a growing bubble this assumption is valid when the Jakob number is larger than unity. The assumption will be satisfied also for a collapsing bubble as long as the thickness of the thermal boundary layer is smaller than the bubble radius (see Figures II-1 and II-2). For sufficiently small radii, however, Equation II-12 indicates that an equation which is based on the "thin boundary" assumption will underestimate the collapse rate. This question appears to be important for bubble dynamics in subcooled liquids, a topic which

is taken up in the next section.

II-7. Dynamics of a Vapor Bubble in a Subcooled Liquid

Bubble dynamics in a subcooled liquid was investigated experimentally by Gunther and Kreith (7) and by Ellion (15) in a non-flow system, and by Gunther (43) and by Treshov (41) in a flow system. The problem was investigated also analytically be various researchers. The growth problem in a non-uniform temperature field was analyzed by Griffith (44) and by Savic (39). An analysis of a bubble growing and collapsing in a sub-cooled liquid was reported by Bankoff and Mikesell (45, 46). The time needed for a bubble to reach the maximum radius before collapsing was considered by Forster (47). The collapse of a bubble in a uniformly subcooled liquid was analyzed by Plesset and Zwick (48). The condensation rate of a vapor bubble which is introduced in a subcooled liquid was discussed by the writer (49). In the following, the growth and collapse rates predicted by the extended Bosnjakovic-Jakob model will be compared to the experimental results of Gunther and Kreith and of Ellion.

Ellion's experiments were performed with water at atmospheric pressure; Figures 47, 49, 53 and 57 from Ellion's dissertation are reproduced in this Chapter as Figures II-5, 6, 7 and 8. Figures II-5 and II-6

show the effect of increasing the heat flux density
from 5.29×10^5 Btu/hr ft^2 to 11.5×10^5 Btu/hr ft^2
at a constant bulk liquid temperature $T_L = 135^\circ$F, i.e.,
at a constant subcooling of $T_s - T_L = 77^\circ$F. Whereas
Figures II-7 and II-8 show the effect of increasing the
bulk liquid temperature from $T_L = 78^\circ$F ($T_s - T_L = 134^\circ$F),
to $T_L = 177^\circ$F ($T_s - T_L = 35^\circ$F), at a constant heat flux
density of 7.79×10^5 Btu/hr ft^2. It can be seen from
these figures that a given average heat flux and
average temperature variations occur in the dynamics
of different bubbles. Ellion noted that, because of
these large variations, an agreement closer than 25%
should not be expected. The large changes which are
indicated by these figures point to the importance of
local conditions which exist in the vicinity of a
nucleating center and, consequently, to the statistical
nature of the overall process when an ensemble of nucle-
ating centers, i.e., of bubbles, is considered.

We shall compare now the growth and collapse
rates predicted by Equation II-17 with Ellion's experi-
mental data. It is seen from Equation II-16 that the
maximum radius R_m is reached when,

FIGURE II-5. ELLION'S EXPERIMENTAL DATA (REFERENCE 15) FOR BUBBLES GROWING AND COLLAPSING IN SUBCOOLED WATER

$q = 5.29 \times 10^5$ Btu/hr ft^2, $T_L = 135°F$, $T_s - T_L = 77°F$
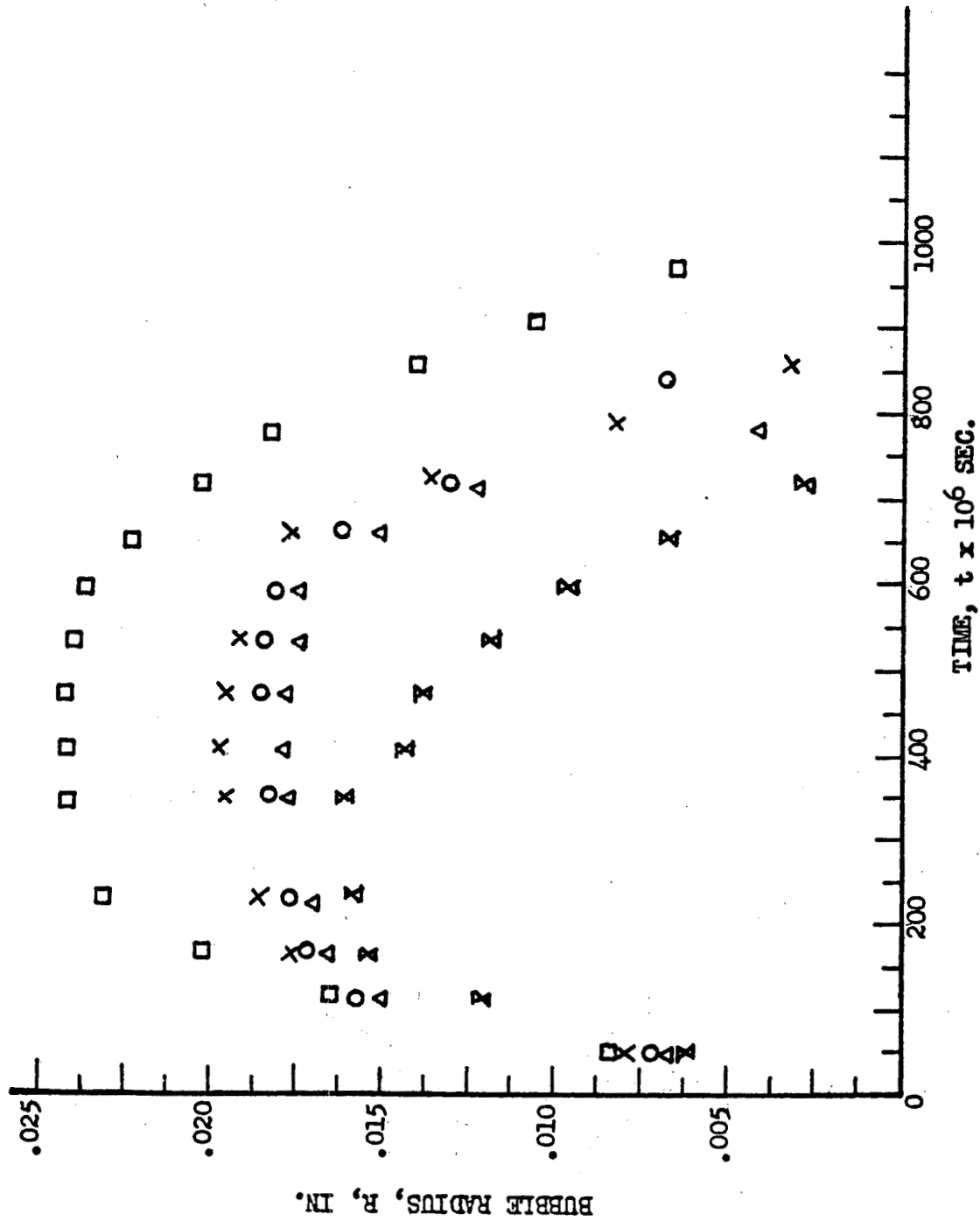
FIGURE II-6. ELLION'S EXPERIMENTAL DATA (REFERENCE 15)
FOR BUBBLES GROWING AND COLLAPSING IN SUBCOOLED WATER

$q = 11.5 \times 10^5$ Btu/hr ft^2, $T_L = 135°F$, $T_s - T_L = 77°F$
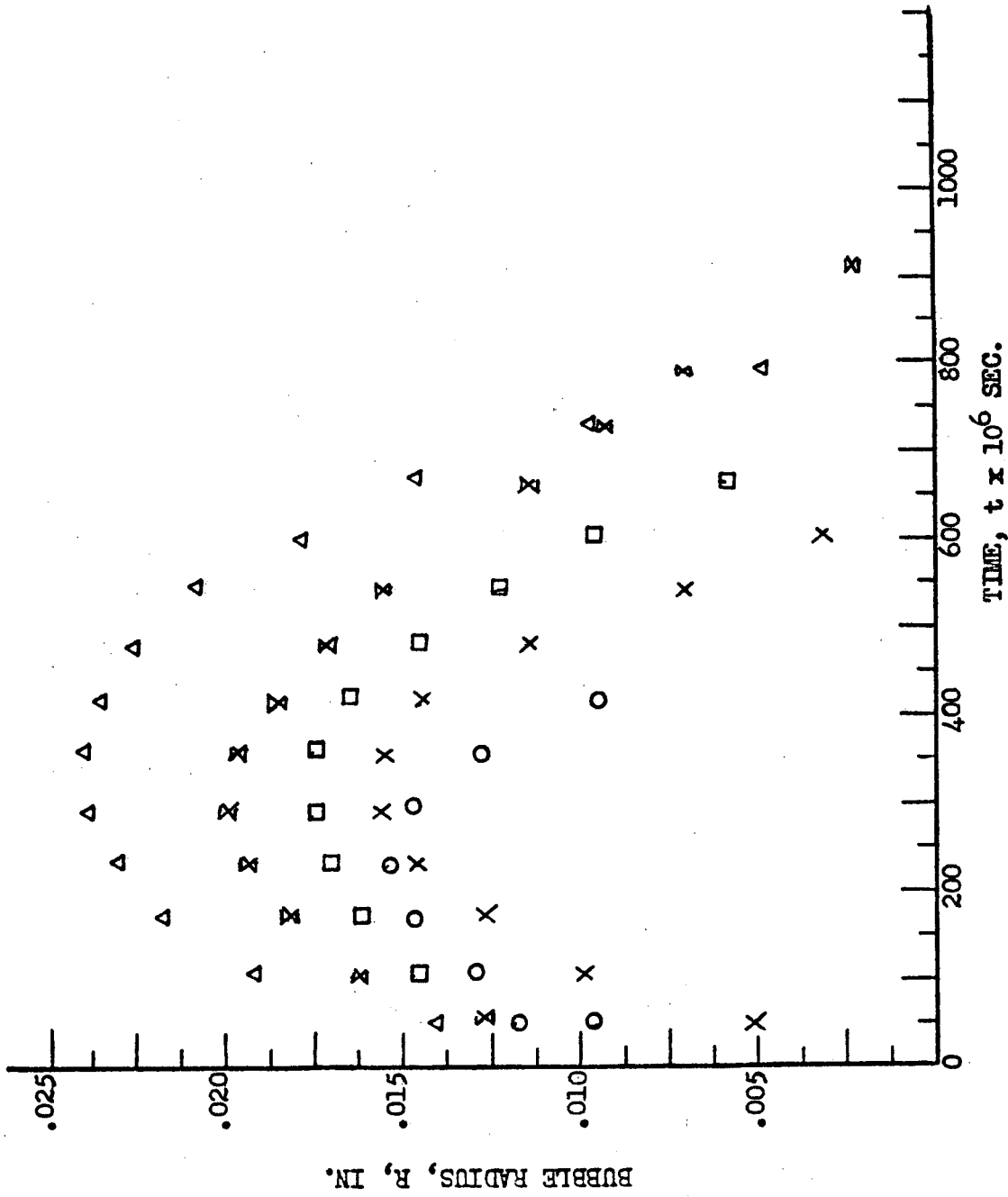
FIGURE II-7. ELLION'S EXPERIMENTAL DATA (REFERENCE 15)
FOR BUBBLES GROWING AND COLLAPSING IN SUBCOOLED WATER

$q = 7.79 \times 10^5$ Btu/hr ft^2, $T_L = 78^\circ F$, $T_s - T_L = 134^\circ F$

TIME, $t \times 10^6$ SEC.
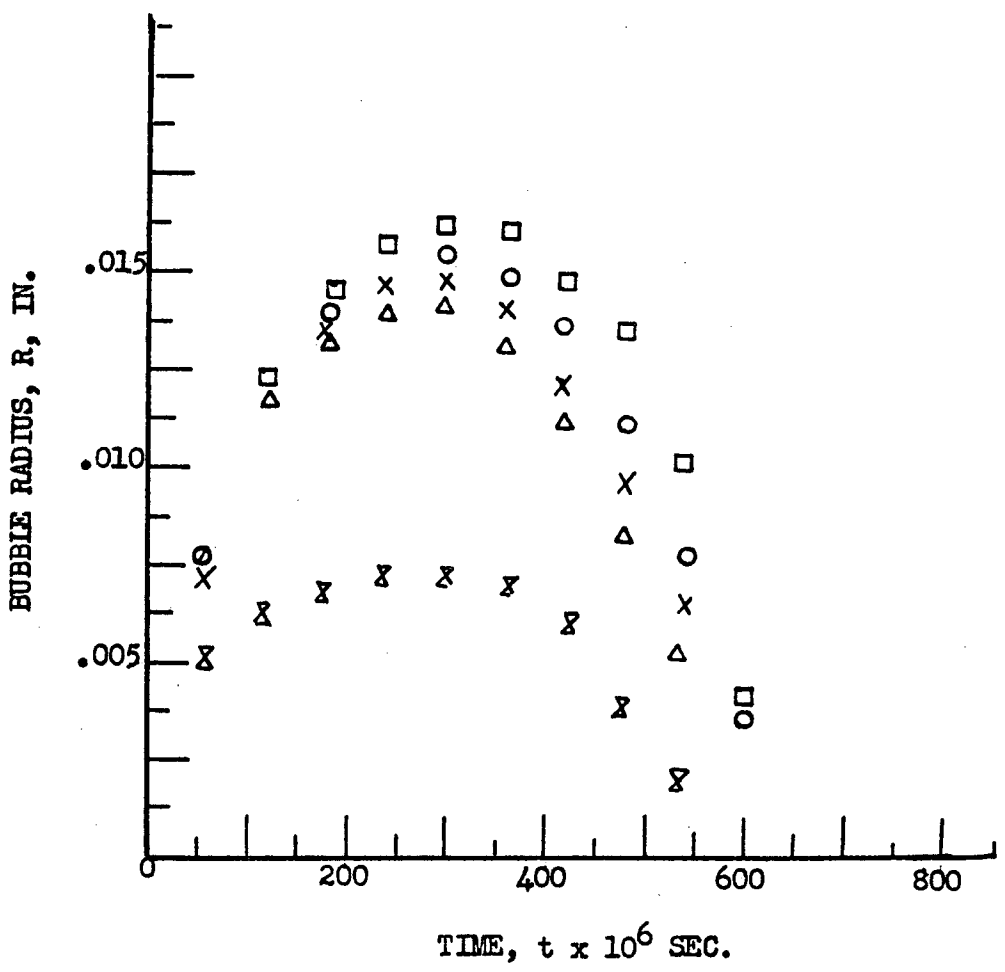
FIGURE II-8. ELLION'S EXPERIMENTAL DATA (REFERENCE 15)
FOR BUBBLES GROWING AND COLLAPSING IN SUBCOOLED WATER

$$q = 7.79 \times 10^5 \text{ Btu/hr ft}^2, \quad T_L = 177°F, \quad T_s-T_L = 35°F$$
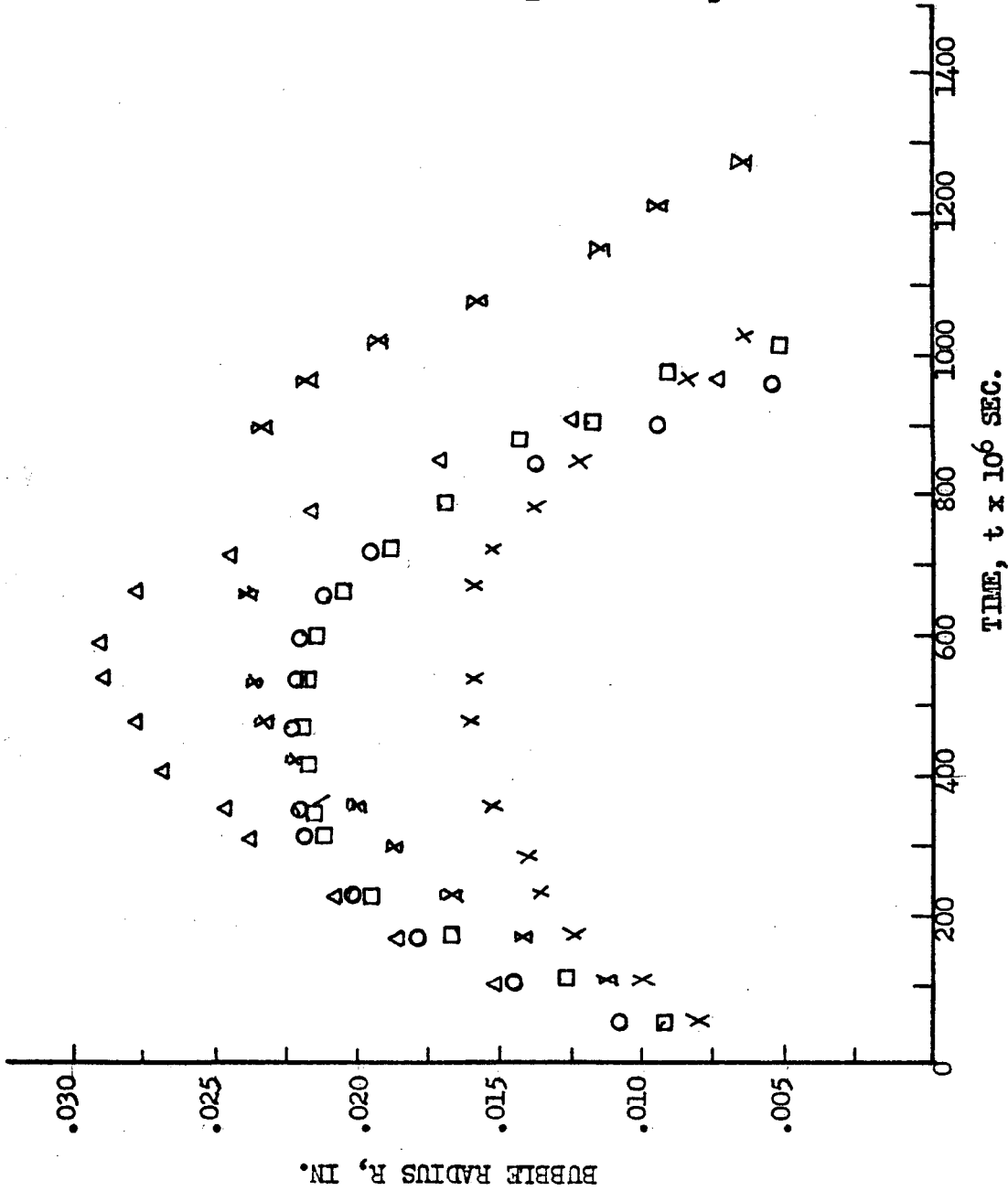
at

$$\sqrt{\pi a t_m} = k \frac{T_w - T_s}{q} \qquad \text{II-27}$$

The radius vs. time relation given by Equation II-17 can
be expressed in terms of the maximum growth time t_m, thus

$$R = b \frac{2}{\pi} \frac{(T_w - T_s) c \rho_L}{L \rho_v} \left[1 - \frac{1}{2} \sqrt{\frac{t}{t_m}} \right] \sqrt{\pi a t} \qquad \text{II-28}$$

The maximum bubble radius is then given by:

$$R_m = \frac{b}{\pi} \frac{(T_w - T_s) c \rho_L}{L \rho_v} \sqrt{\pi a t_m} \qquad \text{II-29}$$

It is advantageous to introduce a dimensionless radius
given by R/R_m and a dimensionless form is obtained from
Equation II-28 and II-29, thus

$$\frac{R}{R_m} = \sqrt{\frac{t}{t_m}} \left[2 - \sqrt{\frac{t}{t_m}} \right] \qquad \text{II-30}$$

Equation II-30 is plotted on Figures II-9, 10, 11 and 12
together with Ellion's data shown on Figures II-5, 6,
7, and 8 respectively. The advantage of normalizing the
data becomes apparent.
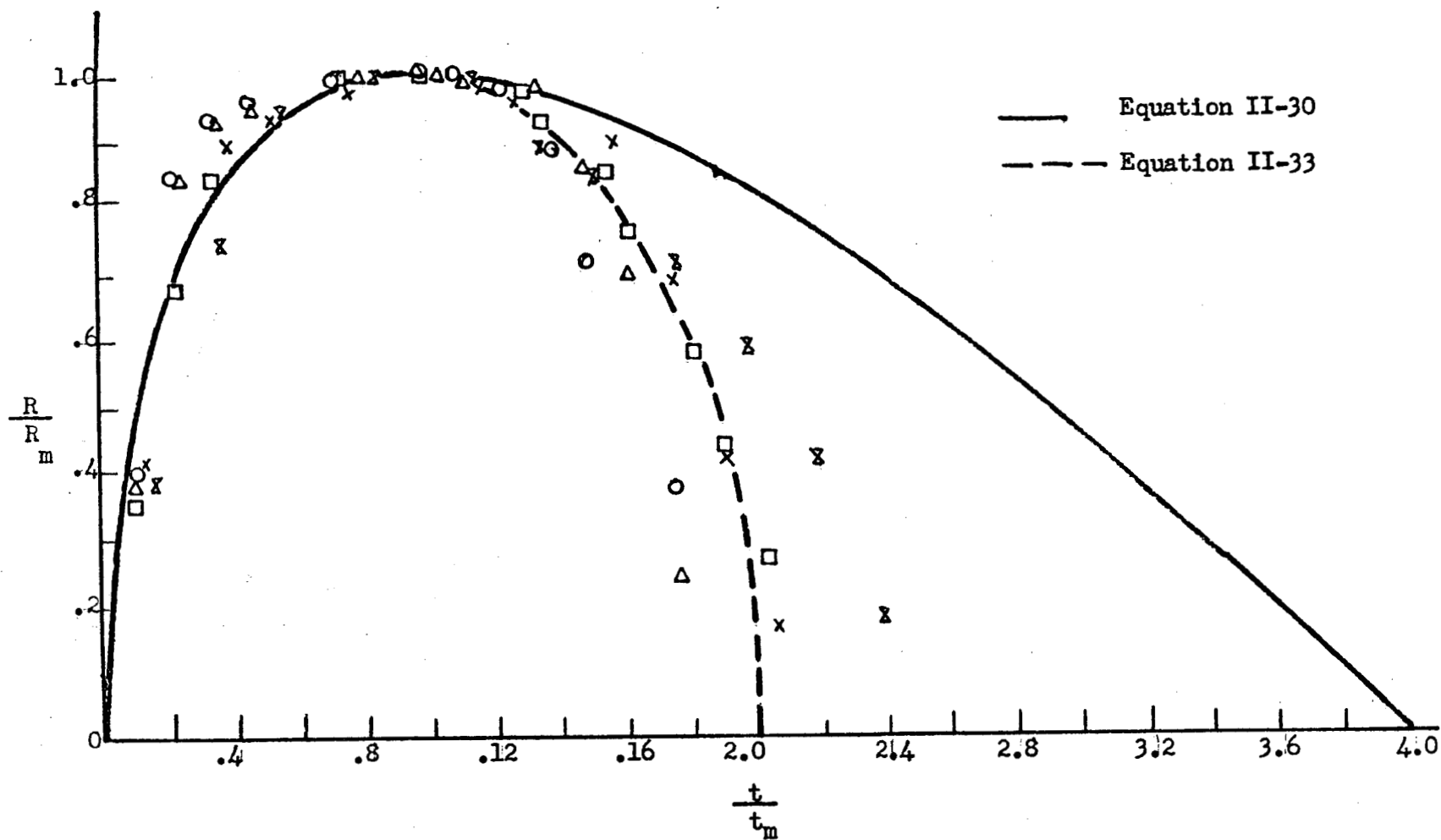
FIGURE II-9. COMPARISON OF EQUATION II-30 and II-33 WITH ELLION'S
EXPERIMENTAL DATA SHOWN ON FIGURE II-5
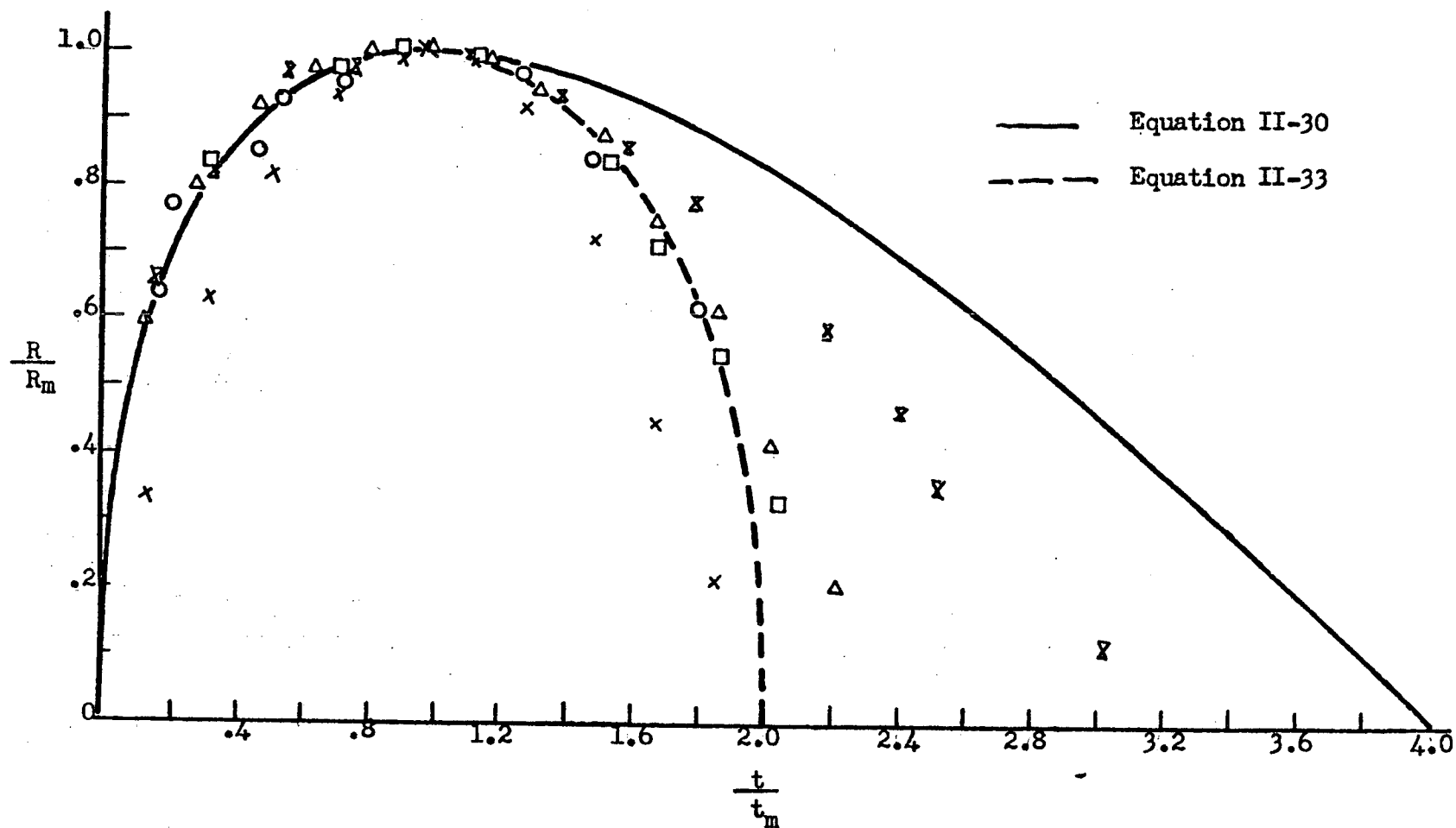
FIGURE II-10. COMPARISON OF EQUATION II-30 AND II-33 WITH ELLION'S
EXPERIMENTAL DATA SHOWN ON FIGURE II-6
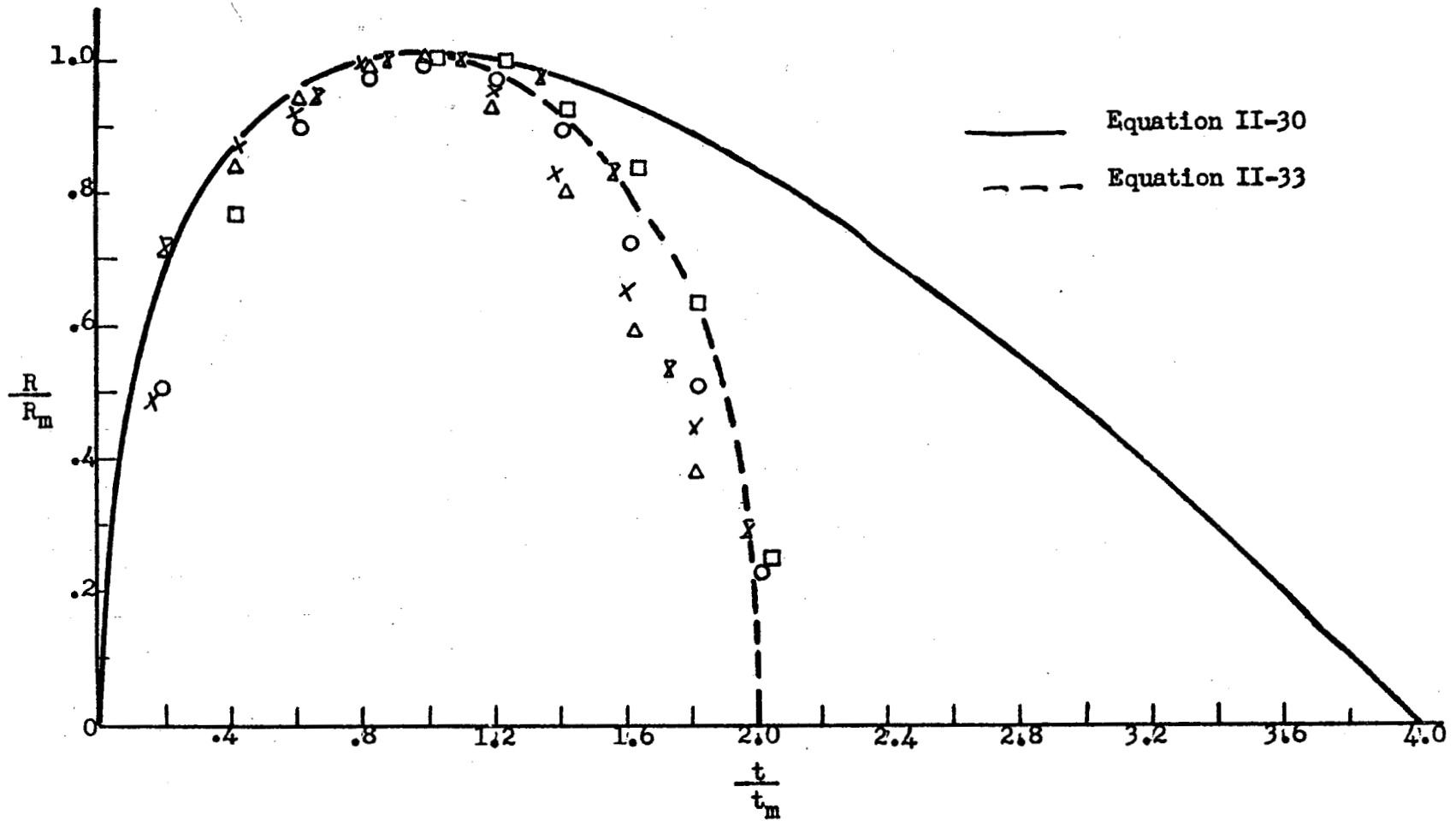
FIGURE II-11. COMPARISON OF EQUATION II-30 AND II-33 WITH ELLION'S
EXPERIMENTAL DATA SHOWN ON FIGURE II-7
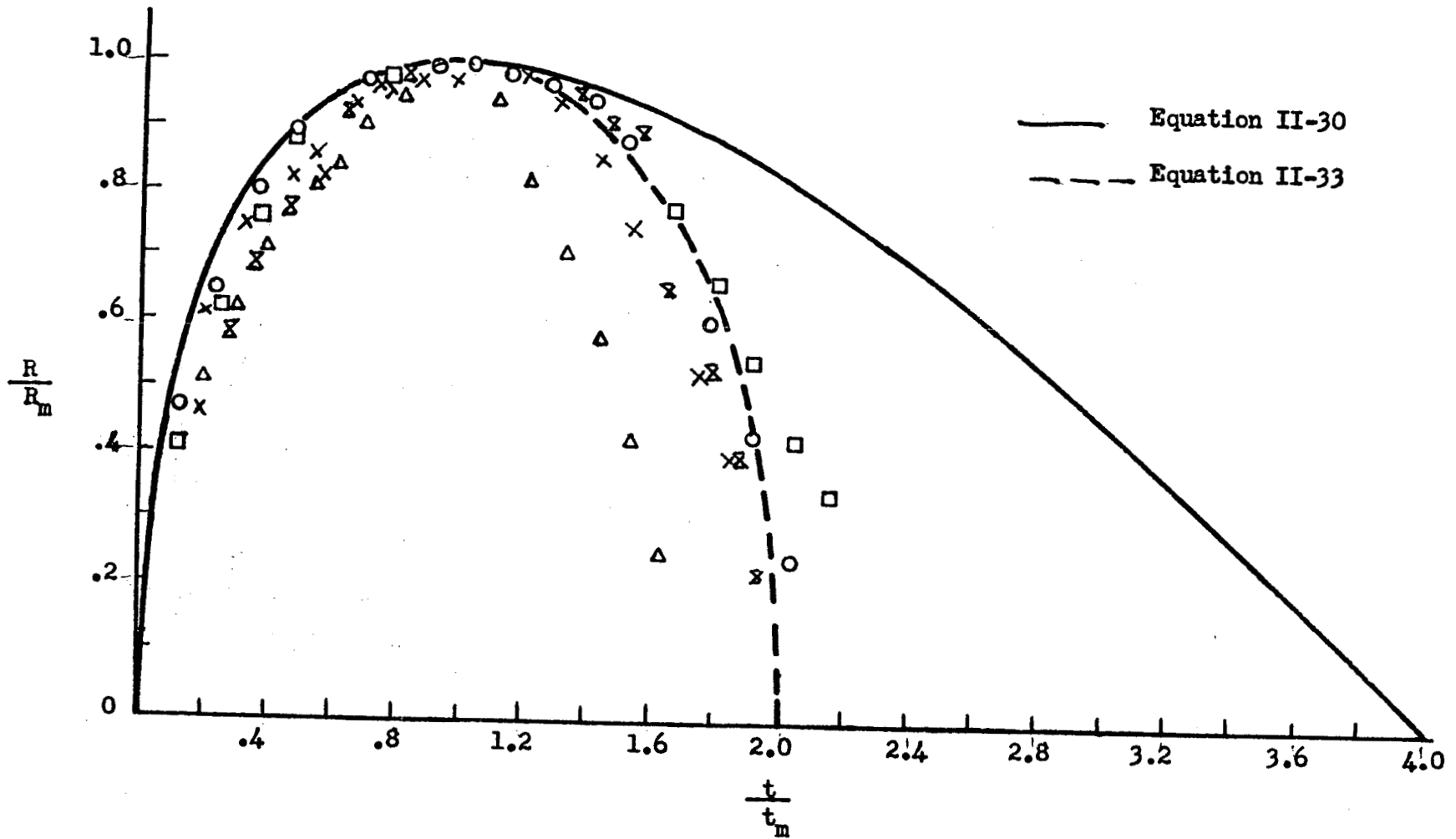
FIGURE II-12. COMPARISON OF EQUATION II-30 AND II-33 WITH ELLION'S
EXPERIMENTAL DATA SHOWN ON FIGURE II-8

It appears from these figures that Equation II-30
adequately approximates the growth process. It is seen,
also, that the model is not adequate for predicting the
collapse stage. The reason for this inadequacy can be
understood in terms of the discussion of the preceding
section.

The inertia of the liquid and the buoyant force
tend to pull the bubble away from the surface, causing
a deformation of the bubble after it reaches the maximum
radius. This deformation and motion of the bubble
increase the thermal gradients causing a faster conden-
sation. As the vapor condenses the thermal boundary
layer increases, whereas the radius decreases. Conse-
quently, the "thin boundary layer approximation"
becomes progressively worse. Because the curvature
increases with a decrease of radius, it is seen from
Equation II-12 that the thermal gradients increase
enabling faster condensation rate than predicted by the
thin boundary approximation. Heat transfer and conse-
quently, the condensation rate during the collapse is
enhanced also by the turbulence of the liquid, as noted
already by Griffith (44) and by Bankoff and Mikesell (45).

Let us examine now the significance of these
favorable heat transfer conditions. As the vapor condenses
at the bubble interface latent heat is liberated and the

temperature of the interface increases. Unless this
energy is transferred to the bulk liquid the rate of
condensation will decrease. High heat transfer rates to
the bulk liquid thus minimize the temperature variations
at the interface and in the vapor due to the latent heat.
Thus, when large thermal gradients are present it appears
permissible to consider, in the limit, an isothermal
collapse process. For an isothermal process the inertia
of the liquid becomes important.

It was shown already by Plesset and Zwick (48)
that, for bubbles collapsing in a liquid at uniform
temperature, the thermal effects on restricting the
collapse rate are unimportant. Consequently, only the
inertial terms in Rayleigh's equation of motion are of
significance. The inertial effects were used by Bankoff
and Mikesell (45) to explain both the growth and the
collapse of a bubble in a subcooled liquid. We shall
examine the inertia effect in terms of the extended
Bosnjakovic-Jakob model.

Assuming spherical symmetry, the liquid inertia
can be taken into account by combining Rayleigh's equation
of motion, Equation II-6, with the energy equation. As
an analogy to the bubble growth problem in a uniformly
superheated liquid, the bubble growth and collapse
equation for a subcooled liquid becomes:

$$R\ddot{R} + \frac{3}{2}\dot{R}^2 + \frac{2\sigma}{\rho_L R} = \frac{1}{\rho_L}\frac{dP}{dT}\left[T_w - T_s - \frac{L\rho_v \dot{R}\sqrt{\pi a t}}{K}\frac{1}{b} - \frac{q\sqrt{\pi a t}}{K}\right] \text{II-31}$$

where the term dP/dT is given by Clausius-Clapeyron equation. With the term q = 0, and b = $\pi/2$, Equation II-31 is reduced to the equation which describes the growth of a bubble in a uniformly superheated liquid; an equation which was analyzed already in References 32, 33 and 34, 35.

During the growth process, the effects of the inertia and of the surface tension are small in comparison with the heat transfer effect. Consequently, during the growth the left hand side can be neglected, and Equation II-31 is reduced to Equation II-17. As the bubble radius goes through the maximum, the right hand side of Equation II-31 changes signs and becomes negative. In this domain then, the liquid inertia cannot be neglected. It was noted already that, because of the combined effects of liquid turbulence and of bubble curvature, the collapse stage could be approximated by an isothermal process. Neglecting the effect of surface tension, Rayleigh's equation for an isothermal process becomes:

$$R \ddot{R} + \frac{3}{2} \dot{R}^2 = - \frac{\Delta P}{\rho_L} = \text{const.} \qquad \text{II-32}$$

The solution of this equation for the initial conditions given by: $t = 0$, $R = R_m$, $\dot{R} = 0$, can be obtained from Lamb (50), thus

$$\frac{t}{t_{ca}} = 1 - \frac{\int_0^y \frac{y^{3/2}}{(1-y^3)^{1/2}} \, dy}{\int_0^1 \frac{y^{3/2}}{(1-y^3)^{1/2}} \, dy} \qquad \text{II-33}$$

where:

$$y = \frac{R}{R_m} \qquad \text{II-34}$$

and t_c is the time needed for the total collapse. Equation II-33 is plotted on Figure II-9, 10, 11 and 12; the initial time for collapse was taken to correspond to t_m, in order to satisfy the initial conditions. The agreement appears satisfactory. Note that the large variations in experimental data shown on these figures point out the poor reproducibility of the data and the statistical nature of the process.

In closing, we note that if a bubble is suddenly introduced in a subcooled liquid, or if the saturation temperature of the liquid is suddenly increased (by increasing the pressure), then, initially, the thickness of the thermal boundary layer is much smaller than the bubble

radius. Under these conditions, as discussed in Reference 49, the initial collapse rate will be given by:

$$L \rho_v \overset{o}{R} = -\frac{\pi}{2} \kappa \frac{T_s - T_L}{\sqrt{\pi a t}}$$

II-35

We shall summarize now the results presented in this chapter.

1) It appears that experimental data for bubbles growing and collapsing in a subcooled liquid can be approximated by considering the growth and collapse process separately.

2) The growth process is governed by the rate of heat transfer to the bubble wall. The experimental data can be approximated by growth rates obtained from the extended Bosnajakovic-Jakob model.

3) The collapse stage can be approximated by the solution of Rayleigh's equation for an iso-thermal process.

4) The growth and collapse equations thus obtained are matched at the maximum bubble radius.

5) The large variation of experimental data point out the poor reproducibility of the data and the statistical nature of the process.

6) Experimental data tend to indicate that the diameter of an active cavity can be related to the thickness of the superheated liquid film.

CHAPTER III

HYDRODYNAMIC ASPECTS OF NUCLEATE BOILING

Two aspects of bubble dynamics, the nucleation
and the growth, were discussed and analyzed in the pre-
ceding chapters. It was seen that the growth equation
can predict the dynamics of a bubble while it is still
attached to the surface. However, the analysis cannot
predict when and how the bubble will depart from the
surface. The mechanism of nucleate boiling was
discussed in Chapter I. It was noted that growing and
departing bubbles agitate the superheated liquid film;
thus, colder liquid is brought in contact with the
heating surface resulting in high heat transfer rates.
Since this renewal rate depends upon the rate at which
bubbles depart from the surface, the heat transfer rates
in nucleate, pool boiling will depend upon the mechanism
which governs the departure of bubbles. This mechanism
of heat transfer and the dependence of the heat flux
upon the frequency of bubble emission was described and
used by Jakob and co-workers (2, 3, 4, 5) in their
analysis of nucleate boiling. It was taken into account
also in the studies reported by Rohsenow (51, 52),

77

Kutateladze (53), Kruzhilin (54, 55) and Sterman (56, 57), among others. Indeed, an analysis which would omit from consideration the mechanism of vapor removal from the heated surface can be considered as incomplete. This statement is supported by the recent experiments of Siegel and Usiskin (58) which were conducted in a gravity-free field. The importance of the gravity in removing the vapor from the surface and thus its influence on nucleate, pool boiling was clearly demonstrated.

In this chapter we shall analyze the problem of vapor removal. It will be seen that the phenomenon of a bubble growing from a nucleating center, and its subsequent departure from the horizontal surface bears a strong similarity to a gas bubbling from a horizontal orifice. This similarity and some known facts concerning the frequency of bubble emission from an orifice will permit an estimate of the frequency of bubble generation in nucleate pool boiling. It will be seen also that the hydrodynamic aspects of nucleate pool boiling are similar to those which characterize the process of a gas bubbling through a porous plate. This similarity, and the hydrodynamic instability (usually referred to as "flooding"), which occurs when a gas is forced to bubble through a perforated plate or a sieve-tray, will help us gain an

understanding of the basic nature of the phenomenon which induces the change from nucleate to transitional boiling and thus creates the critical heat flux in boiling heat transfer.

III-1. The Similarity Between Bubble Formation at an Orifice and Bubble Formation in Nucleate Boiling

The problem of bubble formation at a submerged orifice has received much attention. For detailed information concerning this problem the reader is referred to the studies reported by Krevelen and Hoftijzer (59), Siemes (61, 62), Hughes and co-workers (63), Davidson and Amick (64) and Silberman (65), among others.

Seimes (61, 62) and Davidson and Amick (64) presented a detailed study of the regimes of bubble formation from a given orifice as a function of the gas flow rate. In what follows we shall summarize their results; the quoted sections are taken from Reference 64.

Static Bubbling Region. At very low gas flow rate the bubble formation is a problem of hydrostatics. The diameter of a bubble can be determined by considering the balance of the buoyant and adhesion forces at the orifice. Denoting by r_o, the radius of the orifice, the bubble diameter is given approximately by

$$D_d = \left[\frac{12 \, r_0 \, \sigma}{q \, (\rho_L - \rho_v)} \right]^{1/3} \qquad \text{III-1}$$

Davidson and Amick noted that stationary bubbles could not be formed at orifices larger than about 0.7 cm. In Chapter IV we shall see the reason for this. In this regime the bubble diameter is independent of the gas flow rate. The frequency of bubble emission increases with the gas flow rate. Bubbles rise with constant velocity. "Therefore for a given orifice the center-to-center spacing of the rising bubbles is inversely proportional to their frequency. At low frequencies the liquid at the orifice may be assumed to come to rest before each bubble escapes. The bubbles are identical at any given point early in their rising path."

Transition Region. "At higher flow rates the bubble volume increases sharply as the frequency levels of the spacing between bubbles has decreased, and each forming bubble is affected by the presence of the preceding bubble, perhaps through the mechanism of a liquid vortex at the orifice. The bubbles now start to form into pairs although still forming individually at regular time intervals at the orifice. A bubble will appear to hover

above the orifice until the next bubble emerges, and the two bubbles will remain together as they rise. This pattern is repeated by the next two bubbles, and so on indefinitely."

Incipient Coalescence. "As the flow rate further increases, the members of a bubble pair touch each other. This condition may be called 'doublet formation'. The first member of the doublet usually assumes a hemispherical shape, and the second bubble is elongated vertically; the assembly resembles a mushroom."

Coalescence. "Further flow-rate increase causes the second bubble to penetrate the first one appreciably. Under other conditions the first bubble absorbs part of the second and leaves the residue as a small satellite."...

Coalescence at the Orifice. "Coalescence takes place closer and closer to the orifice as the flow rate increases. A flow rate is finally reached at which the bubbles coalesce right at the orifice, the first bubble having no time to rise before the second emerges. Under these conditions it will appear that the frequency of bubbles rising from the orifice has suddenly been halved."

Double Coalescence. "As the flow rate further increases, the large coalesced bubbles themselves undergo coalescence as they rise. This may be called 'double coalescence.'

At this stage the fluid is usually quite turbulent and the gas seems to issue from the orifice as a continuous jet."

The reader should compare now the above description to the discussion presented in Section I-3. Indeed, if the expression "increasing the gas flow rate" were changed to "increasing the heat flux density", it would appear as if Davidson and Amick were describing the bubble formation in Yamagata and Nishikawa's experiments of nucleate boiling, see Figure I-5.

It appears thus that both the types of bubbles and the bubble formation regimes in nucleate boiling and in gas bubbling through a submerged orifice are hydrodynamically similar.

In the section which follows we shall make use of this apparent similarity to predict the frequency of bubble emission in nucleate boiling.

III-2.   The Frequency of Bubble Emission and the Value of the Product: Bubble Diameter Times Frequency in Nucleate Boiling

It was noted in Section I-3 that during the departure bubbles deform. The rate of rise of bubbles was analyzed by Pebels and Garber (65). The velocity of rise for deformed bubbles was found to be constant and independent of the size. It was found that the data

for sixteen liquids could be described within ± 3% by
the relation

$$U_{\infty} = 1.18 \left[\frac{\sigma g (\rho_L - \rho_v)}{\rho_L^2} \right]^{1/4}$$ III-2

This equation was derived analytically by Frank-Kamenetskii
also (66). During the process of quasi-static bubble
formation, "simple bubbles" depart under the action of
gravity only. It can be expected that, under these
circumstances, the velocity of rise in the vicinity of
the heated surface will be approximately equal to
Equation III-2. Before proceeding further we shall
verify this statement. Jakob (3, 67) has reported that
the velocity of rise of a bubble immediately after
departure is U_{∞}= 17 cm/sec. For water at saturation
temperature, Equation III-2 predicts a velocity of rise
U_{∞} = 18.6 cm/sec.

Jakob and Linke (4) found that while the bubble
still adhers to the surface its center of gravity rises
with almost the same velocity with which the bubble
later rises when it leaves the surface. This observation
implies that the following relation is approximately valid

$$\frac{D_d}{t_d} = U_\infty = 1.18 \left[\frac{\sigma g (\rho_L - \rho_v)}{\rho_L^2} \right]^{1/4} \qquad \text{III-3}$$

It follows then from Equation I-9 and Equation III-3 that

$$D_d \cdot f = \frac{t_d}{t_c + t_d} \cdot 1.18 \left[\frac{\sigma g (\rho_L - \rho_v)}{\rho_L^2} \right]^{1/4} \qquad \text{III-4}$$

The maximum frequency of bubble emission occurs when bubbles touch each other, i.e., when the contact time t_c is zero. For a spectrum of diameters D_d, Equation III-4 then gives the corresponding frequency spectrum.

The product $D_d \cdot f$ appears in almost every analysis of nucleate boiling (4, 5, 51, 52, 53, 54, 55, 56, 57). It was discussed in Section I-3 that this product was a constant for a nucleating center. For different liquids the average value of $D_d \cdot f$ was found to be of the same order of magnitude. Consequently, Jakob and Linke (5) proposed that a constant value of $D_d \cdot f = 77$ mm/sec be assigned to this product, whereas Fritz and Ende proposed a value of 95 mm/sec. We shall compute this value now.

Jakob and co-workers (2, 3, 4, 5, 24, 67) have observed that in their experiments the contact time t_c was almost equal to the time at departure t_d. Taking

t_c equal to t_d, Equation III-4 becomes

$$D_d \cdot f = \frac{1.18}{2} \left[\frac{\sigma g (\rho_L - \rho_v)}{\rho_L^2} \right]^{1/4} \qquad \text{III-5}$$

For water at saturation at one atmosphere Equation III-5 gives a value of 93 mm/sec, whereas for methanol and carbon tetrachloride it predicts 73 mm/sec and 64 mm/sec respectively. On Figure III-1, which is reproduced from References 3 and 67, Equation III-5 (for water) is compared with experimental data of Jakob and co-workers. On the same figure are plotted experimental data of Yamagata and Nishikawa (27) and of Westwater and co-workers (1, 25). The agreement appears to be satisfactory.

III-3. A Possible Relation Between the Diameter of a
Quasi-Static Bubble and the Diameter of a Cavity

The indicated similarity between bubble formation at orifices and bubble formation in nucleate boiling offers an interesting possibility for further investigation. It was noted that for low gas flow rates the diameter of a departing, quasi-static bubble was given by Equation III-1. It was observed in Section I-3 that at low heat transfer rates in nucleate boiling the bubble formation can be considered as a quasi-static process. If the bubble growing from a nucleating center is
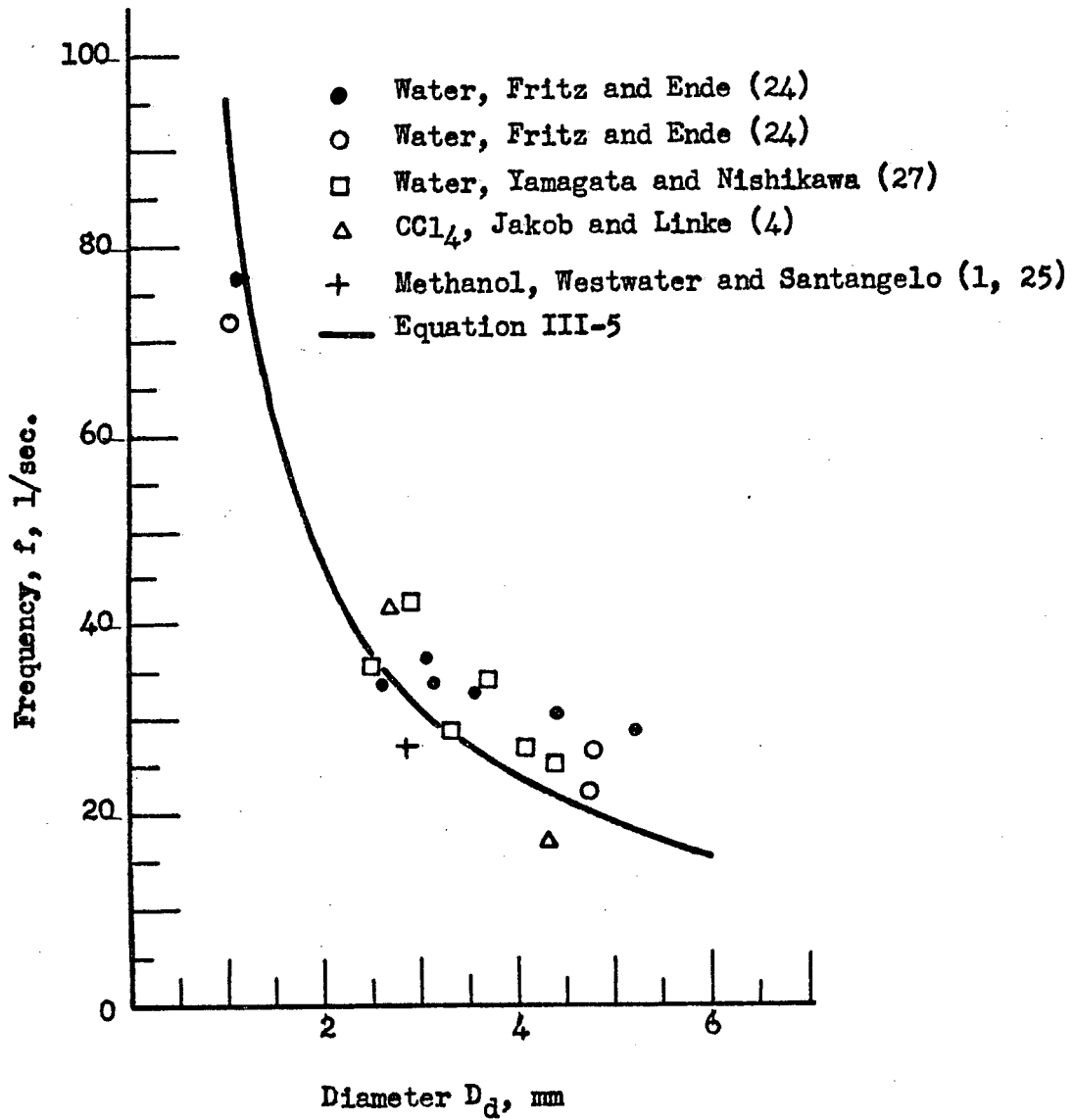
FIGURE III-1. THE RELATION BETWEEN THE FREQUENCY
OF BUBBLE EMISSION AND THE DIAMETER OF A BUBBLE
DEPARTING FROM A HORIZONTAL SURFACE

prevented from wiping the wall clear of water (see
discussion in Section II-6), it could be assumed that
in nucleate boiling the radius of the cavity could be
substituted for the radius r_o of the orifice in Equa-
ation III-1. This would enable us to compute the
spectrum of diameters of departing bubbles in terms of
the spectrum of cavity diameters. We cannot test this
assumption because no experimental data are available.
This can be done somewhat indirectly for the experiments
of Fritz and Ende (24) and of Zmola (42), who reported
the values of D_d. No data was given however for cavity
dimensions $D_c = 2 r_o$. The analysis in Section II-5
indicated a possible relation between the diameter of
the cavity D_c and the thickness of the superheated liquid
film X_s. If we substitute $X_s/2$ from Equation II-26 for
r_o in Equation III-1, it follows that

$$D_d = \left[\frac{6 \sigma}{g(\rho_L - \rho_v)} \frac{K \Delta T}{q} \right]^{1/3} \qquad \text{III-6}$$

On Table III-1 the experimental data of Zmola are tabu-
lated together with the computed value of D_d.

TABLE III-1

Comparison of Equation III-6

with Experimental Data of Zmola

ΔT $^\circ F$	q $\dfrac{Btu}{hr\ ft^2}$	D_d in	D_d (Equation III-6) in
9.4	9600	30×10^{-3}	32×10^{-3}
9.4	9600	31×10^{-3}	32×10^{-3}
9.4	9600	34×10^{-3}	32×10^{-3}

The same is done on Table III-2 for the experiments of
Fritz and Ende and of Jakob and Linke.

TABLE III-2

Comparison of Equation III-6 with Experimental Data of

Fritz and Ende and of Jakob and Linke

	Fritz and Ende		Jakob & Linke	Equation III-6
ΔT $^\circ C$	q $\dfrac{Kcal}{hr\ m^2}$	D_d cm	D_d cm (average value)	D_d cm
9	19000	5.42×10^{-1}	2.81×10^{-1}	2.15×10^{-1}
9	19000	4.04×10^{-1}		2.15×10^{-1}
9	19000	4.64×10^{-1}		2.15×10^{-1}

It is seen that the computed values are of the
same order as the measured one. In view of the possi-
bilities which a relation of this kind could open, it
appears that further experimental investigations are
warranted.

III-4. <u>On the Similarity Between Nucleate Boiling and</u>
<u>Flow of a Gas Bubbling Through a Perforated</u>
<u>Surface</u>.

We shall discuss in this section the similarity
which exists between nucleate boiling and a gas bubbling
through a perforated or porous surface. From this simi-
larity and from some phenomena which occur in fluidized
bubble-bed apparatus, the mechanism leading to the
critical heat flux in nucleate boiling will become
apparent.

The problem of a gas bubbling through a porous
surface has received much attention recently. The
reader is referred to the papers by Verschoor (68),
Siemes (60, 61), Kolbel and Siemes (69), Siemes and
Borchers (70) and Houghton, McLean and Ritchie (71) for
detailed discussion and additional references. It was
suggested already by Kolbel and Siemes that experiments
performed with bubble-beds, i.e., with a gas flowing
through a porous plate, may be used to help our under-
standing of nucleate boiling. Such experimental studies
of two-phase flow phenomena conducted with perforated
and porous surfaces were recently reported by Petrik (72)
and by Wallis and Griffith (73).

We shall first examine the relation between the gas flow rate and the pressure drop across the porous surface; the discussion is based on the studies reported in References 61, 70 and 71. Take a capillary of a given radius r_0, the pressure difference which is required for the formation of a bubble is given by Equation I-1. Thus the problem of initiating the bubbling process in nucleate boiling and from a porous plate are identical.

Consider now the effect of increasing the gas flow rate. At low gas flow rates only few of the largest pores are bubbling. As the gas flow increases the pressure difference increases and an increasing number of smaller pores become active. Vershoor noted that in addition to these new pores coming into action the first ones are yielding larger bubbles. Smaller pores can be brought into action also by reducing the surface tension of the liquid. The porosity of the surface determines the slope of the curve. This can be seen on Figure III-2, which is reproduced from Reference 70.

The reader should compare now the experimental results listed above to the discussion, given in Section I-4, of the effect of surface roughness upon the relation between the heat flux density and superheat
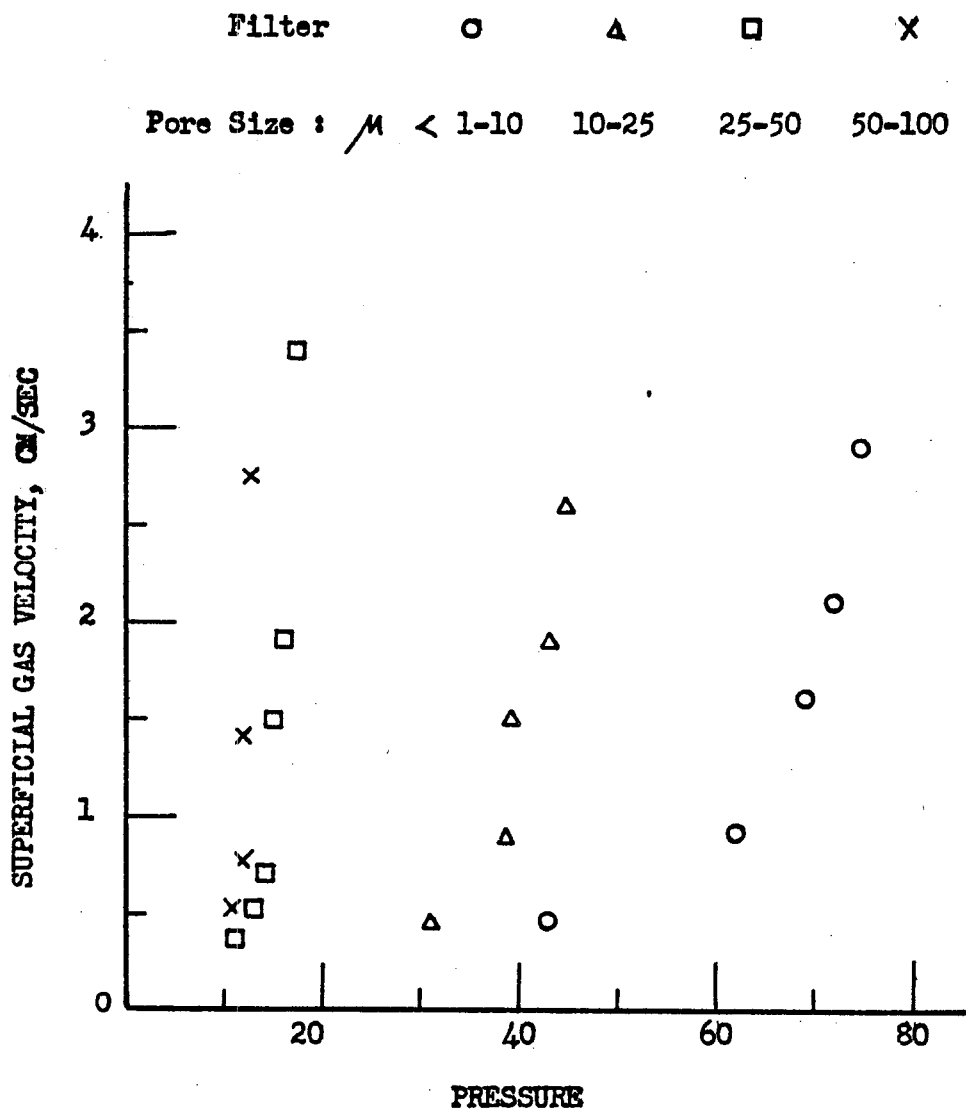
FIGURE III-2. THE RELATION BETWEEN THE SUPERFICIAL
GAS VELOCITY AND THE PRESSURE DROP ACROSS A POROUS
PLATE AS A FUNCTION OF THE PORE SIZE (This figure
is reproduced from the paper by Siemes and Borchers, 70)

temperature difference $T_w - T_s$, in nucleate boiling.
If, as it was suggested in Section III-1, "gas flow
rate" is substituted for "heat flux density", both
descriptions are alike. Note that through Clausius-
Clapeyron's equation the superheat temperature difference
can be expressed in terms of a pressure drop.

We shall now examine some hydrodynamic charac-
teristics of fluidized bubble-beds. For additional
information the reader is referred to the excellent
study of Siemes. The flow process of gas bubbling
through a porous plate is characterized by two distinct
flow regimes. At low gas flow rates a so-called "laminar"
regime exists, whereas a "turbulent" regime is associated
with high gas flow rates. At low gas flow rates few pores
are active. Bubbles of constant volume rise with a
constant velocity without interacting. At these low gas
flow rates an increase of flow rate results mostly in an
increase of the number of acting pores, i.e., of the
bubble population. At still higher rates both the popu-
lation and the bubble volumes increase and bubbles start
interacting. This process continues until, at a critical
gas flow rate, the flow changes to a turbulent process.
Houghton and co-workers (71) observed that this change
in the flow regimes is associated with bubble coalescence.
If the gas flow rate is still further increased large
plugs of gas are formed.

The distinct difference between these two flow regimes is shown on Figure 2 in Reference 69. It was noted that hydrodynamically, nucleate boiling is similar to the process of a gas bubbling from a porous or perforated plate. Indeed, if Figure 2 from Reference 69 is compared to the photographs of nucleate boiling which were published by Westwater and co-workers (1, 25), no difference can be seen. The "laminar" regime corresponds to nucleate boiling at low heat transfer rates, whereas the "turbulent" regime corresponds to the region close to the critical heat flux. It appears thus that the critical heat flux is characterized by a change in the flow regime. We shall explore this statement further.

III-5. The Phenomenon of "Flooding"

The change of flow regimes and, consequently, of the operating conditions is not a characteristic of fluidized bubble-beds only, but is a phenomenon which occurs in the performance of other apparatus. It has been recognized that the liquid and gas throughput in packed columns is subject to an upper limit above which the column ceases to operate satisfactorily as a counter-current device. This upper limit is designated either as the "loading" or the "flooding" point. For a given apparatus "flooding" is determined by both gas and liquid rates. At any given gas rate there is a definite liquid

rate above which a packed column will flood. Similarly, at any given liquid rate there is a definite gas rate above which the column will flood.

The mechanism of "flooding" in a sieve-tray distillation tower was recently described by McAllister, McGinnis and Plank (74). Among other effects, "flooding" resulted from a complete lifting of the liquid from the tray floor and subsequent carry-over of all the liquid on the tray as entrainment.

The generality of the "flooding" phenomenon was best discussed by Elgin and Weiss (75) and we shall quote now their description of the mechanism.

"It is believed desirable to emphasize here the generality of flooding and to visualize it as a requisite consequence in any apparatus in which one fluid passes discontinuously through an immiscible second one. The flooding of the packed tower is a special case of this general viewpoint. Bubble-cap, spray, bubble, or film type gas-liquid or liquid-liquid towers exhibit flooding in essentially the same manner. Preliminary visual laboratory studies of the flooding of such equipment indicate no fundamental or radical difference in the operative mechanism producing flooding. A difference in the visual behavior of such equipment arises from differences in the phase initially discontinuous. The

behavior of an evaporator or vaporizer operated at an
excessive heat rate for its diameter or a tube containing
a column of water into which air is bubbled at an in-
creasing rate is believed to be an evidence of the same
basic phenomenon.

"The general character of flooding is visualized
as follows: As pointed out the holdup of any discontin-
uous phase passing through another, whether the latter
is in motion or not, necessarily increases with its rate
of flow since its linear velocity in the continuous is
less than proportional to the rate at which it enters.
That its holdup must eventually approach the free volume
or cross section of the apparatus and result in a ten-
dency for it to become continuous and displace the phase
initially continuous is obvious. The continuous phase,
if in countercurrent motion, retards the passage of the
discontinuous through frictional drag to a greater or
less extent. An increase in the holdup of the latter
follows. This in turn results in a corresponding increase
of holdup. Since the countercurrent velocities are
mutually interdependent, the effect is multiplied at a
rapidly accelerating pace with further increase in volume
of either phase fed to the apparatus and must eventually
culminate in flooding. When the flooding point is
reached, either of two things may happen. Depending

upon the rate of passage of the continuous phase if made
discontinuous in the other and its corresponding holdup
at the relative volume flow rates at which flooding has
occurred, either the discontinuous phase is reversed,
and the only evident change is a transition say, from
a spray to a bubble device; or if the flow conditions
are such that the corresponding holdup of each would be
sufficient to fill the available volume, a competition
results and either is discharged more or less violently
from one or both ends of the apparatus. Both conditions
occur in packed tower or a spray type liquid-liquid
tower. Only the latter situation is observed in a film
type or a bubble type gas-liquid tower. The first may
be regarded as flooding with respect to liquid, the
second to gas."

We can interpret now the critical heat flux as
the region where vapor and liquid compete for the free
volume. It is a hydrodynamic phenomenon like other
"flooding" phenomena. We may expect, therefore, that
it will occur when the velocity of the vapor phase reaches
a critical value. Like in the experiments of McAllister
and Plank (74) the liquid will be pushed away from the
surface and the whole system will oscillate at some
characteristic frequency. In Chapter VI we shall determine
the critical velocity of the vapor phase, and this fre-

quency. In the next section we shall discuss the heretofore proposed correlations of the critical heat flux.

III-6. <u>Previous Empirical Correlations of the Critical Heat Flux</u>

The observation of Elgin and Weiss which was quoted in the preceding section is, to the knowledge of the writer, the first reference in the literature which interpreted the critical heat flux as a hydrodynamic phenomenon. The first correlation of experimental data of the critical heat transfer rates which used the concept of "flooding" was reported by Bonilla and Perry (75).

The correlation of experimental data for column flooding are plotted in terms of two dimensionless groups

$$\Pi_1 = \frac{\rho_g u_g^2}{\rho_L 2g \, m} \qquad\qquad \text{III-7}$$

$$\Pi_2 = \frac{u_g}{u_L}$$

where U_g, U_L, and ρ_g, ρ_L are the superficial velo-
cities and densities of the gas and liquid phase respec-
tively; whereas m and g are the hydraulic radius and the
acceleration due to gravity. To apply the above dimen-
sionless groups to the critical heat flux, Bonilla and
Perry substituted the group $q/L\rho_v$ for U_g, and
ρ_L/ρ_v for U_g/U_L. The hydraulic radius was expressed
in terms of the diameter D_d given by Equation I-7. The
correlation was expressed thus in terms of

$$\Pi_3 = \frac{(q/L\rho_v)^2 \rho_v}{\rho_L \, 2g \frac{1}{4}\left[\frac{\sigma}{g(\rho_L - \rho_v)}\right]^{1/2}} \qquad \text{III-8}$$

$$\Pi_4 = \frac{\rho_L}{\rho_v}$$

The experimental values of the critical heat flux q,
for boiling binary liquid mixtures, were inserted in
Equation III-8, and the data was plotted on a log-log
scale using Π_3 and Π_4 as coordinates. From the
results Bonilla and Perry concluded, "The points do not
fall too far from the flooding line." However, in their
subsequent publications this approach to the critical
heat flux was not pursued further.

The view that the critical heat flux marks a
transition from one regime to another was adopted by
Kutateladze (78, 77), Borishanskii (80, 79), Sterman
(56), and by Rohsenow and Griffith (80). The analysis
of Kutateladze will be discussed in greater detail
because he was responsible for the investigation and
interpretation of the critical heat flux as a hydrody-
namic phenomenon.

Kutateladze noted (78, 77), "At heat transfer
rates close to the critical heat flux, the amount of
vapor forming on the surface is so large that it is
impossible to consider separate nucleating centers
and separate bubbles. Consequently, in this case the
meaning and the concept of the frequency of bubble
generation is lost . . . the essential feature of the
theory of the phenomenon can be derived if one assumes
that the crisis in the boiling process is purely a
hydrodynamic phenomenon: the destruction of stability
of two-phase flow existing close to the heating surface."
According to this view the change from nucleate to
transitional boiling occurs when the velocity in the
vapor phase reaches a critical value. Starting from
the non-linear Euler equation of motion and the energy
equation he derived by dimensional analysis, the following
equation for the critical heat flux in pool boiling of

liquids at saturation:

$$\frac{q}{L (\rho_v)^{\frac{1}{2}}[\sigma g (\rho - \rho_v)]^{1/4}} = K = const.$$

III-9

The constant K was determined from experiments and its value was found to be

$$K = 0.16$$

III-10

The same equation, using dimensional analysis but a different thought model, was re-derived by Sterman (56).

It is interesting to note here that the dimensionless group K defined by Equation III-9 is equal to the square root of the dimensionless group π_3 defined by Equation III-8.

In two recent papers Borishanskii (80, 79) extended Kutateladze's analysis to include the effect of viscosity. In the discussion he pointed out several interesting aspects of nucleate boiling close to the critical heat flux. These comments are worth repeating here. According to Borishanskii the continuous existence of steady heat transfer rates in the neighborhood of the critical nucleate heat flux leads to the conclusion that there exists a direct steady movement of liquid toward the heating surface and of vapor away from it. Because

of the density difference between the two phases,
Borishanskii reasoned that a large part of a cross-
sectional area close to the heating surface is occupied
by vapor rather than by liquid. Therefore, near the
heating surface one can consider a two-phase boundary
layer whose thickness is of the order of a disengaged
bubble. This two-phase boundary region may be visua-
lized as consisting of liquid streams flowing toward
the surface and surrounded by vapor. The shapes of the
filaments of liquid as they flow towards the wall are
not well defined because of the inherent randomness in
the bubble dynamics and coalescence in the nucleate
regime.

At low nucleate boiling heat transfer rates the
discrete phase appears as a vapor bubble surrounded by
a mass of liquid; whereas close to the critical heat
flux it is, rather, a liquid stream filament bounded by
a group of bubbles. The change from nucleate to transi-
tional boiling occurs when the steady flow of the liquid
toward the wall is disrupted, i.e., when at critical
velocity of the vapor phase the liquid streams are
destroyed. Borishanskii noted further that: "This
problem seems analogous from a theoretical point of
view to the disturbance of steady flow of a liquid
stream in gas which moves coaxially with it. The

solution of the problem leads to a relationship between
the increment of the oscillation and the wave length.
Further analysis of the equation for the limiting case
of stable flow leads to the conclusion that the critical
boiling point corresponds to the establishment of a
definite geometrical structure of the two-phase boundary
layer." Borishanskii, therefore, considered that the
phenomenon was to be explained by analyzing the stability
of a liquid jet surrounded by a moving, coaxial, vapor
phase. From the equation which determines the amplitude
of the wave and from the energy equation he established,
by dimensional analysis, two similarity criteria: K
given by Equation III-9 as previously found by Kutateladze,
and N, given by

$$N = \frac{\rho_L \, \sigma^{3/2}}{\mu^2 \left[g(\rho_L - \rho_v) \right]^{1/2}} \qquad \text{III-11}$$

By plotting K versus N he found the following approximate
relation:

$$K = 0.13 + 4 \, N^{-0.4} \qquad \text{III-12}$$

In order to establish the above correlation, 117 experimental data points were used. The experimental data represent the following liquid-solid combination: Water boiling on a graphite surface (77), ethanol, benzene, n-heptane, and n-pentane boiling on a chromium plated surface (82), ethanol (83) and water (84) boiling from a nichrome surface. The viscosity of the liquid appears in Equation III-12 only in the additive correction factor N. Inasmuch as the deviation from a horizontal line is small it can be seen from Figure III-3, that the effect of the viscosity is also small.

Good agreement with experimental data was achieved, also, by the correlation proposed by Rohsenow and Griffith (80):

$$\frac{q}{L\rho_v} = C \left[\frac{\rho_L-\rho_v}{\rho_v}\right]^m$$

III-13

The value of the constant $C = 143$ f.p.h., which has dimensions of a velocity, and the exponent $m = 0.6$ were determined from experimental data by plotting $q/L\rho_v$ versus the buoyancy term $\rho_L - \rho_v/\rho_v$.

Equations III-9 and III-13 are remarkable for three reasons. We note first that they do not relate heat transfer to a temperature difference. Also, they

1 water   6 heptane   11 ethanol
2 benzene   7 propane   12 heptane
3 ethanol   8 propane   13 water
4 pentane   9 water
5 pentane   10 benzene
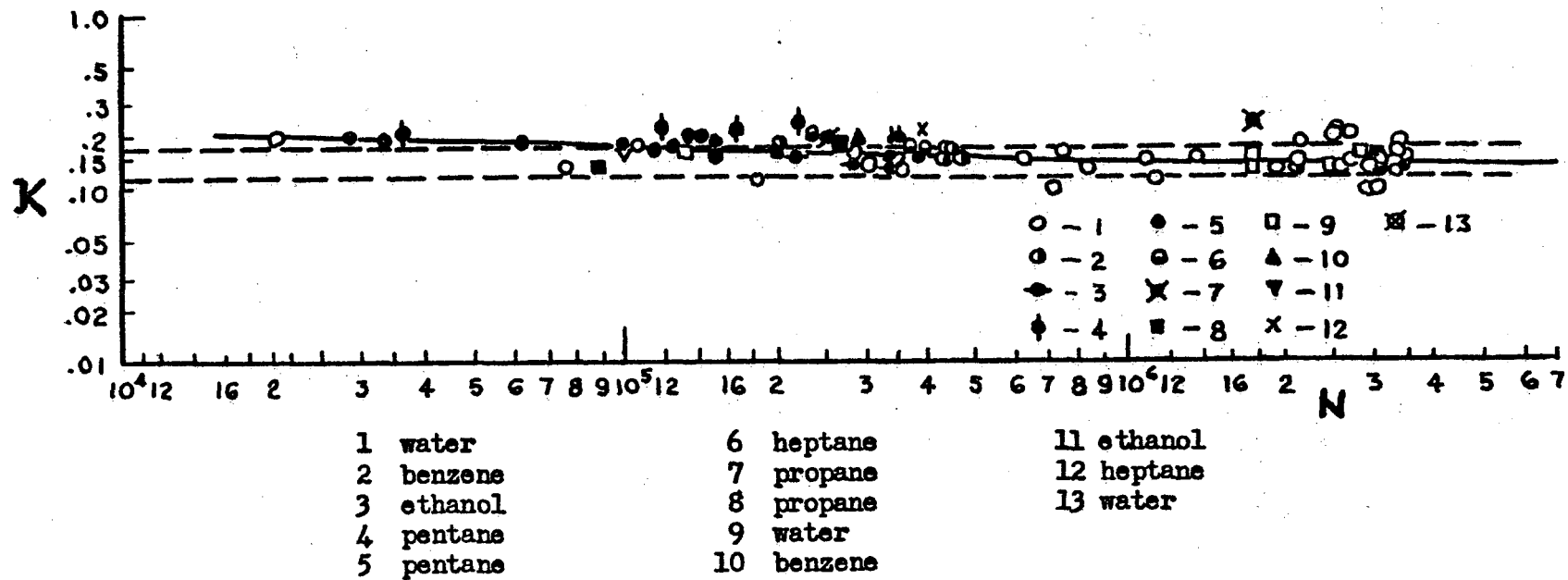
FIGURE III-3. CORRELATION OF DATA FOR VARIOUS LIQUIDS AT THE
CRITICAL HEAT FLUX DENSITY IN POOL BOILING.
This figure is reproduced from the report by Borishanskii (79,80).
The solid line (Equation III-12) is his best fit curve to 117 data
points. The two dashed lines represent the upper and lower bounds
on K (Equation VI-13) derived by the considerations in the paper.

do not depend upon the thermal and transport properties
of the liquid. And, we note their striking simplicity.
These characteristics of Equations III-9 and III-13 are
surprising when an interpretation of the phenomenon is
sought in terms of the conventional convective heat
transfer concepts where the thermal and transport pro-
perties of the liquid are of paramount importance. It
is not surprising, however, if the critical heat flux
is interpreted as a hydrodynamic phenomenon of "flooding"
which occurs at a critical velocity of the vapor phase.
This statement is confirmed when Equation III-13 is
compared to the equation which gives the critical, i.e.,
the limiting, vapor velocity at which a bubble-cap
column floods (85).

$$U_c = K \left[\frac{\rho_L - \rho_v}{\rho_v} \right]^{1/2} \qquad \text{III-14}$$

where U_c is the maximum permissible velocity, in feet
per second, based on the area of the bubbling section of
the plate and K is an empirical constant.

III-7. <u>Nucleate Boiling and the Region of the Critical</u>
<u>Heat Flux</u>

In Chapter I we have reviewed experimental results
of nucleate boiling. In the preceding sections of this
chapter, nucleate boiling and the process of a gas
bubbling through a liquid were compared and two simi-
larities were analyzed. We have considered first the
similarity which exists between a gas bubbling through
an orifice and bubbles growing from a nucleus in boiling.
Following this, we have considered the similarity which
exists between nucleate boiling and a gas bubbling
through a perforated surface.

By making use of the first similarity and of
some known facts concerning the frequency of bubble
emission from an orifice, an equation (Equation III-4
or III-5) was derived for the product $D_d \cdot f$ in nucleate
boiling. It is possible thus, from Equation III-4, to
estimate the maximum frequency of emission of simple
bubbles in nucleate boiling. The first similarity indi-
cated also the possibility of expressing the diameter
D_d of a simple bubble departing from the heated surface
in terms of the radius of r_o of the nucleating cavity.

The second similarity, i.e., the similarity
which exists between nucleate boiling and the process of
a gas forced to bubble through a perforated surface,

indicated the basic nature of the phenomenon which induces the change from nucleate to transitional boiling. It was seen that the critical heat flux is a hydrodynamic phenomenon. It was concluded also that existing correlations (cf. Equation III-13) can be understood only if the critical heat flux is interpreted as a "flooding" phenomenon.

In this section we shall integrate the discussion given in Chapter I with the results presented in the preceding sections of this chapter. We shall attempt thus to form a composite picture of nucleate pool boiling from a horizontal surface.

Consider the effect of increasing the heat flux density on the process of boiling. At low heat flux densities nucleate boiling takes place in patches. In these patches of nucleate boiling "simple" bubbles are generated (see Figure III-4.a). From a given nucleating center bubbles depart with a regular frequency and with a constant diameter. The product of the diameter and the frequency can be approximated by Equation III-4. To a distribution of nucleating cavities of different dimensions there corresponds probably a distribution of departing bubbles having different diameters and different frequencies of emission. The velocity of bubble rise in the vicinity of the surface can be approximated
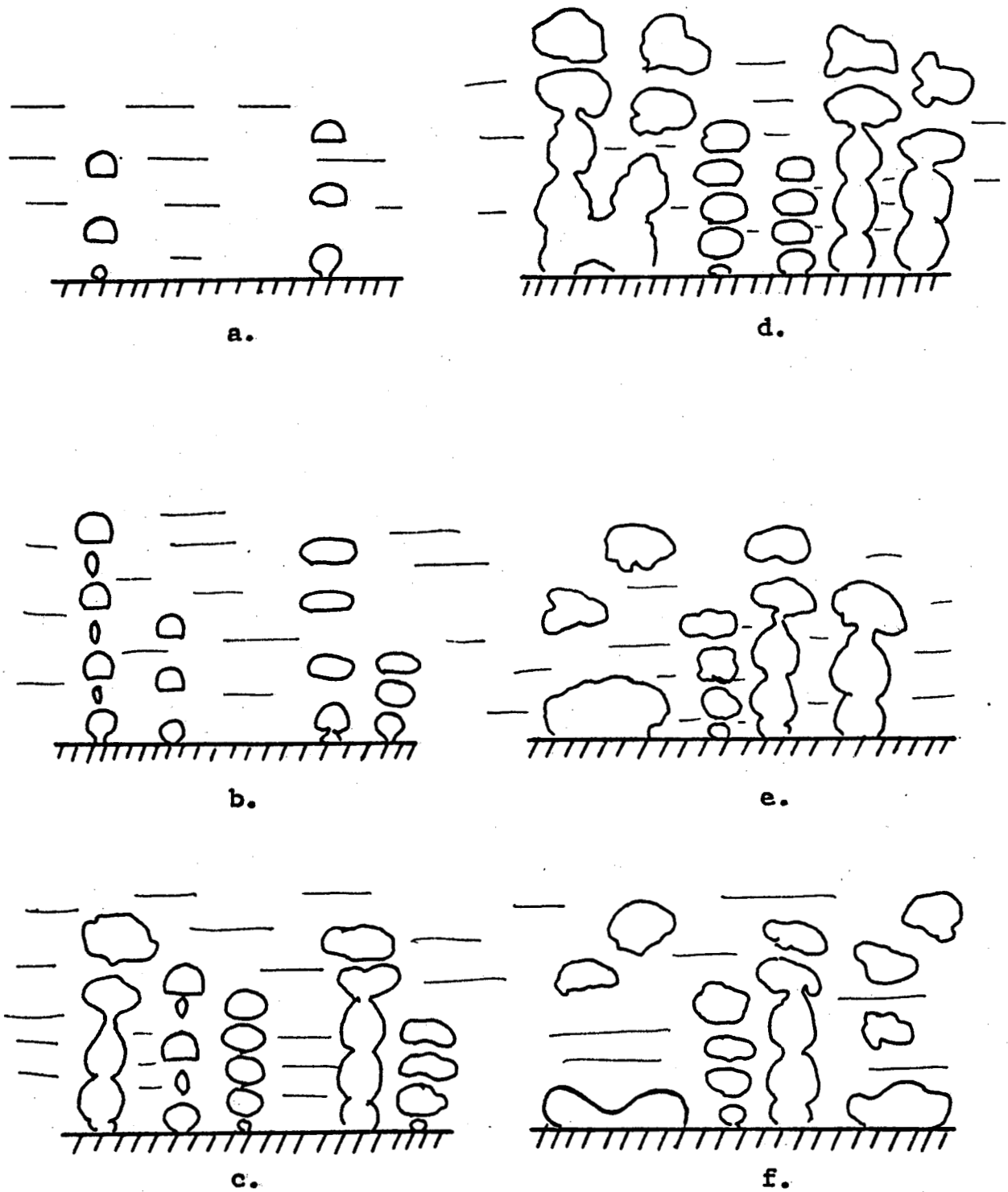
Figure III-4. Schematic Representation of the
Process of Nucleate Boiling

by Equation III-2. As bubbles grow and depart the liquid is agitated. At regular time intervals in the vicinity of a nucleating center colder liquid is brought in contact with the heating surface, thus resulting in high local heat transfer rates. The process of bubble generation and, consequently, the process of local heat transfer are intermittent. The sum of such high local heat transfer rates results in an average total heat flux density which is higher than in a non-boiling system.

As the heat flux density is increased the patches of nucleate boiling spread, i.e., the bubble population increases. In addition to the new active nucleating centers the first active ones are generating "multiple" bubbles (see Figure III-4.b). The process of spreading of patches of nucleate boiling continues with an increase of the heat flux density until the whole surface is covered with active sites.

The bubble population continues to increase with increasing heat flux densities. The frequency of bubble emission increases until bubbles follow each other, ie., the contact time is almost zero. For a given bubble diameter the maximum frequency can be estimated from Equation III-4. Under these conditions coalescence of bubbles takes place. Consequently, from some nucleating

centers continuous vapor columns, i.e., vapor jets, are generated. At some distance from the surface these vapor jets break up into large bubbles (see Figure III-4.c). It is probable that further increase of the heat flux density results mainly in increasing the number of these continuous vapor columns, although the bubble population will keep increasing also.

The vapor velocity in these jets increases with increasing heat flux density. The process continues until at some critical velocity of the vapor two neighboring jets start interacting, i.e., become unstable. The liquid stream between the two jets is interrupted, and the steady flow of the liquid toward the surface ceases (see Figure III-4.d). Using the expression of Elgin and Weiss the vapor and the liquid start competing for the free volume and "flooding" starts.

For a horizontal surface the interaction of the jets occurs at a random place. Thus, at random location on the surface a large patch of vapor is formed (see Figure III-4.e). In order to distinguish the patches of nucleate boiling which appear at low heat flux densities from the large patches of vapor which appear in the region close to the critical heat flux, we shall refer to the latter ones as patches of transitional boiling. Such a patch insulates the surface locally.

Consequently, for a constant heat flux density the temperature of the surface increases. This causes the rate of evaporation to increase and results in higher vapor velocities in other jets. These, in turn, become unstable, start interferring with each other and patches of transitional boiling appear at a compounding rate. Using, again, the expression of Elgin and Weiss the effect of the instability is multiplied at a rapidly accelerating pace. Thus in the region of the critical heat flux a small increase of the heat flux density results in a large increase of the surface temperature. Consequently, in the q = Δ T plane there exists a plateau across which boiling changes from the nucleate to the transitional boiling regime.

The patches of transitional boiling are hydrodynamically unstable; this problem will be analyzed in the chapter which follows. In collapsing, i.e., when the vapor-liquid interface of a patch approaches the heated surface, large rates of evaporation occur and the interface is pushed violently back. The process is similar to explosions or bursts of vapor. Similarly to the "flooding" of sieve-trays, in the region of the critical heat flux, the liquid is pushed away from the surface and the whole system oscillates at some characteristic frequency.

Once the patches of transitional boiling cover the whole surface, transitional boiling sets in. The problem of transitional boiling is taken up in the chapters which follow. It will be seen that a well defined geometry is the characteristic of transitional boiling. Therefore, an analytical solution of the problem can be attained (86, 87, 88). In nucleate boiling the flow configuration is not well defined. As noted by Borishanskii, "the form of the liquid streams differs considerably since it is determined by the not well regulated order of the combination of vapor bubbles." It was observed in Reference 88, that given a field equation and no geometrical data, Kutateladze and Borishanskii found it necessary to use dimensional analysis, which is the best that can be done under the circumstances and which reduces the problem to the determination of an empirical constant.

III-8. <u>Nucleate Boiling Heat Transfer - Methods</u>
<u>of Analysis</u>

In this closing section of the chapter on hydro-dynamic aspects of nucleate boiling we shall discuss briefly two methods of analyzing the process of heat transfer in nucleate boiling. Correlations of experi-mental data which are based on finding empirical relations among dimensionless groups will not be discussed

here. This approach to the problem as well as the correlations which have been proposed are discussed in Reference 88.

It was discussed in the preceding sections that heat transfer rates in nucleate boiling are the result of local effects which are created by bubbles growing and departing from the heated surface. Consequently, an analysis must consider both the effect of bubble population and the mechanism of vapor removal.

The problem can be analyzed either by considering the transport of enthalpy across an imaginary boundary located in the liquid, or by considering the mechanism of energy transfer at the heating surface. A complete analysis cannot be carried out at present because both methods require information on the bubble population; this information is not available yet. In what follows we shall only outline these two methods of analysis and cite the contributions and suggestions which were advanced by various researchers.

The transport of enthalpy which was considered by Sterman (56) and by Treschov (20) is an energy balance: the enthalpy transported by one bubble, multiplied by the frequency of emission and by the number of bubbles per unit area, is equated to the heat flux density, thus.

$$q = \frac{4\pi}{3} \bar{R}^3 \left[c \rho_L \overline{(T_w - T_L)} + L \rho_v \right] \bar{f} \frac{n}{A} \qquad \text{III-15}$$

where the bar refers to mean values.

The second method of analysis was proposed by Kruzhilin (54, 55) and by Rannie (47); they considered the heat transfer process at the heating surface. It was noted that, because of the growth and departure of a bubble, colder liquid is periodically brought in contact with the heating surface. Thus in the vicinity of a nucleating center large temperature gradients are created periodically; conduction is increased and becomes the dominant heat transfer process.

The analysis is formulated (54, 55) by considering the amount of energy which is transferred from the heated surface (x = 0) during a contact time t_c, across an area element F. This area F is the segment of the total heated surface which is influenced by the action of one nucleating center, i.e., it is the "influence domain" of one bubble. The amount of energy Q', which is transferred by the action of one nucleating center, becomes thus

$$Q' = \int_{t_d}^{t_d + t_c} \int_F \kappa \frac{\partial T}{\partial x} \bigg)_{x=0} dt \, dF \qquad \text{III-16}$$

The total amount of energy Q, which is transferred from the surface, is obtained by multiplying Equation III-15 by the total number of nucleating centers.

In order to make use of Equation III-15 it is necessary to evaluate the gradient $(\partial T/\partial x)_{x=0}$. This temperature gradient will be determined, as in similar transient conduction problems, by the coupling of the thermal fields which exist in the solid and in the liquid. It will depend thus upon the thermal properties of both the solid and the liquid. The importance of the thermal characteristics of the solid on nucleate boiling heat transfer were discussed by Rohsenow, Sabersky and Snyder (47). The observation made by Zysina-Molozhen, which was quoted in Section I-4, only adds supporting evidence. It was discussed by Griffith (44) that when the temperature of the heated surface remains approximately constant during the process of intermittent heat transfer, the temperature distribution in the liquid during the contact time t_c, can be approximated by the solution of Equation II-2. The instantaneous temperature gradient is given then by Equation II-4.

When the energy equation for the liquid adjacent to the heating surface can be approximated by Equation II-2, the problem of intermittent heat transfer in nucleate boiling becomes similar to the system which is

described by the "discontinuous film model." This model was developed and used by Highbie (89), Dankwerts (90) and Hanratty (91) to describe the exchange of mass, momentum and energy at a boundary. According to this theory, masses of fluid can be visualized as moving to and from the wall causing a continual change of the fluid in contact with the wall. When a mass of fluid comes in contact with the solid, its surface layer immediately attains the temperature of the wall. It remains in contact with the wall for a period of time t_c, during which energy is transferred from the wall to the liquid by conduction. The problem is similar to the heating of a block of metal. After the contact time t_c, the mass of fluid is replaced and the process is repeated.

The problem is formulated by considering the instantaneous temperature gradient, in this instance it is given by Equation II-4. If all fluid masses had the same contact time t_c, the average, i.e., the measured heat flux density would be

$$q = \frac{1}{t_c} \int_0^{t_c} \frac{k(T_w - T_s)}{\sqrt{\pi a t}} dt = \frac{2(T_w - T_s)}{\sqrt{\pi a t_c}} \qquad \text{III-17}$$

However, different liquid masses will have different
contact times. The effect of the variations is taken
into account by considering the probability $\phi(t_c)\,dt_c$
that a fluid mass has a contact time between t_c and
$t + dt_c$. The average heat flux is obtained by inte-
grating over all variations, thus

$$q = \int_0^\infty \phi(t_c) \frac{2\kappa(T_w - T_s)}{\sqrt{\pi a t_c}}\,dt_c \qquad \text{III-18}$$

It is seen from this brief discussion that the
system which is described by the "discontinuous film
model" resembles the process of intermittent heat
transfer which takes place in nucleate boiling. An
investigation along this line will be given at a later
date. Here we note that this approach can be readily
applied to transitional boiling. It will be seen in
the chapters which follow that, in contrast to nucleate
pool boiling where the frequency of bubble emission
and therefore the contact times are given by a distri-
bution curve, in transitional boiling to a given heat
flux density there corresponds one frequency. Thus, in
transitional boiling Equation III-18 is reduced to
Equation III-17 which permits an analytical solution of
the problem (87, 88).

CHAPTER IV

HYDRODYNAMIC ASPECTS OF TRANSITIONAL BOILING

The region of the critical heat flux was discussed in the preceding chapter. It was observed that when two vaporjets start interferring with each other the flow of liquid toward the surface is interrupted and a patch of vapor, i.e., a patch of transitional boiling, is formed. The region of the critical heat flux is characterized thus by the presence of both nucleate and transitional boiling. When patches of transitional boiling cover the whole surface transient boiling sets in. We shall analyze in this chapter the hydrodynamic aspects of transitional boiling. The first analytical investigation of the characteristics of transitional boiling was reported in Reference 86; the problem was investigated further in Reference 88.

In transitional boiling the heating surface is separated from the liquid phase by an unstable irregular film of vapor. The process is hydrodynamically unstable, because the acceleration is directed from the less dense to the more dense medium. An understanding of the phenomenon requires therefore an understanding of the mech-

anism of hydrodynamic instability, a topic which is taken up in the section which follows.

IV-1. Stability of a Plane Interface - Mathematical Formulation

The problem of hydrodynamic stability of a plane interface has received much attention. The reader is referred to the treatise by Lamb (50) and in particular to the recent monograph by Birkhoff and Zarantonello (92) for a detailed discussion of the problem. In what follows we shall summarize the results which are pertinent to the problem under consideration. The discussion is based on studies which were reported by Taylor (93), Lewis (94), Allred and Blount (95), Bellman and Pennington (96) and by Birkhoff (97, 98).

When two liquids of different densities and having a common interface are accelerated in a direction perpendicular to the boundary, any small irregularity of the interface will tend to change in shape. The interface is stable, i.e., the irregularities will tend to smooth out in time, if the acceleration is directed from the denser to the lighter fluid. The interface is unstable, i.e., the irregularities of the interface will grow with time, when the acceleration is directed from the lighter to the heavier medium. A familiar example of this phenomenon is a glass of water turned upside down. The

air-water interface instead of remaining plane as it falls will tend to form long liquid spikes which subsequently disintegrate into drops. An instability of this kind is referred to as "Taylor instability" because, as pointed out by Birkhoff and Zarantonello, "the first clear formulation of this principle was due to Sir Geoffrey Taylor (93), who also inspired its experimental confirmation by Lewis." (94)

The problem was formulated mathematically by Kelvin (Reference 50, Page 458) using potential theory. Consider a plane interface at $Y = 0$ separating the vapor in $Y < 0$ and the liquid in $Y > 0$. Let an infinitesimal perturbation of this interface be given by

$$\eta = H_o\, e^{i(\omega t - mx)} \qquad\qquad \text{IV-1}$$

Under the usual perturbation approximation the frequency equation of the interface becomes (Reference 50, Page 459, Equation 2)

$$\omega^2 = \frac{\sigma m^3}{\rho_L + \rho_v} - \frac{g(\rho_L - \rho_v)m}{\rho_L + \rho_v} \qquad\qquad \text{IV-2}$$

The condition of stability is that ω be real; when ω becomes imaginary the disturbance η , given by Equation IV-1, will grow exponentially with time. The wave length can be expressed in terms of the wave number m , thus,

$$\Lambda = \frac{2\pi}{m} \qquad \text{IV-3}$$

Equation IV-2 indicates that the disturbances of the interface can be stable or unstable according to whether the wave length is shorter or longer than a critical value. This critical value is obtained by equating Equation IV-2 to zero, thus

$$\Lambda_{o_1} = 2\pi \left[\frac{\sigma}{g(\rho_L - \rho_v)} \right]^{1/2} \qquad \text{IV-4}$$

Equations IV-1 and IV-2 indicate the existence of a continuum of unstable perturbations, each of which has its own growth rate. Because of the exponential nature of the instability the wave length which maximizes - ω^2 will be the "most dangerous", i.e., it will result in a disturbance which has the most rapid growth. Differentiating ω^2 with respect to the wave number m , the "most dangerous" wave length then becomes (96):

$$\Lambda_{o_2} = 2\pi \left[\frac{3\sigma}{g(\rho_L - \rho_v)} \right]^{1/2} \qquad \text{IV-5}$$

Substituting Equation IV-5 into Equation IV-2, the maximum value of $-\omega^2$ becomes

$$\omega^2 = -\frac{2}{3} \frac{g(\rho_L - \rho_v)}{\rho_L + \rho_v} \left[\frac{g(\rho_L - \rho_v)}{3\sigma} \right]^{1/2} \qquad \text{IV-6}$$

The most unstable disturbance is obtained from Equation IV-1 and IV-6, thus

$$\eta_m = H_0 e^{\beta t} e^{imx} \qquad \text{IV-7}$$

where

$$\beta = \left[\frac{2 \, g(\rho_L - \rho_v)}{3 \, (\rho_L + \rho_v)} \right]^{1/2} \left[\frac{g(\rho_L - \rho_v)}{3\sigma} \right]^{1/4} \qquad \text{IV-8}$$

The comparison of these theoretical results with experimental data is discussed in the section which follows.

IV-2. Stability of a Plane Interface - Experimental

Results

We shall first note some phenomena which can be
interpreted in terms of Taylor instability. It was
observed by Bellman and Pennington (96) that, "This
phenomenon explains the hanging of water drops on the
underside of a horizontal surface, such as a ceiling.
Such a droplet is undergoing an upward acceleration of
980 cm/sec^2 and will tend to drip because of Taylor
instability unless its effective wave length is about
λ_{01} = 1.73 cm. Droplets of larger diameter will tend
to drip, while smaller ones will tend to hang." Another
evidence is cited by Lamb (50) and Milne-Thompson (99)
who point to experiments "in which water is retained by
atmospheric pressure in an inverted tumbler whose mouth
is closed by a gauze of sufficiently fine meshes." The
mesh size should not exceed $\lambda_{01}/2$.

It was noted in Section III-1 that Davidson and
Amick (64) reported "... stable stationary bubbles could
not be found at an orifice having a diameter of 0.79 cm,
but stable bubbles formed at an orifice of 0.64 cm."
The reason for this becomes apparent when Taylor insta-
bility is considered. For water the critical wave
length λ_{01} is 1.73 cm; because of probable fluctuation
at the orifice or in the liquid, the orifice diameter

of 0.79 cm was too close to the value of $\lambda_{01}/2$ for
the stability to be maintained.

The occurrence of capillary waves in stable film
boiling has been reported and described by Bromley (100)
and by Westwater and Santangelo (1). In a recent paper
Chang (101) observed that in stable film boiling the
bubble spacings computed from Equation IV-4 are in
agreement with experimental results reported by West-
water and Santangelo (1).

The analytical prediction of Taylor and of Bellman
and Pennington were verified by the experiments reported
by Lewis (94) and by Allred and Blount (95). These
experiments were conducted to determine the growth of
sinusoidal perturbations with wave length λ at a
liquid-gas interface, accelerated at a = 30g - 75 g
over a distance of 5λ - 15λ. Lewis (94) concluded
that "the instability is made up of the following stages:

1) "An exponential increase in amplitude as
given by the first order theory until the
amplitude is about 0.4λ.

2) "A transition stage during which the amplitude
increases from 0.4λ to 0.75λ and the
surface disturbance changes to the form of
round-ended columns of air penetrating into
the liquid, which forms narrow upstanding

columns in the interstices.

3) "A final stage of penetration through the
liquid of the columns at a uniform velocity
proportional to $\sqrt{a - g}$."

Two additional stages to be expected are discussed
by Birkhoff (97); these are:

4) "A stage in which the boundaries of the air
columns will deform irregularly under the
influence of Helmholtz instability and the
growth of vorticity, until

5) "the mixing zone separating the two fluids
is turbulent, and must be analyzed (like
turbulence) by statistical methods."

For detailed information concerning Taylor instability
the reader is referred to this excellent report by
Birkhoff.

The initial exponential growth rate as predicted
by Taylor's theory was verified further by the experiments
of Allred and Blount (95). They observed also that during
the final stage of deformation (Stage 3), the interface
consists of spikes of heavy liquid extending into the
light fluid, and of rounded regions which may be thought
of as bubbles of lighter fluid rising into heavier fluid.
The spacing of these spikes, i.e., the effective "wave
length" was found to be in good agreement with the "most

dangerous" wave length given by Equation IV-5. It is important to emphasize here that this equation was derived from two-dimensional considerations.

Lewis (94) reported that the growth rates during the asymptotic stage can be predicted from an equation, derived by Davies and Taylor (102), for the rise of a large bubble:

$$ U = \frac{2}{3} \left[r g \right]^{1/2} \qquad \text{IV-9} $$

where r is the radius of curvature of the bubble vertex. Similar conclusions for the asymptotic growth were reported by Allred and Blount (Reference 95, Page 11)*. The asymptotic growth rate of Taylor instability was investigated also theoretically in the recent papers by Garabedian (103) and by Birkhoff and Carter (104).

In this and the preceding section we have briefly summarized results of theoretical and experimental investigations of Taylor instability. It will be seen in the sections which follow that transitional boiling is closely related to this instability.

---

* See also Reference 97, Page 16 and Page 31.

IV-3.   Westwater and Santangelo's Description of

Transitional Boiling

The only quantitative, experimental investigation

of transitional boiling in the literature was reported

by Westwater and Santangelo (1). It is fortunate to

have as a guide for theoretical analysis the results of

these and other outstanding experiments reported by

Professor Westwater and his co-workers. Westwater and

Santangelo give the following description of transition

boiling.

"Most prior workers have failed to realize that

this boiling is entirely different from both nucleate

boiling and film boiling. No active nuclei exist. In

fact, no liquid-solid contact exists either. The tube

is completely blanketed by a film of vapor, but the

film is not smooth nor stable. The film is irregular

and in violent motion.

"Vapor is formed by sudden bursts at random

locations along the film. Liquid rushes in toward the

hot tube, but before the two can touch, a miniature

explosion of vapor occurs and the liquid is thrust back

violently. The newly formed slug of vapor finally

ruptures, and the surrounding liquid again surges toward

the tube. The process is repeated indefinitely.

128

"One observer of these high speed motion pictures
has expressed an opinion that occasional liquid-solid
contact does occur during transition boiling. If so,
these contacts are rare and exceedingly short. The
present writers do not believe there is a real contact.

"The frequency of the vapor burst is surprisingly
high. For an over-all $T_w - T_s$ of 133°F (and of
h = 164 Btu/hr ft^2 °F) each inch of the photographed
side of the tube exhibited 84 bursts per second. The
burst occurs so suddenly and unexpectedly that even in
slow motion they resemble explosions.

"If the temperature is increased still further,
the blanket becomes thicker and more stable. ... The
increase of vapor thickness results in a better damping
of the explosive burst until finally a thick rather
stable film results and no more bursts occur. This is
the beginning of film boiling."

The minimum heat flux, i.e., point D on Figure I
is described by Westwater and Santangelo as follows:

"As vapor gathers at the top of the tube, a rod-
like mass forms along the top of the entire length of
tube. At first the rod is smooth and rather uniform in
thickness, although faint movements occur constantly.
As the gas rod increases in volume, peaks and valleys
form until the upper boundary becomes sinusoidal in shape.

The entire rod ruptures, between all the nodes, and a horizontal row of bubbles rise side by side. After the rupture, the whole process is repeated. One cycle requires 0.06 second when the over-all temperature difference is 184°F.

"A second gas rod ruptures at points directly under the centers of the last released individual bubbles. This means that the even-numbered rows of bubbles are displaced sideways by a half space from the odd-numbered ones. Viewed from the side the bubbles are similar to marchers arranged in triangular spacing rather than the conventional square spacing."

In the section which follows we shall relate these observations to the discussion which was presented in the preceding section. We shall thus interpret transitional boiling in terms of Taylor instability.

IV-4.   The Hydrodynamic Instability of Transitional
        Boiling

Consider a vapor patch in transitional boiling from a horizontal surface (see Figure IV-1.a). The liquid vapor interface is hydrodynamically unstable because the acceleration is directed from the vapor to the liquid. It can be expected that, because of agitation, the interface has random initial perturbations,
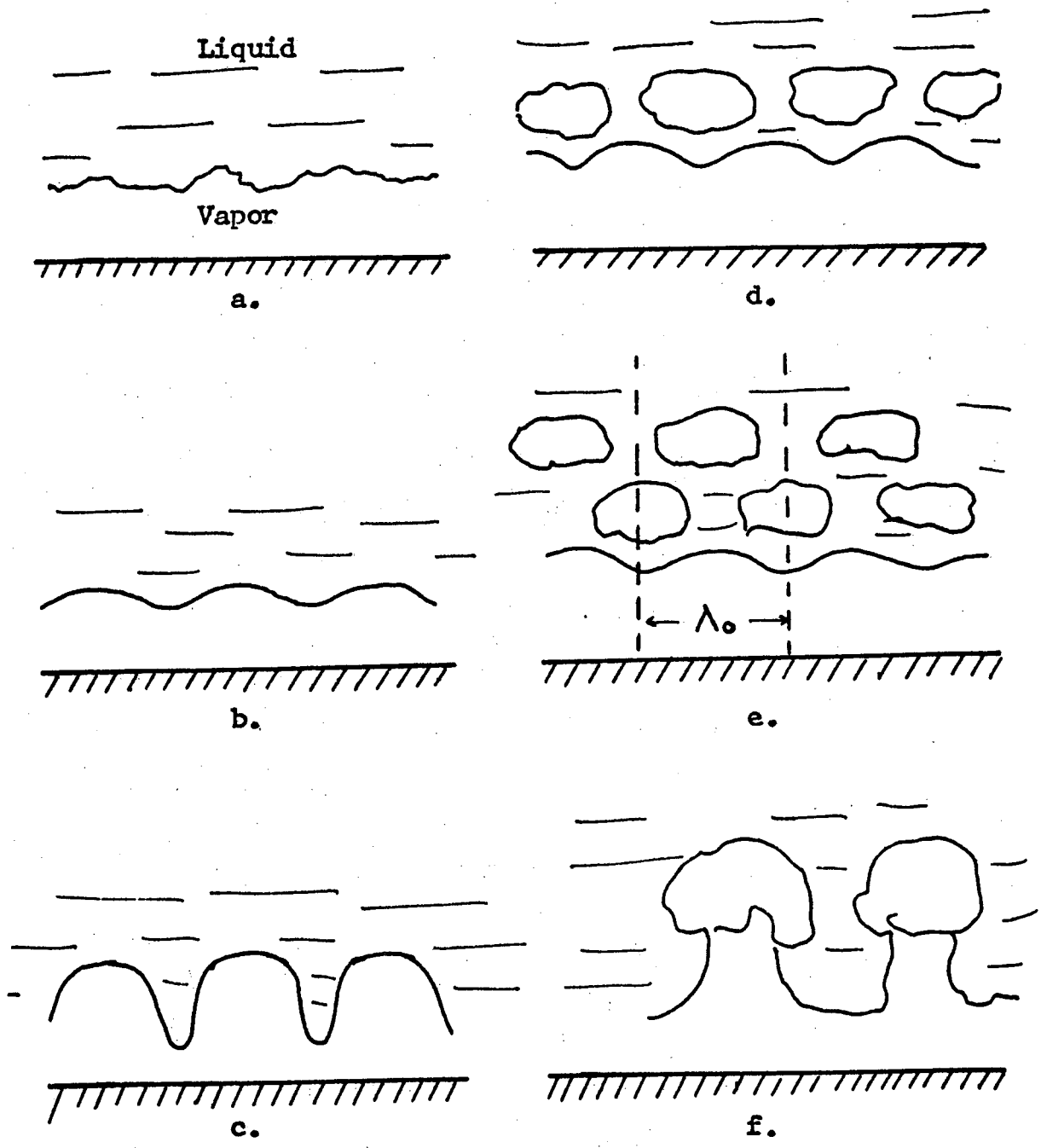
Figure IV-1 Schematic Representation of
the Process of Transitional Boiling

distributed over a spectrum of wave lengths.

It was seen in Section IV-2 that the growth rates and wave lengths which are obtained by two-dimensional considerations are in good agreement with experimental results. It appears, therefore, that the essential characteristics of the physical process are well described by two-dimensional equations. In view of the above agreement we shall, in what follows, make use of this two-dimensional thought model. The analysis can be easily extended to three dimensions. Indeed, the three-dimensional frequency equation was published by Maxwell (Reference 50, Page 461).

It was seen in Section IV-1 that for a two-dimensional system all perturbations with wave lengths longer than the critical one, i.e., than λ_{o1}, are unstable. For an interface which has random initial perturbations it can be expected that, because of the initial exponential growth, wave lengths near the "most dangerous" one, i.e., near λ_{02}, will be the first to achieve finite observable amplitude. In line with the experiments of Lewis and of Allred and Blount, the interface will consist of spikes of liquid and of rounded regions similar to cylindrical bubbles which rise into the liquid. Therefore, as a consequence of Taylor instability a definite geometrical configuration in

transitional boiling can be expected (see Figure IV-1.b).
This chape of the interface is shown by the photograph
on Figure 10.4 in Reference 105. For a two-dimensional
system this geometry should be characterized by distur-
bances with wave lengths in the spectrum

$$\Lambda_{o1} \leq \Lambda_o \leq \Lambda_{o2} \qquad \text{IV-10}$$

In contrast to nucleate boiling, where the dis-
turbances of the superheated liquid film originate at
randomly distributed nucleating centers, in transitional
boiling the disturbances occur away from the surface and
are selected by the properties of the fluid field.

In their downward fall the spikes approach the
heated surface and rapid evaporation occurs. As liquid
evaporates from the spikes the vapor flows in the region
between two spikes. It was noted that this region
resembles rising bubbles (see Figure IV-1.c). The same
form of the interface is shown by the photographs on
Figure 7, Reference 1, and on Figures 3.6, 3.7, 3.8,
and 3.9 in Reference 95. These and other photographs
are reproduced in Reference 88. Thus in transitional
boiling because of Taylor instability a release of
bubbles at regular intervals can be expected.

As a row of bubbles is released an unstable interface is formed again. Because of the downward flow of the liquid a spike will be formed now underneath the released bubble and the process is renewed (see Figure IV-1.d). The successive rows of bubbles will appear displaced therefore by half a wave length (see Figure IV-1.e). To quote Westwater and Santangelo, "the bubbles are similar to marchers arranged in triangular spacing." This spacing is shown by photographs on Figure 8, Reference 1, and on Figure 14.3, Reference 106.

The alternate interchange of position between the spikes and the rounded cylindrical bubbles bears similarity to the phenomenon known as Faraday's crispations which is discussed by Rayleigh (107). We shall quote his description of the phenomenon. When a horizontal plate on which liquid is spread is set to vibrate, "the motion of the liquid interface consists of two sets of stationary vibrations superposed, the ridges and furrows of the two sets being perpendicular to one another and usually parallel to the edges of the plate . . . At one moment the ridges form a set of parallel and equidistant lines, the interval being λ . Midway between these are the lines which represent, at that moment, the position of the furrows. After a lapse of a 1/4 period, the surface is flat; after another 1/4

period, the ridges and furrows are again at their maximum development but the positions are exchanged."

In the region of transitional boiling close to the critical heat flux, the rates of evaporation are high. Consequently, the release of bubbles will resemble small explosions or bursts of vapor (see Figure IV-1.f). A similar form of the interface is shown by photographs on Figures 4 and 5 in Reference 1 and Figure 5.6 in Reference 95. The mushrooming of the interface during the growth of Taylor instability was observed in the experiments by Allred and Blount who noted: "It seems reasonable to ascribe this effect to the Helmholtz instability, in view of the fact that the necessary velocities for the production of Helmholtz instability are present." A similar effect can be expected to take place in transitional boiling at high heat flux densities when large rates of evaporation occur, i.e., when the velocities in the vapor phase are large. This aspect of the problem will be analyzed in Chapter VI.

It was observed that the geometry of the interface in transitional boiling is determined by the properties of the fluid field. Inasmuch as the factors which influence the "most dangerous" wave length will remain constant at a given pressure, it can be expected that, in transition boiling, changes in heat transfer rates

are associated with changes in the frequency of bubble release, i.e., of the vapor bursts. The critical heat flux and the minimum heat flux correspond, therefore, to the maximum and the minimum frequencies of the system. At a given heat flux the process of transitional boiling can continue indefinitely; it is therefore thermally stable. However, it is hydrodynamically unstable; indeed, it is this instability which is the cause of the phenomenon.

In this chapter we have qualitatively analyzed the hydrodynamic aspects of transitional boiling. It was seen that experimental results of transitional boiling can be understood and interpreted in terms of Taylor instability. We shall summarize now the results of this chapter.

1) As a consequence of Taylor instability a definite geometrical configuration can be expected in transitional boiling. For a two-dimensional system this geometry is characterized by disturbances with wave length in the spectrum.

2) As a consequence of the exponential character of the instability it can be expected that the interface takes the form of spikes of heavy liquid moving downward and of rounded

regions of lighter fluid moving upward.

3) As a consequence of the definite geometrical configuration a release of bubbles from the interface at regular intervals can be expected. For large evaporation rates the release of a bubble will appear as a burst.

4) Because of the release of vapor and of Taylor instability the process exhibits, also, a periodicity in time. The phenomenon is hydrodynamically unstable but thermally stable.

5) Inasmuch as the factors which influence the geometry remain invariant, it can be expected that, in transitional boiling, changes in heat transfer rates are associated with changes in frequency only. The critical heat flux and the minimum heat flux correspond, therefore, to the maximum and the minimum allowable frequencies of the system.

In the chapters which follow, the problem will be formulated mathematically and the results quantitatively compared to experimental data.

CHAPTER V

THE MINIMUM HEAT FLUX DENSITY IN TRANSITIONAL BOILING FROM A HORIZONTAL SURFACE

The geometrical regularity and the periodicity of the process of transitional boiling was discussed in the preceding chapter. It was noted that inasmuch as the geometry should remain invariant, changes of heat transfer rates should be associated only with changes of the frequency of the system. The phenomenon thus bears a similarity to a release of bubbles from a set of orifices of fixed geometry but with a variable frequency. Although, at first, this similarity appears to be rather tenuous the agreement of the detail and the gross characteristics of the idealized system with experimental data seems to support it. The problem is, therefore, to determine the geometry of "orifices" and the maximum and minimum frequency of the releases. According to the hypothesis, these frequencies should correspond to the maximum (critical) and to the minimum heat transfer rates in transitional boiling from a horizontal surface. In this chapter we shall analyze the minimum heat flux density; the critical heat flux

density is taken up in Chapter VI.

V-1. Minimum Heat Flux Density - Formulation and Solution of the Problem

In order to formulate the problem a simplifying idealization must be made concerning the form of the vapor slugs which are released from the vapor liquid interface. Westwater and Santangelo observed (see Section IV-3) that the disturbed vapor liquid interface breaks at the nodes. It will be assumed therefore in what follows that the vapor slugs can be approximated by spheres of radius

$$R = \frac{\Lambda_o}{4} \qquad\qquad V-1$$

For the two dimensional thought model* it follows from Equation IV-10 that the diameter is given within the limits

$$\pi\left[\frac{\sigma}{g(\rho_L - \rho_v)}\right]^{1/2} \leq D \leq \pi\left[\frac{3\sigma}{g(\rho_L - \rho_v)}\right]^{1/2} \qquad V-2$$

---

* See Section IV-4 for the discussion concerning the two-dimensional approximation.

The mass of vapor associated with one vapor slug is

$$G = \rho_v \frac{4\pi}{3} \left(\frac{\lambda_o}{4} \right)^3 \qquad \text{V-3}$$

Denoting the frequency of bubble release by f, the number of bubbles released per unit time is

$$m = \frac{a}{\lambda_o} \cdot \frac{b}{\lambda_o} f \qquad \text{V-4}$$

where a·b is the area of interest. The vapor flow rate per unit area is obtained from Equation V-4 and V-3, thus

$$\overset{o}{M} = \rho_v \frac{\pi}{48} \lambda_o f \qquad \text{V-5}$$

The heat transfer is obtained from an energy balance. In transitional boiling of liquids at saturation the only energy requirements of the system is the energy needed to generate the vapor flux density given by Equation V-5. Therefore the heat transfer rate from a horizontal surface in transitional boiling of liquids at saturation is

$$q = L \, \rho_v \, \frac{\pi}{48} \, \Lambda_o \, f \qquad \qquad \text{V-6}$$

At a constant pressure the geometry does not change; Equation V-6 can be written as

$$q = (constant) \cdot f \qquad \qquad \text{V-7}$$

The problem now is to determine the frequency of bubble release f, for the minimum heat flux density. It was discussed in the preceding chapter that at the minimum heat flux the rates of evaporation are low, consequently in this region small velocities in the vapor phase can be expected. In the absence of dynamic effects of the vapor phase, the rate of penetration of the rounded vapor regions into the liquid (see Figure IV-1.c) cannot be faster than that which is predicted by Taylor instability. In other words, at the minimum heat flux in transitional boiling from a horizontal surface, the frequency of release of bubbles from the vapor-liquid interface cannot be slower than that which would be expected by considering the effect of Taylor instability only. The relation between the frequency of bubble release f, and the rate of penetration of the interface $d\eta/dt$, then becomes

$$f = \frac{2}{\Lambda_o} \frac{d\eta}{dt} \qquad\qquad \text{V-8}$$

The above relation implies that bubbles follow one another very closely in a strip of width Λ_o, which extends from the heating surface into the liquid (see Figure IV-1.e). The photograph on Figure 14-3 in Reference 106 confirms the validity of this approximation.

To make use of Equation V-8 we have to determine the value $d\eta/dt$. It was discussed in Sections IV-1 and IV-2, that the growth of Taylor instability passes through several stages. During the initial stage the growth rate can be predicted from the linearized theory, whereas during the final stage the rate of growth can be approximated by Equation IV-9. We shall express the frequency in terms of both growth rates.

Consider the "most dangerous" wave length Λ_{02}. If the amplitude H_o, of the disturbance η, was known then Equation IV-7 could be used to estimate the time which is required for the disturbance to reach a value of $\eta_m = \Lambda_{02}/2$. This method was used by Birkhoff (Reference 97, Page 41) in analyzing the penetration of a disturbance. However, in boiling the values of H_o are not reported. In order to estimate the initial rate

of growth we shall make use of the experimental obser-
vation of Lewis (94) that the amplitude increases at an
exponential rate until it reaches a value of $\eta = 0.4\lambda$
(see Section IV-2). From Equation IV-7 the rate of
growth during the initial stage is given by:

$$\frac{d\eta}{dt} = \beta\,\eta_m \qquad\qquad \text{V-9}$$

During the exponential growth the disturbance η_m
increases from an infinitesimally small value to approxi-
mately $0.4\,\lambda_{02}$. The average velocity corresponding to
this average disturbance is

$$\overline{\frac{d\eta}{dt}} = \beta\,\frac{0.4\,\lambda_{02}}{2} \qquad\qquad \text{V-10}$$

Substituting Equations V-10 and IV-8 into Equation V-8,
the estimated frequency of bubble release becomes

$$f = 0.4\beta = 0.4\left[\frac{2}{3}\,\frac{g(\rho_L - \rho_v)}{\rho_L + \rho_v}\right]^{1/2}\left[\frac{g(\rho_L - \rho_v)}{3\sigma}\right]^{1/4} \qquad \text{V-11}$$

From Equations V-6 and V-11 the estimated minimum heat
flux density is then given by

$$q = L\rho_v \frac{\pi}{48} \; 2\pi \left[\frac{3\sigma}{g(\rho_L-\rho_v)}\right]^{1/2} 0.4 \left[\frac{2}{3}\frac{g(\rho_L-\rho_v)}{\rho_L+\rho_v}\right]^{1/2} \left[\frac{g(\rho_L-\rho_v)}{3\sigma}\right]^{1/4} \quad \text{V-12}$$

or

$$q = L\rho_v \frac{\pi}{24} \left(\frac{\pi \; 0.4 \sqrt{2}}{(3)^{1/4}}\right) \left[\frac{\sigma g(\rho_L-\rho_v)}{(\rho_L+\rho_v)^2}\right]^{1/4} \quad \text{V-13}$$

We shall now use the growth rate of the final
stage, i.e., Equation IV-9 to estimate the frequency
and the heat flux density. Including the effect of
buoyancy in Equation IV-7 and substituting Equation V-1
for the radius of curvature r_o, Equation IV-9 becomes

$$u = \frac{2}{3} \left[\frac{\lambda_o}{4} \frac{g(\rho_L-\rho_v)}{\rho_L}\right]^{1/2} \quad \text{V-14}$$

The frequency is obtained from Equation V-14 and V-8, thus,

$$f = \frac{2}{3}\left[\frac{g(\rho_L - \rho_v)}{\rho_L}\frac{1}{\Lambda_\omega}\right]^{1/2}$$

V-15

Because of the spectrum of unstable disturbances, the wave length in the above expression can be determined between the limits given by Equation IV-10, i.e., by Equations IV-4 and IV-5. It follows from Equation V-15, IV-4 and IV-5 that the frequency can be determined within the limits

$$\frac{2}{3}\left[\frac{g(\rho_L - \rho_v)}{\rho_L}\frac{1}{2\pi}\left(\frac{g(\rho_L - \rho_v)}{3\sigma}\right)^{1/2}\right]^{1/2} \leq f \leq$$

V-16

$$f \leq \frac{2}{3}\left[\frac{g(\rho_L - \rho_v)}{\rho_L}\frac{1}{2\pi}\left(\frac{g(\rho_L - \rho_v)}{\sigma}\right)^{1/2}\right]^{1/2}$$

Consequently the period can be estimated within the range

$$\frac{3}{2}\left[\frac{\rho_L}{g(\rho_L - \rho_v)}\cdot 2\pi\left(\frac{\sigma}{g(\rho_L - \rho_v)}\right)^{1/2}\right]^{1/2} \leq \tau \leq$$

V-17

$$\leq \frac{3}{2}\left[\frac{\rho_L}{g(\rho_L - \rho_v)}\cdot 2\pi\left(\frac{3\sigma}{g(\rho_L - \rho_v)}\right)^{1/2}\right]^{1/2}$$

Equations V-4 and V-16 give the range of the minimum heat flux, thus

$$L\rho_v \frac{\pi}{48} \Lambda_o \frac{2}{3} \left[\frac{g(\rho_L - \rho_v)}{\rho_L} \frac{1}{\Lambda_{o1}} \right]^{1/2} \leq q \leq$$

$$q \leq L\rho_v \frac{\pi}{48} \Lambda_{o2} \frac{2}{3} \left[\frac{g(\rho_L - \rho_v)}{\rho_L} \frac{1}{\Lambda_{o2}} \right]^{1/2} \quad \text{V-18}$$

Hence from Equations IV-4 and IV-5 it follows that

$$L\rho_v \frac{\pi}{24} \frac{\sqrt{2}\pi}{3} \left[\frac{\sigma g(\rho_L - \rho_v)}{\rho_L^2} \right]^{1/4} \leq q$$

$$q \leq L\rho_v \frac{\pi}{24} \frac{\sqrt{2}\pi}{3} (3)^{1/4} \left[\frac{\sigma g(\rho_L - \rho_v)}{\rho_L^2} \right]^{1/4} \quad \text{V-19}$$

By comparing Equation V-19 to V-13 and Equation V-16 to V-11, it is seen that they exhibit identical dependence upon physical properties. These equations vary only in the values of the numerical constants; the variations being of the order of unity. We note also that the above equations are of the same form as those which have been reported in Reference 86 and 88. The latter ones were derived by considering the similarity between the oscillations of the interface in transitional boiling and the Faraday's crispations, a similarity

which was noted in Section IV-4.

In the section which follows we shall compare theoretical predictions to experimental data.

V-2. The Minimum Heat Flux Density - Comparison of Analytical with Experimental Results

In the following, the theoretical predictions are compared with experimental data for boiling methanol at atmospheric pressure reported by Westwater and Santangelo (1).

The Diameter of Bubbles at the Minimum Heat Flux

	Analysis (inches)	Experiment (inches)
Equation V-2	$0.2 \leq D \leq 0.345$	$0.2 \leq D \leq 0.36$

The Period at the Minimum Heat Flux

	Analysis (seconds)	Experiment (seconds)
Equation V-11	$\tau = 1/f = 0.052$	0.06
Equation V-17	$0.048 \leq \tau \leq 0.063$	

The Minimum Heat Flux in Transition Boiling

	Analysis (Btu/hr ft^2)	Experiment (Btu/hr ft^2)
Equation V-13	q = 8740	q = 5470
Equation V-19	$5500 \leq q \leq 7100$	

It appears from the above comparisons that this simple idealized system exhibits the detailed and general features of the observed phenomenon. The spectrum of bubble diameters as determined from experiments tends to support the original assumption concerning the spectrum of unstable disturbances and the approximation related to the form of the vapor slugs. The frequency of bubble release and the minimum heat flux density determined from the theory are in close agreement with experimental data. Thus, the description and statements concerning transition boiling which were shown, in the preceding chapter, to be in qualitative agreement are also in quantitative agreement with experimental data.

It should be noted that this agreement was achieved by two dimensional considerations; further experiments should indicate whether a three dimensional modification is necessary. Further experiments in transitional

boiling should be performed in order to investigate, in detail, the growth of a disturbance during both the exponential stage and the final stage of penetration.

We shall proceed with an analysis of the critical heat flux.

CHAPTER VI

THE CRITICAL HEAT FLUX IN BOILING
FROM A HORIZONTAL SURFACE

The region of the critical heat flux was discussed
in Section III-7. It was seen that the phenomenon occurs
at some critical velocity in the vapor phase when the
vapor jets start interferring with each other. It was
seen also that because of the spreading of the patches
of transitional boiling the region of the critical heat
flux corresponds to a plateau in the q -ΔT plane. This
region is clearly shown by the experimental results of
Perkins and Westwater (25). Consequently, an analysis
of the critical heat flux can be undertaken at either
end of this plateau. Because the flow configuration in
nucleate boiling is not well defined, an analysis of the
critical heat flux performed by considering nucleate
boiling is reduced to dimensional analysis. It was seen
in the preceding chapter that, because of Taylor insta-
bility, a definite geometrical configuration can be
expected in transitional boiling. We shall make use of
this defined geometry and analyze, therefore, the critical
heat flux by considering transitional boiling.

VI-1. The Critical Heat Flux - Formulation and Solution of the Problem

It was discussed in the preceding chapter that in transitional boiling at high flux densities the release of bubbles appears like vapor explosions. As the interface rushes toward the surface rapid evaporation starts, the interface is pushed violently back, and the vapor is released in the form of explosive jets (see Figure IV-1.f). The process is repeated indefinitely and, as in "flooding", the whole system oscillates at some characteristic frequency. In Section IV-4 the observation of Allred and Blount was quoted which related the mushrooming form of the interface (see Figure IV-1.f) to Helmholtz instability. A similar effect can be expected to take place at the critical heat flux when, because of the large rates of evaporation, the velocity of the vapor phase is large. Thus, at the critical heat flux the dynamic effect of the vapor phase upon the motion of the interface become s important. This is in contrast to the minimum heat flux where this dynamic effect is negligible. Whereas the minimum heat flux is characterized by Taylor instability only, the critical heat flux is characterized by the combined effects of Taylor and Helmholtz instabilities. In order to formulate the problem it is necessary to determine in what way these instabilities manifest

themselves and interact.

It was noted that the phenomenon of transitional boiling, because of Taylor instability, bears similarity to a release of bubbles with variable frequency from a set of regularly spaced orifices of fixed geometry. In accordance with the hypothesis, at the critical heat flux the frequency reaches a maximum and the release resembles explosive vapor jets. In view of Taylor instability we are lead, therefore, to consider vapor columns of width, $\Lambda_o/2$, spaced Λ_o units apart. In view of Helmholtz instability we have to investigate the stability of such a jet. In accordance with the previous analysis the stability of a two-dimensional system is investigated again.

Consider a coordinate system in which the direction y is parallel to the surface and z is perpendicular to the surface. Let the plane y = 0 denote an interface between the vapor leaving the heated surface and the fluid rushing toward it. For a vortex sheet which oscillates under the influence of surface tension, the propagation equation of a small disturbance is given by Lamb (50) and Milne-Thomson (99):

$$c^2 = \frac{\sigma m}{\rho_L + \rho_v} - \frac{\rho_L \rho_v}{(\rho_L + \rho_v)^2} (U_v + U_L)^2 \qquad \text{VI-1}$$

The condition of stability is that C shall be real.

The velocity in the liquid phase is obtained from the continuity

$$\rho_V U_V = \rho_L U_L \qquad \text{VI-2}$$

Substituting U_L from Equation VI-2 into Equation VI-1 the critical velocity in the vapor phase is then obtained, thus

$$U_V = \left[\frac{\sigma m}{\rho_V}\right]^{1/2} \left[\frac{\rho_L}{\rho_L + \rho_V}\right]^{1/2} \qquad \text{VI-3}$$

It is noted that if, in a three-dimensional problem, the continuity equation was corrected for the areas occupied by the vapor and the liquid, the right hand side of Equation VI-3 would be multiplied by the factor $\rho_L (16-\pi) + \rho_V \pi / \rho_L (16-\pi)$. The value of this factor is unity and it is omitted therefore.

We have to determine now the value of the wave number m in Equation VI-3. Rayleigh (107) has examined the stability of a circular gas jet in a liquid. For a disturbance with axial symmetry the instability occurs only for disturbances whose wave length is longer than the circumference of the jet. Thus, the critical wave length is given by

$$\Lambda = 2\pi R \qquad\qquad \text{VI-4}$$

where R is the radius of the jet. If the jet is to break
into spheres, it can be expected that the wave lengths
will be of the same order of magnitude axially as circum-
ferentially. Expressing therefore the wave number m in
Equation VI-3 in terms of the wave length Λ , given by
Equation VI-4, the critical vapor velocity then becomes

$$\mathcal{U}_v = \left[\frac{\sigma}{\rho_v R}\right]^{1/2} \left[\frac{\rho_L}{\rho_L + \rho_v}\right]^{1/2} \qquad\qquad \text{VI-5}$$

In Appendix I, the above equation is derived by
considering the stability of a circular jet. It was
assumed that the radius R, of the vapor column was given
by $\Lambda_0/2$; substituting this value in Equation VI-5 it
follows that

$$\mathcal{U}_v = \left[\frac{\sigma\,4}{\rho_v \Lambda_0}\right]^{1/2} \left[\frac{\rho_L}{\rho_L + \rho_v}\right]^{1/2} \qquad\qquad \text{VI-6}$$

The mass flow rate associated with one vapor
column is:

$$G = \rho_v \pi \left(\frac{\Lambda_0}{4}\right)^2 U_v \qquad \text{VI-7}$$

The vapor mass flow rate per unit area is obtained from Equations VI-6 and VI-7, thus

$$\dot{M} = \rho_v \frac{\pi}{16} \left[\frac{\sigma 4}{\rho_v \Lambda_0}\right]^{1/2} \left[\frac{\rho_L}{\rho_L + \rho_v}\right]^{1/2} \qquad \text{VI-8}$$

Expressing the wave length Λ_0 in Equation VI-8 in terms of the wave number m_0, it follows that

$$\dot{M} = \rho_v \frac{\pi}{24} \frac{3}{\sqrt{2\pi}} \left[\frac{\sigma m_0}{\rho_v}\right]^{1/2} \left[\frac{\rho_L}{\rho_L + \rho_v}\right]^{1/2} \qquad \text{VI-9}$$

For liquids at saturation temperature the only energy requirement of the system is the energy needed to generate the vapor flux density given by Equation VI-9. Therefore the critical heat flux density in pool boiling from a horizontal surface is

$$q = L \rho_v \frac{\pi}{24} \frac{3}{\sqrt{2\pi}} \left[\frac{\sigma m_0}{\rho_v}\right]^{1/2} \left[\frac{\rho_L}{\rho_L + \rho_v}\right]^{1/2} \qquad \text{VI-10}$$

It was seen in Section V-2 that experimental data supported the assumption concerned with the spectrum of unstable disturbances given by Equation V-2. Because of this spectrum the wave number m_0 can be determined within the range

$$\left[\frac{4(\rho_L-\rho_v)}{\sigma}\right]^{1/2} \geqslant m_0 \geqslant \left[\frac{9(\rho_L-\rho_v)}{3\sigma}\right]^{1/2} \qquad \text{VI-11}$$

The critical heat flux density is determined therefore within the limits:

$$L\rho_v \frac{\pi}{24} \frac{3}{\sqrt{2\pi}} \left[\frac{\sigma g(\rho_L-\rho_v)}{\rho_v^2}\right]^{1/4} \left[\frac{\rho_L}{\rho_L+\rho_v}\right]^{1/2} \geq q \geqslant$$

$$q \geqslant \frac{\pi}{24} \frac{3}{\sqrt{2\pi}} \frac{1}{(3)^{1/4}} L\rho_v \left[\frac{\sigma g(\rho_L-\rho_v)}{\rho_v^2}\right]^{1/4} \left[\frac{\rho_L}{\rho_L+\rho_v}\right]^{1/2} \qquad \text{VI-12}$$

Equation VI-12 can be written as

$$K_1 L\rho_v \left[\frac{\sigma g(\rho_L-\rho_v)}{\rho_v^2}\right]^{1/4} \left[\frac{\rho_L}{\rho_L+\rho_v}\right]^{1/2} \geqslant q \geqslant$$

$$q \geqslant K_2 L\rho_v \left[\frac{\sigma g(\rho_L-\rho_v)}{\rho_v^2}\right]^{1/4} \left[\frac{\rho_L}{\rho_L+\rho_v}\right]^{1/2} \qquad \text{VI-13}$$

where

$$K_1 = \frac{\pi}{24} \frac{3}{\sqrt{2\pi}} = 0.157 \qquad \text{VI-14}$$

and

$$K_2 = \frac{\pi}{24} \frac{3}{\sqrt{2\pi}} \frac{1}{(3)^{1/4}} = 0.12 \qquad \text{VI-15}$$

The algebraic mean is, therefore

$$K_m = 0.138 \qquad \text{VI-16}$$

A convenient average value for the critical heat flux can be obtained by replacing m_o in Equation VI-10 by the upper limit obtained from Equation VI-11, and by approximating the numerical constant $3/\sqrt{2\pi}$ by unity. The resulting equation is given by

$$q = \frac{\pi}{24} L\rho_v \left[\frac{\sigma g (\rho_L - \rho_v)}{\rho_v^2} \right]^{1/4} \left[\frac{\rho_L}{\rho_L + \rho_v} \right]^{1/2} \qquad \text{VI-17}$$

The value of the numerical constant in this case is:

$$K = \frac{\pi}{24} = 0.131 \qquad \text{VI-18}$$

In the section which follows, the theoretical results will be compared with experimental data.

VI-2. The Critical Heat Flux - Comparison of Theoretical with Experimental Results

It is assumed that in transitional boiling changes in heat transfer rates are associated with changes of frequency only. We shall verify this assumption first. According to this postulate and to Equation V-7, the following relation should hold in transitional boiling:

$$\frac{q_1}{q_2} = \frac{f_1}{f_2} \qquad\qquad \text{VI-1}$$

where the subscripts 1 and 2 refer to two different operating conditions.

Westwater and Santangelo have reported that for an overall temperature difference $T_w - T_o = 133°F$, and a heat transfer coefficient $h = 164$ Btu/hr ft^2 °F, the frequency was 84 bursts per second per inch length of tube. Whereas at a heat flux of $q = 5470$ Btu/hr ft^2, the frequency was 22 bursts per second per inch length. Substituting these values into Equation VI-19 it follows that

$$\frac{q_1}{q_2} = \frac{21\,800}{5470} = 3.98$$

$$\text{VI-20}$$

$$\frac{f_1}{f_2} = \frac{84}{22} = 3.82$$

As a further check of the hypothesis the ratio of the frequencies computed from the analysis will be compared with the ratio of the maximum and minimum heat flux determined from experiments.

The frequency of the bursts of vapor at the critical heat flux is obtained from the equation of continuity

$$\frac{4\pi}{3}\left(\frac{\Lambda_0}{4}\right)^3 f_c = \pi\left(\frac{\Lambda_0}{4}\right)^2 \mathcal{U}_v$$

<div align="right">VI-21</div>

hence

$$f_c = \frac{3}{\Lambda_0} \mathcal{U}_v$$

<div align="right">VI-22</div>

Substituting Equation VI-6 into Equation VI-22 and neglecting the density ratio $\rho_L + \rho_v/\rho_L$ it follows that

$$f_c = \frac{3}{\Lambda_0}\left[\frac{\sigma}{\rho_v}\frac{4}{\Lambda_0}\right]^{1/2}$$

<div align="right">VI-23</div>

The two frequencies which correspond to the disturbances Λ_{01} and Λ_{02} are obtained by substituting alternately Equation IV-4 and IV-5 into Equation VI-23, thus

$$f_{c01} = \frac{6}{\sqrt{2\pi}}\frac{1}{\Lambda_{01}}\left[\frac{\sigma g(\rho_L - \rho_v)}{\rho_v^2}\right]^{1/4}$$

<div align="right">VI-24</div>

$$f_{co2} = \frac{6}{\sqrt{2}\pi} \frac{1}{(3)^{1/4}} \frac{1}{\lambda_{o2}} \left[\frac{\sigma g (\rho_L - \rho_v)}{\rho_v^2} \right]^{1/4}$$ VI-25

The corresponding frequencies at the minimum heat flux
are given by Equation V-16; thus, after some rearrangement

$$f_{mo1} = \frac{2\sqrt{2}\pi}{3} \frac{1}{\lambda_{o1}} \left[\frac{\sigma g (\rho_L - \rho_v)}{\rho_L^2} \right]^{1/4}$$ VI-26

$$f_{mo2} = \frac{2\sqrt{2}\pi}{3} (3)^{1/4} \frac{1}{\lambda_{o2}} \left[\frac{\sigma g (\rho_L - \rho_v)}{\rho_L^2} \right]^{1/4}$$ VI-27

The ratio of the frequencies of vapor release at the
critical and minimum heat flux densities are then given by

$$\frac{f_{co1}}{f_{mo1}} = \frac{9}{2\pi} \sqrt{\frac{\rho_L}{\rho_v}}$$ VI-28

and

$$\frac{f_{co2}}{f_{mo2}} = \frac{9}{2\pi \sqrt{3}} \sqrt{\frac{\rho_L}{\rho_v}}$$ VI-29

The critical and the minimum heat flux densities
for boiling methanol were reported by Westwater and
Santangelo (1). Substituting the theoretical and experi-
mental values in Equation VI-19 the following result is
obtained

	Analysis	Experiment
Equation VI-28	$\dfrac{f_{col}}{f_{mol}} = 35.3$	$\dfrac{q_{crit}}{q_{min}} = \dfrac{172000}{5470} = 31.4$
Equation VI-29	$\dfrac{f_{co2}}{f_{mo2}} = 20.6$	

It appears from this comparison and from Equation
VI-20 that experimental results tend to support the hypo-
thesis that in transitional boiling changes of heat
transfer are associated with changes of frequency only.

We shall compare now the critical heat flux densities
predicted by the theory with experimental data. Inasmuch
as the square root term in Equations VI-12 and VI-17 is
close to unity except in the neighborhood of the thermo-
dynamic critical state, it is seen that both Equations
III-9 and III-12 are of the same form as Equation VI-12.
The agreement of the heat transfer rates predicted by
Equation III-9 with experimental data was discussed in
Section III-3; this agreement is shown also on Figure III-3.
Therefore, for a comparison of the present analysis with
experiments it suffices to compare the value of the

coefficients K determined analytically with the values determined by Kutateladze and Borishanskii from experiments.

<u>Analysis</u>   <u>Experiment</u>

Equation VI-13 $0.12 \leq K \leq 0.157$ Kutateladze

                                        $K = 0.16$

Equation VI-17 $K = \dfrac{\pi}{24} = 0.131$ Borishanskii

                                         $K = 0.13$

The values of the constant K given by the theoretical limits

$$\frac{\pi}{24} \frac{3}{\sqrt{2\pi}} = 0.157 \geqslant K \geqslant 0.12 = \frac{\pi}{24} \frac{3}{\sqrt{2\pi}} \frac{1}{(3)^{1/4}}$$

are indicated on Figure III-3.

In Figure VI-1 the heat transfer rates predicted by Equation VI-17 are compared with experimental data for water by Kazakova (108). Another comparison with experimental data for ethanol reported by Cichelli and Bonilla (82) is shown on Figure VI-2.

It appears from the above comparisons that this simple idealized system exhibits the detailed and general features of the phenomenon. It is interesting to note that the analysis predicts an inherent uncertainty in determining the exact heat flux. The width of this uncertainty band is approximately $\pm$ 14%. It follows from the theory that a certain irreproducibility of the experimental results can be expected. The scatter of experi-
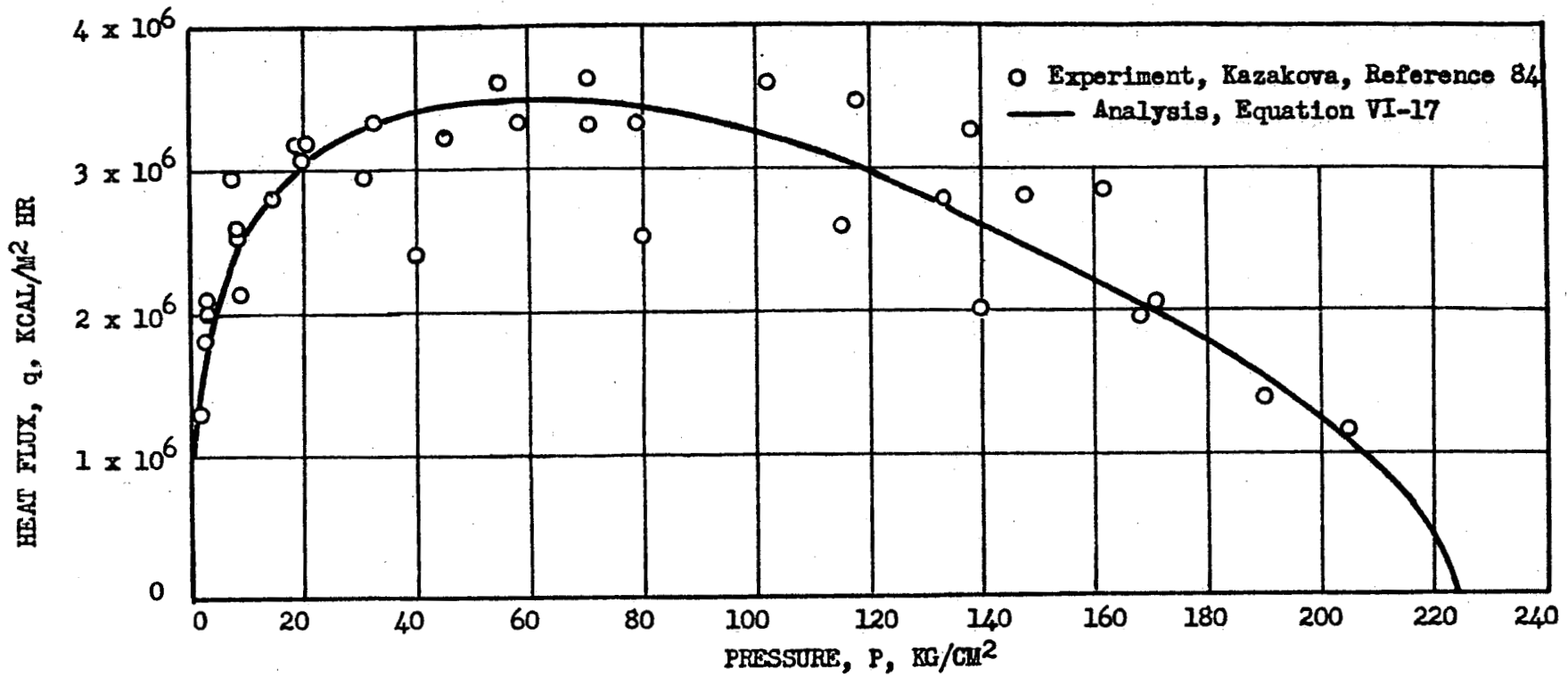
FIGURE VI-1. COMPARISON OF PREDICTED WITH EXPERIMENTALLY DETERMINED CRITICAL
HEAT FLUX DENSITIES IN POOL BOILING FOR WATER AT SATURATION TEMPERATURE
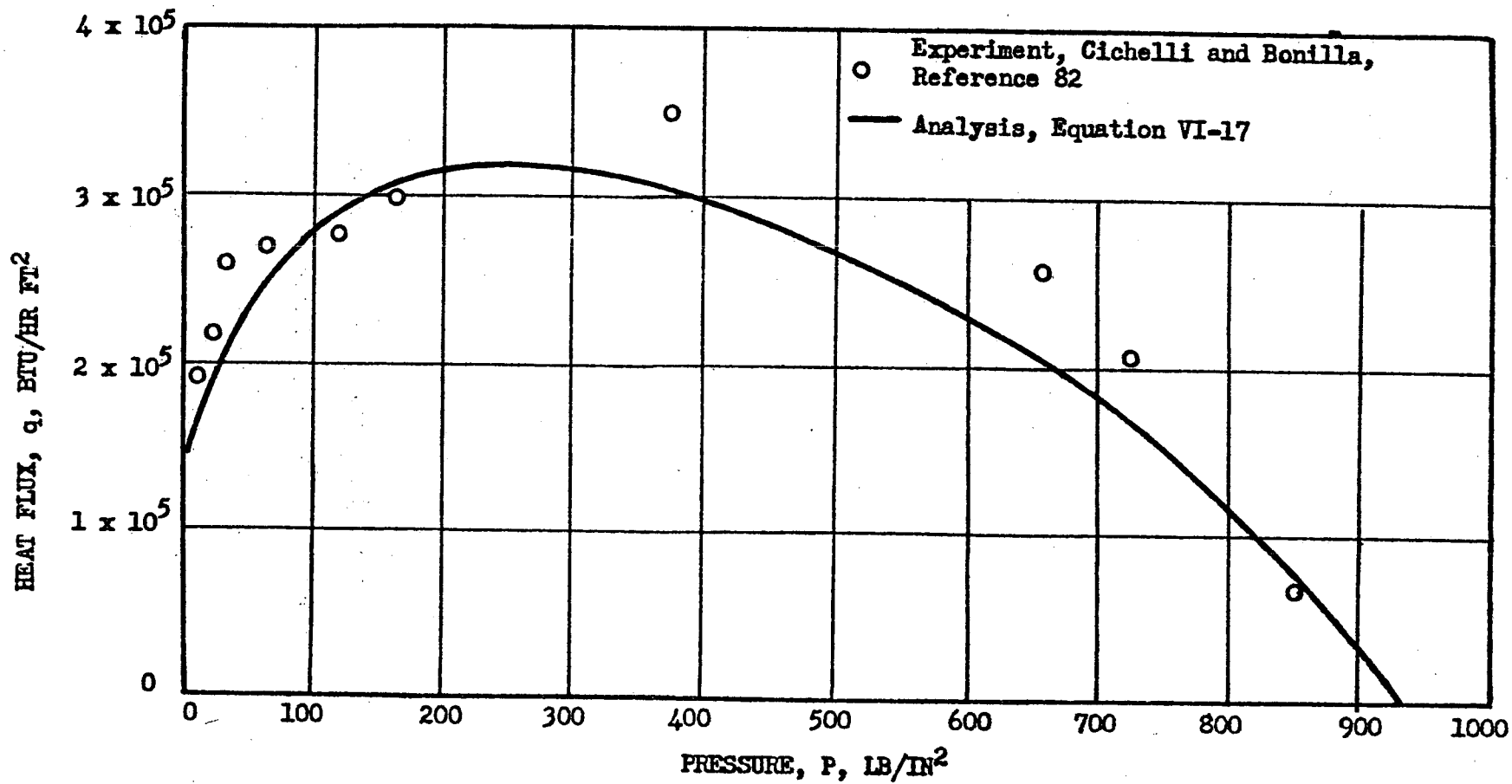
FIGURE VI-2. COMPARISON OF PREDICTED WITH EXPERIMENTALLY DETERMINED CRITICAL HEAT
FLUX DENSITIES IN POOL BOILING FOR ETHYL ALCOHOL AT SATURATION TEMPERATURE

mental data is often reported in the literature.

In the following section the analysis will be extended to transition boiling of subcooled liquids.

VI-3. The Critical Heat Flux in Pool Boiling of a Subcooled Liquid

Equations VI-12 and VI-17 which predict the critical heat flux were determined from stability consid- erations and an energy balance for liquids at saturation temperature. To extend the analysis to subcooled liquids a basic assumption will be made: The change from nucleate to transitional boiling is determined only by the hydro- dynamic stability; in pool boiling, i.e., in the absence of a forced flow, the change occurs when the vapor flux attains a given value. Therefore, if the liquid is at saturation and the viscosity is neglected, the heat transferred across the solid surface is equal to the energy required for the generation of that particular vapor mass flow. Since the stability is the mechanical aspect of the problem it will be unaffected by whether the liquid is subcooled or not, but will depend only on the mass transport. However, as the heat flux across the solid surface is determined by an energy balance it will depend on the subcooling. Therefore all energy requirements will appear as additive terms to the energy needed for the generation of the critical vapor flow. The problem

is reduced now to the determination of energy requirements associated with a boiling, subcooled liquid.

In transitional boiling the vapor-liquid interface is at saturation temperature; when the bulk liquid is subcooled, the problem is to determine the energy transferred from the interface to the bulk liquid. It was discussed in the preceding sections that in transitional boiling vapor is periodically released from the interface. Because of this release both the interface and the temperature distribution are periodically renewed. The process can be described therefore by the "discontinuous film model" which was discussed in Section III-8. If the assumption is made that the "contact time" is short compared to the ratio of the scale of turbulence to the intensity of turbulence, the energy will be transferred mainly by conduction. This is equivalent, therefore, to the assumption that the "depth of penetration" is small compared to the "scale of turbulence." Assuming a plane interface the energy problem is described by Equation II-2. In transitional boiling to a given heat flux there corresponds a given frequency. Consequently, the average heat flux from the interface to the bulk liquid is given by Equation III-17 (instead of Equation III-18), thus

$$q = 2 \kappa \frac{(T_S - T_L)}{\sqrt{\pi a \tau}} \qquad \text{VI-30}$$

where $\mathcal{T}$ is the period. In References 87 and 88 the equations which correspond to Equations II-4 and VI-30 of this dissertation were multiplied by the factor $b = \pi/2$ (see Section II-1) in order to account for the distortion of the interface. Experimental data of Kutateladze and Schneiderman (109) indicate that this correction is not needed. The factor b is omitted therefore from Equation VI-30. Expressing the period in terms of the frequency given by Equation VI-24, Equation VI-30 becomes

$$q_2 = 2 \kappa \frac{(T_s - T_L)}{\sqrt{\pi a}} \sqrt{f_{col}} \qquad \text{VI-31}$$

The heat transferred across the solid surface is obtained again from an energy balance, i.e., by adding Equations VI-17 and VI-31. Consequently the critical heat flux in subcooled, pool boiling from a horizontal surface is given by

$$q_{c.s.} = L \rho_v \frac{\pi}{24} \left[\frac{\sigma g (\rho_L - \rho_v)}{\rho_v^2} \right]^{1/4} + \frac{2 \kappa (T_s - T_L)}{\sqrt{\pi a}} \sqrt{f_{col}} \qquad \text{VI-32}$$

where

$$f_{c01} = \frac{6}{\sqrt{2\pi}} \frac{1}{\Lambda_{01}} \left[\frac{\sigma g (\rho_L - \rho_v)}{\rho_v^2} \right]^{1/4} \qquad \text{VI-33}$$

$$\Lambda_{01} = 2\pi \left[\frac{\sigma}{g(\rho_L - \rho_v)} \right]^{1/2} \qquad \text{VI-34}$$

In Figure VI-3 the heat transfer rates predicted by Equation VI-31 are compared to the experimental data reported by Gunther and Kreith (7) for water boiling at atmospheric pressure from a horizontal surface. A comparison is shown also with experimental results for ammonia and carbon tetrachloride reported by Bartz (110) and by Ellion (15). The experimental data of Kutateladze and Schneiderman are reported as the ratio $q_{c.sub}/q_{c.sat}$. In order to predict this ratio we divide Equation VI-32 by Equation VI-17, thus

$$\frac{q_{c.sub}}{q_{c.sat}} = 1 + \frac{2 \kappa (T_s - T_L)}{\sqrt{\pi a}} \sqrt{f_{c01}} \frac{24}{\pi} L \rho_v \left[\frac{\rho_v^2}{\sigma g (\rho_L - \rho_v)} \right]^{1/4} \qquad \text{VI-35}$$
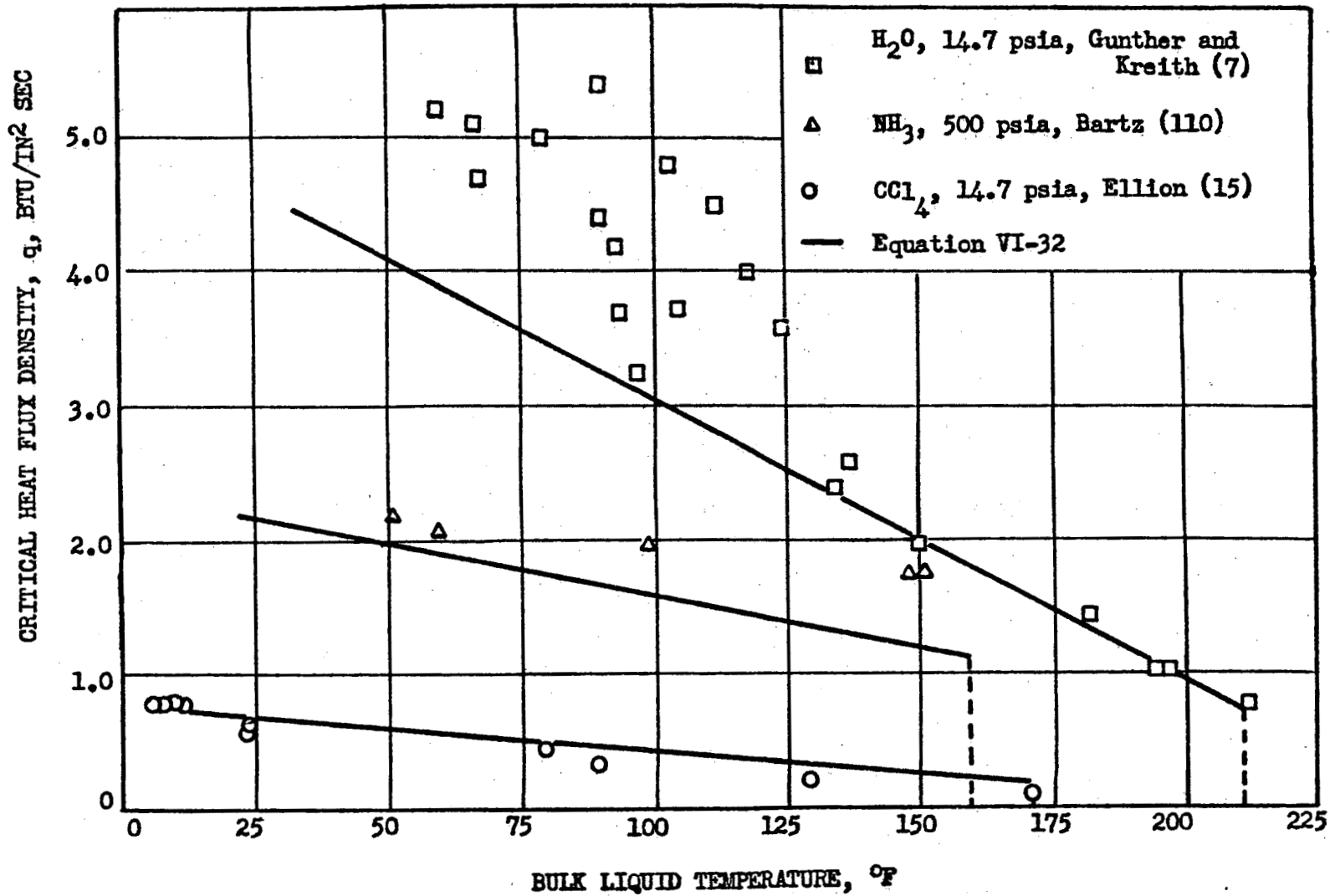
FIGURE VI-3.   COMPARISON OF PREDICTED WITH EXPERIMENTALLY DETERMINED CRITICAL
HEAT TRANSFER RATES IN POOL BOILING OF SUBCOOLED LIQUIDS

On Figures VI-4 and VI-5, Equation VI-34 is plotted together with the experimental data of Kutateladze and Schneiderman. The agreement appears to be satisfactory.

It should be noted that the interface in subcooled boiling is not plane, and the treatment of the interface as though it were a plane is introduced as the simplest idealization. However, it will follow that no matter what geometry is postulated, the form of the resulting solution is unchanged and only the numerical constant will be affected in Equation VI-33. This change will alter each of the slopes of Figures VI-3, 4 and 5 in the same way. The group $k\sqrt{f/a}$ will still determine the relative slopes for different liquids and the ratios of the slopes will be unaffected by the numerical constant. The agreement shown by Figures VI-3, 4 and 5 concerning absolute as well as relative slopes serves to indicate that the conception of the process is proper. Similar remarks apply to the use of a "contact time."

As a closing remark we note that in some experiments, in order to maintain the subcooling, the liquid is circulating slowly. The velocity of circulation is low, so that the process can be considered pool boiling. When the subcooling is low, bubbles will depart from the interface and will be removed by the circulating liquid. The mass of vapor is replaced by an equivalent
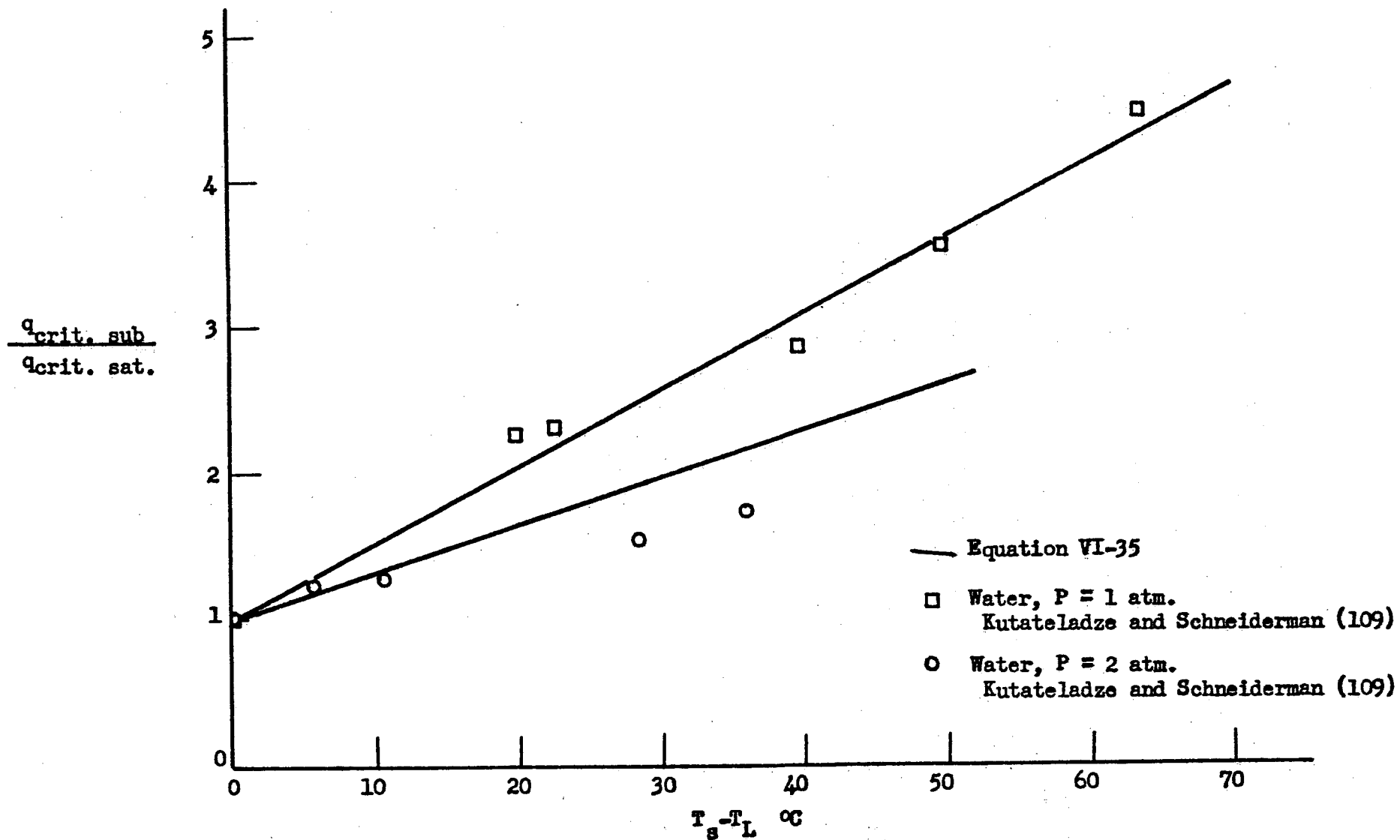
FIGURE VI-4. COMPARISON OF PREDICTED WITH EXPERIMENTALLY DETERMINED CRITICAL
HEAT TRANSFER RATES IN POOL BOILING OF SUBCOOLED WATER
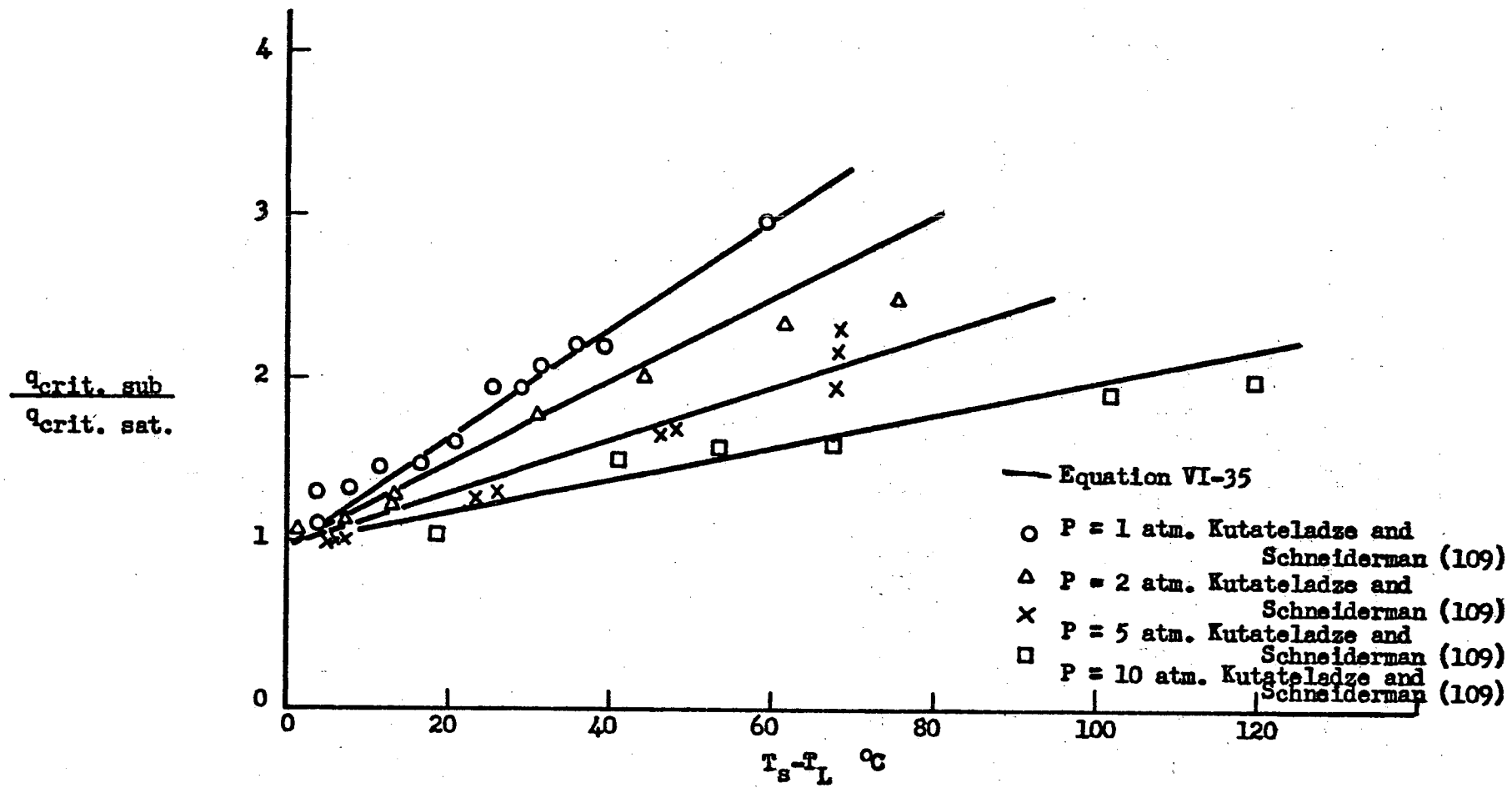
FIGURE VI-5. COMPARISON OF PREDICTED WITH EXPERIMENTALLY DETERMINED
CRITICAL HEAT TRANSFER RATES IN POOL BOILING
OF SUBCOOLED ETHYL ALCOHOL AT VARIOUS PRESSURES

mass of liquid which, as the bulk temperature is subcooled, has to be heated up to saturation temperature first before the evaporation can occur. From Equation VI-17, the critical vapor mass flow rate is given by

$$\overset{o}{M} = \rho_v \ \frac{\pi}{24} \left[\frac{\sigma g (\rho_L - \rho_v)}{\rho_v^2} \right]^{1/4}$$

VI-36

The enthalpy change ΔH, of the liquid thus becomes

$$\Delta H = \left[\frac{\pi}{24} \rho_v \left[\frac{\sigma g (\rho_L - \rho_v)}{\rho_v^2} \right]^{1/4} \right] c (T_S - T_L)$$

VI-37

Because in the experiments of Gunther and Kreith and of Kutateladze and Schneiderman the liquid did not circulate, Equation VI-37 was not included in the energy balance.

SUMMARY AND CONCLUSIONS

Chapter I. - A Review of Nucleate Boiling

The problems of nucleation from a solid surface and the dynamics of a bubble departing from the heating surface were considered. The characteristics of nucleate boiling and the relation between the heat flux density, the surface roughness and the liquid superheat temperature difference were discussed. It was seen that, in nucleate boiling, the heat flux density is not a single valued function of the temperature; in order to determine the q - T relation it is necessary to specify the characteristics of the surface.

Chapter II.- The Problem of Bubble Growth

The problem of bubble growth in a superheated liquid was discussed. It was pointed out that the original conceptual and mathematical formulation of the problem as given by Bosnjakovic and Jakob contain the essential features of the phenomenon.

The theory of Bosnjakovic and Jakob was extended to include the effects of a non-uniform temperature field; the growth rates predicted by Equations II-17 and II-30 are in satisfactory agreement with experimental data.

These equations are not adequate for predicting the collapse of a bubble in subcooled boiling. Experimental data indicate that the collapse can be approximated by an isothermal process; it can be predicted by the solution of Rayleigh's equation, i.e., by Equation II-33. Experimental data for bubbles growing and collapsing in subcooled boiling can be approximated therefore by considering the growth and collapse process separately. The growth and collapse equations are matched at the maximum bubble radius.

If a bubble is suddenly introduced into a subcooled liquid, or if the saturation temperature is suddenly increased (by increasing the pressure), then, initially, the thickness of the thermal boundary layer is much smaller than the bubble radius. Under these conditions the bubble collapse rate is given by Equation II-35.

Experimental data tend to indicate that the diameter of an active nucleating cavity can be related to the heat flux and superheat temperature by the simple relation given by Equation II-26. Further experimental investigations are needed to verify this relation.

Chapter III. - Hydrodynamic Aspects of Nucleate Boiling

The similarity between bubble formation at an orifice and bubble formation in nucleate boiling was pointed out and discussed. Using this similarity an

equation (Equation III-4 or III-5) was derived for the product bubble diameter times frequency of bubble emission in nucleate boiling. Equation III-5 was shown to be in good agreement with experimental data. From Equation III-4 it is possible to estimate the maximum frequency of bubble release in nucleate boiling. The similarity also indicates the possibility of relating (by Equation III-1 or III-6) the diameter, D_d, of a bubble departing from a heated horizontal surface to the radius, r_o, of the nucleating cavity. From such a relation it would be possible to estimate the spectrum of departing bubbles in terms of a distribution of nucleating cavities. Further experiments are needed to verify this relation.

The hydrodynamic aspects of nucleate boiling and the region of the critical heat flux were analyzed. It was seen that nucleate boiling at low heat flux densities is characterized by the presence of single bubbles; whereas the region of the critical heat flux is characterized by the presence of vapor columns and large patches of vapor.

The similarity between nucleate boiling and the bubbling of a gas from a porous plate was discussed. This similarity indicated that the change from nucleate to transitional boiling is a hydrodynamic phenomenon known as "flooding". It occurs when the stability of

two-phase flow is disrupted. It was concluded that existing correlations of experimental data can be understood only if the critical heat flux is interpreted as a "flooding" phenomenon.

Chapter IV. Hydrodynamic Aspects of Transitional Boiling

The hydrodynamic stability of a plane interface was analyzed and experimental results pertaining to Taylor instability were discussed. The hydrodynamic aspects of transitional boiling were qualitatively analyzed and the phenomenon was interpreted in terms of Taylor instability. It was concluded that, as a consequence of Taylor instability, a definite geometrical configuration can be expected in transitional boiling. As a consequence of this definite geometrical configuration, a release of bubbles occurs at regular intervals. At a constant pressure the factors which influence the geometry remain invariant. Consequently, in transitional boiling, changes in heat transfer rates are associated only with changes in the frequency of bubble release. The critical heat flux and the minimum heat flux in transitional boiling correspond, therefore, to the maximum and minimum allowable frequencies of the system.

Chapter V. - The Minimum Heat Flux in Transitional

Boiling from a Horizontal Surface

The diameters of the vapor slugs in transitional boiling were estimated by considering the critical and the "most dangerous" wave length (Equation V-2) given by Taylor instability. It was noted that, at the minimum heat flux density, the dynamic effect of the vapor phase upon the motion of the interface is small. It was concluded therefore that the rate of penetration of the vapor into the liquid cannot be faster than the rate which would be predicted from Taylor instability. Because this rate of penetration is initially exponential and later reaches a constant value, two equations (Equation V-11 and V-16) were derived for the frequency of bubble release. Using the two frequencies and making an energy balance, two equations (Equation V-13 and V-19) were derived for the minimum heat flux density in transitional boiling. The theoretical results were found to be in good agreement with experimental data.

Chapter VI. - The Critical Heat Flux Density from a

Horizontal Surface

The critical heat flux density was analyzed by considering transitional boiling. Because of large evaporation rates, at the critical heat flux, the dynamic effect of the vapor upon the motion of the

liquid-vapor interface is important. The problem was
formulated by considering the combined effect of Taylor
and Helmholtz instabilities. Analytical expressions were
derived which permit the prediction of the critical heat
flux density in pool boiling of saturated or subcooled
liquids. The numerical values of the empirical constants
which appear in the Kutateladze and Borishanskii criteria
for the critical heat flux are derived from the theory.
The theoretical results are in good agreement with
experimental data.

BIBLIOGRAPHY

1. Westwater, J. W. and J. G. Santangelo, "Photographic Study of Boiling," Ind. Engr. Chem., 47, 1955, 1605.

2. Jakob, M. and W. Fritz, "Versuche uber den Verdampfungsvorgang," Forschung, 2 Bd. Heft 12, 1931, 435.

3. Jakob, M., "Kondensation and Verdampfung," Zetschr. d. Ver. Deutsch. Ingr., Bd. 76, 1932, 1161.

4. Jakob, M. and W. Linke, "Der Wärmeübergang von einer Waagerechten Platte an Siedenes Wasser," Forschung, 4 Bd., Heft 2, 1933, 75.

5. Jakob, M., and W. Linke, "Der Wärmeübergang beim Vergampfen von Flussigkeiten an Senkrechten und Waagerechten Flächen," Phys. Zeitsch., 36, 1935, 267.

6. Jakob, M., "Heat Transfer in Evaporation and Condensation," Mech. Engr., 58, 1936, 643 and 729.

7. Gunther, F. C. and F. Kreith, "Photographic Study of Bubble Formation in Heat Transfer to Subcooled Liquids," Heat Transfer and Fluid Mechanics Inst., Berkeley, 1949, 113.

8. Rohsenow, W. and J. Clark, "A Study of the Mechanism of Boiling Heat Transfer," Trans. A.S.M.E., 73, 1951, 609.

9. Bankoff, S. G., "Ebullition from Solid Surfaces in the Absence of Pre-existing Gaseous Phases," Trans. A.S.M.E., 79, 1957, 735.

10. Clark, H. B., P. H. Strenge and J. W. Westwater, "Active Sites for Nucleate Boiling," Preprint No. 13, A.I.Ch.E.-A.S.M.E. Heat Transfer Conference, Chicago, 1958.

11. Dzhandzhgava, Sh. G., "Investigation of the Formation of Bubbles and of the Superheat," Dok. Ak. Nauk S.S.S.R., 70, No. 3, 1950, 417.

12. Nesis, E. I., "Boiling under Real Conditions," Zh. Tekh. Fiz., 22, 1952, 1506.

13. Courty, C., "Surface Variables in Nucleate Boiling," Ph. D. Thesis, Purdue Univ., Lafayette, Ind., 1952.

14. Courty, C. and A. Foust, "Surface Variables in Nucleate Boiling," Chem. Engr. Progr. Symposium, Series 51, 1955, 1.

15. Ellion, M. E., "A Study of the Mechanism of Boiling Heat Transfer," Ph. D. Thesis, Calif. Inst. Tech., 1954, Jet Prop. Lab Rept. Memo. 20-88, Calif. Inst. Tech., 1954.

16. Griffith, P. and J. D. Wallis, "The Role of Surface Conditions in Nucleate Boiling," Tech. Rept. No. 14, Mass. Inst. Tech., Dec., 1958.

17. Bankoff, S. G., "The Entrapment of Gas in the Spreading of a Liquid Over a Rough Surface," A.I.Ch.E. Journal, 4, 1958.

18. Bankoff, S. G., "The Prediction of Surface Temperatures at Incipient Boiling," Preprint 4, A.I.Ch.E.-A.S.M.E. Heat Transfer Conference, Chicago, 1958.

19. Sabersky, R. H. and C. W. Gates, "On the Start of Nucleation in Boiling Heat Transfer," Jet Propulsion, 1955, 67.

20. Treschov, G. G., "Experimental Investigation of the Mechanism of Heat Transfer in Surface Boiling," Teploenergetika, 3, No. 5, 1957, 44.

21. Wark, J. W., "The Physical Chemistry of Flotation," J. Phys. Chem., 37, 1933, 623.

22. Fritz, W., "Berechnung des Maximalvolumens von Dampfblasen," Phys. Zeitsch., 36, 1935, 379.

23. Bashforth, F. and C. Adams, An Attempt to Test the Theories of Capillary Action, Cambridge Univ. Press, 1883.

24. Fritz, W. and W. Ende, "Verdampfungsvorgang nach Kinematographischen Aufnahmen an Dampfblasen," Phys. Zeitsh., 37, 1936, 401.

25. Westwater, J. W. and A. S. Perkins, "Measurements of Bubbles Formed in Boiling Methanol," A.E.Ch.E. Jour., 2, 1956, 471.

26. Donald, M. B. and F. Haslam, "The Mechanism of the Transition from Nucleate to Film Boiling," Chem. Engr. Sc., 8, 1958, 287.

27. Yamagata, K. and K. Nishikawa, "Nucleate Boiling of Water on the Horizontal Heating Surface," Memoirs of the Faculty of Engr., Kyushu Univ., 15, No. 1, 1955.

28. Averin, E. K., "Effect of Material and Machining of Surface on Heat Transfer to Boiling Water," Izv. Akad. Nauk S.S.S.R., Otd. Tekh. Nauk No. 3, A.E.R.E. Tr. 562, 1954, 116.

29. Zysina-Molozhen, L. M., "Some Data on the Number of Centers of Vaporization in Boiling on Industrial Heating Surfaces," published in Problems of Heat Transfer During a Change of State, G. E. I., Moscow, 1953.

30. Bosnjakovic, F., "Verdampfung und Flüssigheitsüberhitzung," Tech. Mech. und Therm., Bd. 1, 1930, 358.

31. Prüger, W., "Die Verdampfungsgeschwindigkeit der Flüssigkeiten," Zeitsch. fur Physik, B-115, 1940, 202.

32. Plesset, M. and S. A. Zwick, "A Non-Steady Diffusion Problem with Spherical Symmetry," J. Appl. Phys., 23, 1952, 95.

33. Plesset, M. and J. A. Swick, "The Growth of Vapor Bubbles in Superheated Liquids," J. Appl. Phys., 25, 1954, 493.

34. Romie, F., "The Growth of Bubbles in Superheated Liquids," Memorandum, Dept. of Engr., Univ. of Calif., Los Angeles, 1952; see also M. L. Greenfield, et al., "Density Transients in Volume Heated Boiling Systems," Rept. 53-17, Dept. of Engr., Univ. of Calif., Los Angeles, 1953.

35. Forster, H. K. and N. Zuber, "Growth of a Vapor Bubble in a Superheated Liquid," J. Appl. Phys., 25, 1954, 474.

36. Dergarabedian, P., "The Rate of Growth of Vapor Bubbles in Superheated Water," J. Appl. Mech., 20, 1953, 537.

37. Birkhoff, G., R. S. Margulies, and W. A. Horning, "Spherical Bubble Growth," Phys. of Fluids, 1, 1958, 201.

38. Scriven, L. E., "On the Dynamics of Phase Growth," Report P 659, Shell Development Co., Emeryville, California, 1958.

39. Savic, P., "The Cooling of a Hot Surface by Drops Boiling in Contact with It," Nat. Res. Council of Canada, Div. of Mech. Engr., Rept. No. MT-37, April, 1958.

40. Carslaw, H. S. and J. C. Jaeger, Heat Conduction in Solids, Oxford Univ. Press

41. Treschow, G. G., "Experimental Investigation of the Mechanism of Heat Transfer in Surface Boiling," Teploenergetika, 3, 1957, 44.

42. Zmola, P., "Investigation of the Mechanism of Boiling in Liquids," Ph.D. Thesis, Purdue Univ., Lafayette, Ind., 1950.

43. Gunther, F., "Photographic Study of Surface Boiling Heat Transfer to Water with Forced Convection," Trans. A.S.M.E., 73, 1951, 115.

44. Griffith, P., "Bubble Growth Rates in Boiling," Ph.D. Thesis, Mass. Inst. Tech., 1956, Tech. Rept. No. 8, Mass. Inst. Tech., 1956, Trans. A.S.M.E., 80, 1958.

45. Bankoff, S. G. and R. D. Mikesell, "Bubble Growth Rates in Highly Subcooled Nucleate Boiling," Preprint 2, A.S.M.E-A.I.Ch.E. Heat Transfer Conference, Chicago, 1958.

46. Bankoff, S. G. and R. D. Mikesell, "Growth of Bubbles in a Liquid of Initially Nonuniform Temperature," Paper 58-A-105, A.S.M.E. Annual Meeting, New York, 1958.

47. Bankoff, S. G., Colahan, W. J., and D. R. Bartz, "Summary of Conference on Bubble Dynamics and Boiling Heat Transfer Held at the Jet Propulsion Laboratory, June 14 and 15, 1956," Jet Propulsion Lab Memo. No. 20-137, Calif. Inst. Tech., 1956.

48. Plesset M. and S. A. Zwick, "On the Dynamics of Vapor Bubbles in Liquids," J. Math. and Phys., 33, 1955, 308.

49. Zuber, N., "Boiling Heat Transfer to Subcooled Liquids," Memorandum, Dept. of Engr., Univ. of Calif. at Los Angeles, 1956.

50. Lamb, H., Hydrodynamics, Dover Publ., New York, 1957.

51. Rohsenow, W., "A Method of Correlating Heat Transfer Data for Surface Boiling of Liquids," A.S.M.E. Trans., 74, 1952, 969.

52. Rohsenow, W., "Heat Transfer with Evaporation," Heat Transfer Symposium, University of Michigan, 1952.

53. Kutateladze, S. S., Heat Transfer in Boiling and Condensation, Mashgiz, Moscow, 1952.

54. Kruzhilin, G. N., "Generalization of Experimental Data of Heat Transfer to Boiling Liquids in Free Convection," Izv. Akad. Nauk S.S.S.R. No. 3, 1949, 701, A.E.C. Translation RT 2542.

55. Kruzhilin, G. N., "Heat Transmission from a Heating Surface to a Boiling One-component Liquid in Free Convection," Izv. Akad. Nauk, Otd. Tekh. Nauk., 1948, 967, A.E.C. Translation RT 2792.

56. Sterman, L. S., "Theory of Heat Transfer in Boiling Liquids," Zh. Tekh. Fiz., 23, 1953, 342.

57. Sterman, L. S., "Investigation of Heat Exchange by Boiling Liquids in Tubes," Zh. Tekh. Fiz., 24, 1954, 2046, A.E.R.E. Translation 565.

58. Siegel, R. and G. Usiskin, "A Photographic Study of Boiling in the Absence of Gravity," A.S.M.E. Paper 59-AV-37, 1959 Aviation Conference, Los Angeles.

59. Van Krevelen, D. W. and P. J. Hoftijzer, "Studies of Gas Bubble Formation, Calculation of Interfacial Area in Bubble Contactors," Chem. Engr. Progress, 46, 1950, 29.

60. Siemes, W., "Über die Erzengung und den Aufstieg von Gasblasen in Flüssigkeiten," Chem. Ingr. Technik, 26, 1954, 479.

61. Siemes, W., "Gasblasen in Flüssigkeiten", Chem. Ingr. Techn., <u>26</u>, 1954, 614.

62. Siemes, W. and J. F. Kaufman, "Die Periodische Enstehung von Gasblasen an Dusen," Chem. Engr. Sc., <u>5</u>, 1956, 127.

63. Hughes, R. R., Handlos, A. E., Evans, H. D., and R. L. Maycock, "The Formation of Bubbles at Simple Orifices," Chem. Engr. Progress, <u>57</u>, 1955, 557.

64. Davidson, L. and E. Amick, "Formation of Gas Bubbles at Horizontal Orifices," A.I.Ch.E. Journal, <u>2</u>, 1956, 336.

65. Peebles, F. N. and H. J. Garber, "Studies on the Motion of Gas Bubbles in Liquids," Chem. Engr. Progress, <u>49</u>, 1953, 88.

66. Kutateladze, S. S. and M. A. Styrikovich, <u>Hydraulics of Air-Liquid Systems</u>, Gosenergoizdat, Moscow, 1958.

67. Jakob, M., <u>Heat Transfer</u>, Vol. 1, Wiley, New York, 1949.

68. Verschor, H., "Some Aspects of the Motion of a Swarm of Gas Bubbles Rising Through a Vertical Liquid Volumn," Trans. Inst. Chem. Engr., <u>28</u>, 1950, 52.

69. Kölbel, H. and W. Siemes, "Eigenschaften von Blasen-säulen," Dechema-Monographien, Bd. 29, 1957, 334.

70. Siemes, W. and M. Borchers, "Begassung von Flüssig-durch Porose Sintermetalle," Chem. Ingr. Tech., <u>28</u>, 1956, 787.

71. Houghton, G., McLean, A. M., and P. D. Ritchie, "Mechanism of Formation of Gas Bubble-Beds," Chem. Engr. Sci., <u>7</u>, 1957, 40.

72. Petrick, M., "Two Phase Air Water Flow Phenomena," Argonne Nat. Lab. Rept. 5787, 1958.

73. Wallis, C. and P. Griffith, "Liquid and Gas Distribution in a Two-Phase Boiling Analogy," Tech. Rept. No. 13, Mass. Inst. Tech., December 1958.

74. McAllister, R. A., McGinnis, P. H. and C. A. Plank, "Perforated Plate Performance," Chem. Engr. Sc., 9, 1958, 25.

75. Elgin, J. G. and F. B. Weiss, "Liquid Holdup and Flooding in Packed Towers," Ind. Eng. Chem., 31, 1939, 435.

76. Bonilla, C. and C. W. Perry, "Heat Transmission to Boiling Binary Liquid Mixtures," Tran. Am. Inst. Chem. Engr., 37, 1941, 685.

77. Kutateladze, S. S., "On the Transition to Film Boiling under Natural Convection," Kotloturbostroenie, No. 3, 1948, 10.

78. Kutateladze, S. S., "A Hydrodynamic Theory of Changes in the Boiling Process under Free Conduction," Izv. Akad. Nauk, S.S.S.R., Otd. Tekh. Nauk, No. 4, 1951, 529.

79. Borishanskii, V. M., "An Equation Generalizing Experimental Data on the Cessation of Bubble Boiling in a Large Volume of Liquid," Zhur. Tekh. Fiz., 25, 1956, 252. (See Soviet Physics - Technical Phys., 1, No. 2, 438.)

80. Borishanskii, V. M., "On the Problem of Generalizing Experimental Data on the Cessation of Bubble Boiling in a Large Volume of Liquids," Ts. K.T.I., 28, Moscow, 1955.

81. Rohsenow, W. and P. Griffith, "Correlation of Maximum Heat Flux Data for Boiling of Saturated Liquids," Preprint No. 9, A.S.M.E.-A.I.Ch.E. Heat Transfer Symposium, Louisville, Ky., 1955.

82. Cichelli, M. T. and C. F. Bonilla, "Heat Transfer to Liquids Boiling under Pressure," Trans. A.I.Ch.E., 41, 1945, 755.

83. Styrikovich, M. A. and G. M. Poliakov, "On the Critical Heat Load with Boiling Liquids in Large Volume," Izv. Akad. Nauk, Otd. Tekh. Nauk, No. 5, 1948.

84. Kazakova, E. A., "The Influence of Pressure on the First Crisis in Boiling Water from a Horizontal Surface," in Problems of Heat Transfer with Change of Phase, G.E.I., Moscow, 1953.

85. McCabe, W. L. and J. C. Smith, *Unit Operation of Chemical Engineering*, McGraw Hill, New York, 1956, 730.

86. Zuber, N., "Stability of Boiling Heat Transfer," Trans. A.S.M.E., 80, 1958, 711.

87. Zuber, N., "On the Maximum Heat Flux in Pool Nucleate Boiling of Subcooled Liquids," Memorandum, Dept. of Engr., Univ. of Calif. at Los Angeles, 1957.

88. Zuber, N. and M. Tribus, "Further Remarks on the Stability of Boiling Heat Transfer," Dept. of Engr., University of California at Los Angeles, Rept. 58-5, 1958, also A.E.C. Report A.E.C.U. 3631, 1958.

89. Higbie, R., "The Rate of Absorption of a Gas into a Still Liquid During Short Periods of Exposure," Trans. A.I.Ch.E., 31, 1935, 65.

90. Dankwerts, P. V., "Significance of Liquid-Film Coefficients in Gas Absorption," Ind. Engr. Chem., 43, 1951, 1460.

91. Hanratty, T. J., "Turbulent Exchange of Mass and Momentum with a Boundary," A.E.Ch.E. Journal, 2, 1956, 359.

92. Birkhoff, G. and E. H. Zarantonello, *Jets, Wakes and Cavities*, Academic Press, New York, 1958.

93. Taylor, G. I., "The Instability of Liquid Surfaces When Accelerated in a Direction Perpendicular to Their Plane," Proc. Roy. Soc. London, A-201, 1950, 192.

94. Lewis, D. J., "The Instability of Liquid Surfaces When Accelerated in a Direction Perpendicular to Their Planes II," Proc. Roy. Soc. London, A-202, 1950, 81.

95. Allred, J. C. and G. H. Blount, "Experimental Studies of Taylor Instability," Univ. of Calif. Los Alamos Sc.Lab., Rept. LA-1600, 1954.

96. Bellman, R. and R. H. Pennington, "Effects of Surface Tension on Taylor Instability," Quar. Appl. Math., 12, 1954, 151.

97. Birkhoff, G., "Taylor Instability and Laminar Mixing," Univ. of Calif. Los Alamos Sc. Lab., Rept. LA-1862, 1955.

98. Birkhoff, G., "Taylor Instability Appendices to Rept. LA-1862," Univ. of Calif. Los Alamos Sc. Lab., Rept. LA-1927, 1955.

99. Milne-Thompson, L. M., Theoretical Hydrodynamics, Macmillan Co., New York, 1950, 37.

100. Bromley, L., "Heat Transfer in Stable Film Boiling," Chem. Engr. Progress, 46, 1950, 221.

101. Chang, Y. P., "A Theoretical Analysis of Heat Transfer in Natural Convection and in Boiling," A.S.M.E. Trans. 79, 1957, 1501.

102. Davies, R. M. and G. I. Taylor, "The Mechanism of Large Bubbles Rising Through Extended Liquids and Through Liquids in Tubes," Proc. Roy. Soc. London, A-200, 1949, 375.

103. Garabedian, P. R., "On the Steady-State Bubbles Generated by Taylor Instability," Proc. Roy. Soc. London, A-241, 1957, 423.

104. Birkhoff, G. and D. Carter, "Rising Plane Bubbles," J. of Rat. Mech. and Analysis, 6, 1957, 769.

105. Kutateladze, S. S., Borishanskii, V. M., Novikov, I. I. and O. S. Fedjinski, Liquid Metal Heat Transfer, Atomazdat, Moscow, 1958.

106. McAdams, W. H., Heat Transmission (3rd Edition), McGraw Hill, New York, 1954.

107. Lord Rayleigh, Theory of Sound, Dover Publ., New York, 1945.

108. Kazakova, E. A., "The Influence of Pressure on the First Crisis in Boiling Water," Problems of Heat Transfer During a Change of State, Gosenergoizdat, Moscow, 1953.

109. Kutateladze, S. S. and L. L. Schneiderman, "Experimental Study of the Influence of the Temperature of a Liquid on the Change of the Rate of Boiling," Problems of Heat Transfer During a Change of State, Moscow, 1953.

110. Bartz, D., "Factors Which Influence the Suitability of Liquid Propellants as Rocket Motor Regenerative Coolants," Paper presented at the American Rocket Society Spring Meeting, Washington, D. C., April, 1957.

111. Rayleigh, Lord, "Instability of Cylindrical Fluid Surfaces," Philosophical Magazine, 34, Ser. V, 1892, 177.

112. Christiansen, R. M., "Breakup of a Liquid Jet in a Denser Liquid," Ph.D. Dissertation, University of Pennsylvania, 1955.

113. Christiansen, R. M., and A. N. Hixson, "Breakup of a Liquid Jet in a Denser Liquid," Ind. and Engr. Chemistry, 49, 1957, 1017.

114. Weber, C., "Zum Zerfall eines Flüssigkeitsstrahles," Zeitsch. für. angew. Math. und Mech., 11, Heft 2, 1931, 136.

APPENDIX A

The Stability of a Circular Jet

The stability of a cylindrical fluid column under the action of capillary force was analyzed by Rayleigh (106, 111). Considering only the inertia of the liquid inside the column, the angular frequency of an axially symmetric disturbance is given by:

$$\omega^2 = \frac{\sigma m R}{\rho' R^3} \left[(mR)^2 - 1 \right] \frac{I_0'(mR)}{I_0(mR)} \qquad \text{A-1}$$

where ρ' is the density of the fluid within the column; m is the wave number of the disturbance and R is the radius of the jet. This case would correspond to a liquid jet disintegrating in air. When the inertia of the fluid outside, rather than the fluid inside, the column is important, the angular frequency is given by:

$$\omega^2 = \frac{\sigma m R}{\rho R^3} \left[1 - (mR)^2 \right] \frac{K_0'(mR)}{K_0(mR)} \qquad \text{A-2}$$

189

where ρ is the density of the surrounding medium; this case corresponds to the disruption of a jet of air under water. Since the modified Bessel function of the second kind is given by

$$K_0(\mathfrak{z}) \simeq \sqrt{\frac{\pi}{2\mathfrak{z}}}\ e^{-\mathfrak{z}} \qquad\qquad \text{A-3}$$

it is seen that in both problems the cylindrical column becomes unstable when mR $<$ 1, i.e., when the wave length λ exceeds the circumference of 2 π R of the jet.

The inertial effects of both jet and surrounding medium were considered by Christiansen (112, 113). When the densities of both fluids are taken into account the angular frequency is given by

$$\omega^2 = \frac{\sigma m R\left[(mR)^2 - 1\right]}{R^3\left[\rho' \dfrac{I_0(mR)}{\overset{\bullet}{I}_0(mR)} - \rho\ \dfrac{K_0(mR)}{\overset{\bullet}{K}_0(mR)}\right]} \qquad\qquad \text{A-4}$$

An analysis of the effects of Helmholtz instability upon the disintegration of a liquid jet in air was reported by Weber (114). In his paper the inertia of the jet only was taken into account, i.e., the inertia of the surrounding medium was neglected. In what follows the stability of a cylindrical column will be investigated

and the inertial effects of both media as well as the effect of Helmholtz instability will be considered.

Let a cylindrical jet of radius R flow with velocity u' in the direction of the vertical z axis. Denote by superscript prime the medium inside the jet. The equation of the disturbed boundary is given by

$$r = R + \zeta(z, t)$$

A-5

where the disturbance ζ is of the form

$$\zeta = \zeta_o \, e^{i(\omega t - m z)}$$

A-6

The problem is formulated by considering the equations of continuity for the two flow fields

$$\frac{\partial^2 \phi'}{\partial r^2} + \frac{1}{r}\frac{\partial \phi'}{\partial r} + \frac{\partial^2 \phi'}{\partial z^2} = 0$$

A-7

$$\frac{\partial^2 \phi}{\partial r^2} + \frac{1}{r}\frac{\partial \phi}{\partial r} + \frac{\partial^2 \phi}{\partial z^2} = 0$$

A-8

subject to the boundary conditions

$$r = 0: \quad \frac{\partial \phi'}{\partial r} = 0 \qquad\qquad \text{A-9}$$

$$r = R: \quad -\frac{\partial \phi'}{\partial r} = \frac{d\,y}{d\,t} \qquad\qquad \text{A-10}$$

$$r = R: \quad -\frac{\partial \phi}{\partial r} = \frac{d\,y}{d\,t} \qquad\qquad \text{A-11}$$

$$r \to \infty: \quad \phi \quad \text{finite} \qquad\qquad \text{A-12}$$

$$r = R: \quad P' - P = \sigma\left[\frac{1}{R_c} + \frac{1}{R_z}\right] \qquad \text{A-13}$$

where $1/R_c$ and $1/R_z$ are the curvature in the transverse and axial sections respectively. From Lamb (Reference 50, Page 473) the sum of the principal curvature is

$$\frac{1}{R_c} + \frac{1}{R_z} = \frac{1}{R} - \frac{y}{R^2} - \frac{\partial^2 y}{\partial z^2} \qquad \text{A-14}$$

The pressures P' and P satisfy Bernouilli's equation thus:

$$\frac{P}{\rho} = \frac{\partial \phi}{\partial t} - \frac{1}{2}\left[\left(\frac{\partial \phi}{\partial \xi}\right)^2 + \left(\frac{\partial \phi}{\partial r}\right)^2\right] + const.$$

A-15

$$\frac{P'}{\rho'} = \frac{\partial \phi'}{\partial t} - \frac{1}{2}\left[\left(\mathcal{U}' - \frac{\partial \phi'}{\partial \xi}\right)^2 + \left(\frac{\partial \phi}{\partial r}\right)^2\right] + const$$

A-16

The solutions of Equations A-7 and A-8 which satisfy the kinematic conditions, i.e., Equations A-9 through A-12, are

$$\phi' = -i\left(\frac{\omega}{m} - \mathcal{U}'\right)\frac{I_0(mr)}{\overset{\bullet}{I_0}(mR)}\,\zeta_0\,e^{i(\omega t - m\xi)}$$

A-17

$$\phi = -i\left(\frac{\omega}{m}\right)\frac{K_0(mr)}{\overset{\bullet}{K_0}(mR)}\,\zeta_0\,e^{i(\omega t - m\xi)}$$

A-18

The frequency equation is obtained by satisfying the dynamic conditions, i.e., Equations A-13 through A-16 thus

$$\frac{\sigma[(mR)^2-1]}{R^2} = \frac{\rho' I_o'(mR)}{\dot{I}_o(mR)}\left(\frac{\omega}{m}-u'\right)^2 m - \rho\frac{K(mR)}{\dot{K}(mR)}\left(\frac{\omega}{m}\right)^2 m \quad \text{A-19}$$

We note that for $u' = 0$, Equation A-19 is reduced to Equation A-4. With $u' = 0$ and neglecting the inertia of the surrounding liquid, i.e., $\rho = 0$, Equation A-19 reduces to Equation A-1; with $\rho' = 0$ it reduces to Equation A-2.

Expanding and rearranging Equation A-19 it follows that

$$\frac{\omega}{m} = \frac{\rho' I_o^* u'}{\rho' I_o^* - \rho K_o^*} \pm \frac{[(\rho' I^* - \rho K^*)W + \rho K^* \rho' I^* u'^2]^{1/2}}{\rho' I^* - \rho K^*} \quad \text{A-20}$$

where

$$I^* = \frac{I_o(mR)}{\dot{I}_o(mR)}$$

$$K^* = \frac{K_o(mR)}{\dot{K}_o(mR)} \quad \text{A-21}$$

$$W = \frac{\sigma}{R^2 m}[(mR)^2-1]$$

The first term on the right-hand side may be called the mean velocity of the flow. Relative to this there are waves travelling with velocities $\pm C$, given by

$$c^2 = \frac{\sigma[(mR)^2 - 1]}{R^2 m[\rho' I^* - \rho K^*]} + \frac{\rho' I^* \rho K^* u'^2}{[\rho' I^* - \rho K^*]^2} \qquad \text{A-22}$$

We note that if the density ρ, of the surrounding medium is small compared to the density ρ', of the jet, Equation A-22 becomes

$$c^2 = \frac{\sigma[(mR)^2 - 1]}{R^2 m[\rho' I^*]} + \frac{\rho K^*}{\rho' I^*} u'^2 \qquad \text{A-23}$$

which is the equation derived by Weber. For the present problem the density of the jet ρ' is much smaller than the density of the surrounding liquid; Equation A-22 can be simplified, thus

$$c^2 = \frac{\sigma}{\rho R} \frac{[(mR)^2 - 1]}{mR} \left| \frac{\overset{o}{K_0}(mR)}{K_0(mR)} \right| - \frac{\rho' \overset{'}{I_0}(mR)}{\rho \overset{\cdot}{I}(mR)} \left| \frac{\overset{\cdot}{K_0}(mR)}{K_0(mR)} \right| u'^2 \qquad \text{A-24}$$

For large values of mR, i.e., for short waves, Equation A-24 becomes

$$C^2 = \frac{\sigma m}{\rho} - \frac{\rho' u'^2}{\rho}$$

A-25

which is of the same form as Equation VI-1. The condition of stability is that C shall be real. It is seen from Equation A-24 that if mR = 1 the motion is unstable for any vapor velocity. The critical condition is then given by

$$u'^2 = \frac{\sigma}{\rho' R} \frac{[(mR)^2 - 1]}{mR} \frac{I_0'(mR)}{I_0(mR)}$$

A-26

With mR = 2, Equation A-26 becomes

$$u'^2 = \frac{\sigma}{\rho' R}$$

A-27

which is of the same form as Equation VI-5.